

N° d'Ordre : D.U.

UNIVERSITE BLAISE PASCAL

U.F.R. Sciences et Technologies

ECOLE DOCTORALE DES SCIENCES FONDAMENTALES

N°

THESE

Présentée pour obtenir le grade de

DOCTEUR D'UNIVERSITE

Spécialité : Chimie-Physique

Par **Kristýna MONTÁGOVÁ BERKOVÁ**

**PROCESSING, STRUCTURE AND PROPERTIES OF
COMPOSITES BASED ON NATURAL FILLERS AND
STREOREGULAR POLYOLEFINS:
ENVIRONMENTALLY BENIGN CONCEPT**

A soutenir publiquement devant la commission d'examen :

Président :	-	-
Rapporteurs :	Assoc. Professor	Valerie Massardier-Nageotte
	Professor	Berenika Hausnerová
	Assoc. Professor	Martin Obadal
Examineurs:	Assoc. Professor	Vincent Verney
	Professor	Roman Čermák
	Professor	Sophie Commereuc

TOMAS BATA UNIVERSITY IN ZLÍN
Faculty of Technology
Department of Polymer Engineering

DOCTORAL THESIS

Kristýna Berková

**PROCESSING, STRUCTURE AND PROPERTIES OF
COMPOSITES BASED ON NATURAL FILLERS AND
STEREOREGULAR POLYOLEFINS:
ENVIRONMENTALLY BENIGN CONCEPT**

Programme: Chemistry and Materials Technology
Course: Technology of Macromolecular Compounds
Co-supervisors: Assoc. Prof. Vincent Verney
doc. Ing. Roman Čermák, Ph.D.
Year: 2013

ACKNOWLEDGEMENTS

I would like to take this opportunity to express my cordial gratitude to my supervisors Mr. Vincent VERNEY and Mr. Roman ČERMÁK for giving me the opportunity of Co-supervised Ph.D. study, their encouragement, advice, professional chairmanship and inspiration during my doctoral studies.

Also I would like to thank my colleagues, from Department of Polymer Engineering and Chemical Institute in Clermont-Ferrand for their help and friendly environment.

The special thanks are directed to my husband and my parents for their permanent help, patience, confidence and support.

TABLE OF CONTENTS

ABBREVIATIONS	- 6 -
RÉSUMÉ	- 8 -
ABSTRAKT	- 9 -
ABSTRACT	- 10 -
1 INTRODUCTION	- 11 -
2 STATE OF THE ART	- 13 -
2.1 INTRODUCTION TO WOOD-PLASTIC COMPOSITES.....	- 13 -
2.1.1 Properties of Wood-Plastic Composites.....	- 13 -
2.1.2 Processing of Wood-Plastic Composites	- 15 -
2.1.3 Applications of Wood-Plastic Composites	- 15 -
2.2 WOOD	- 17 -
2.2.1 Chemical Structure of Wood.....	- 17 -
2.2.2 Properties of Wood	- 19 -
2.2.3 Modification of Wood.....	- 20 -
2.2.4 Different Particles of Wood for WPC.....	- 22 -
2.3 POLYPROPYLENE.....	- 23 -
2.3.1 Synthesis	- 23 -
2.3.2 Structures of Polypropylene	- 23 -
2.3.3 Isotactic Polypropylene.....	- 25 -
3 AIMS OF THE WORK	- 30 -
4 EXPERIMENTAL PART	- 31 -
4.1 MATERIALS	- 31 -
4.2 PREPARATION OF COMPOSITES.....	- 32 -
4.3 EXPERIMENTAL METHODS – RHEOLOGICAL CHARACTERIZATION	- 33 -
4.3.1 Backgrounds of Rheology.....	- 33 -
4.3.2 Rheological Measurements	- 36 -
4.4 EXPERIMENTAL METHODS – STRUCTURAL CHARACTERIZATION	- 36 -
4.4.1 Principles of Wide-Angle X-Ray Scattering.....	- 36 -
4.4.2 Measurement of Wide-Angle X-Ray Scattering.....	- 38 -
4.5 EXPERIMENTAL METHODS – THERMAL BEHAVIOR CHARACTERIZATION.....	- 38 -
4.5.1 Introduction to Differential Scanning Calorimetry	- 38 -
4.5.2 Differential Scanning Calorimetry	- 40 -
5 RESULTS AND DISCUSSION	- 41 -
5.1 RHEOLOGICAL CHARACTERIZATION	- 41 -
5.1.1 Effect of Melt Flow Index on Viscoelastic Behavior.....	- 41 -
5.1.2 Effect of Wood Flour Origin and Filler Size	- 51 -
5.1.3 Effect of Polymer Matrix	- 53 -
5.1.4 Effect of Wood Flour Extraction.....	- 58 -

5.2	STRUCTURAL CHARACTERIZATION	- 67 -
5.3	THERMAL BEHAVIOR CHARACTERIZATION	- 76 -
6	CONCLUSIONS.....	- 89 -
7	REFERENCES	- 92 -
	LIST OF THE FIGURES.....	- 98 -
	LIST OF THE TABLES.....	- 102 -
	AUTHOR'S PUBLICATIONS	- 103 -
	CURRICULUM VITAE.....	- 104 -

ABBREVIATIONS

a	<i>Power law index</i>
A_a	<i>Amorphous halo</i>
A_c	<i>Crystal reflections intensities</i>
De	<i>Deborah number</i>
FWHM	<i>Full width in half maximum</i>
G'	<i>Dynamic storage modulus</i>
G''	<i>Dynamic loss modulus</i>
H	<i>Dispersion parameter</i>
h	<i>Relaxation parameter</i>
iPP	<i>Isotactic polypropylene</i>
ISO	<i>International Organization of Standardization</i>
K	<i>Constant</i>
K_β	<i>Amount of beta crystallites</i>
$L_{(hkl)}$	<i>Crystalline domain length</i>
l_c	<i>Crystalline thickness</i>
m	<i>Shape factor</i>
MA	<i>Maleic anhydride</i>
MFI	<i>Melt flow index</i>
M_n	<i>Number average molecular weight</i>
M_w	<i>Weight average molecular weight</i>
PDI	<i>Polydispersity index</i>
PE	<i>Polyethylene</i>
PP	<i>Polypropylene</i>
PPMA	<i>Maleated polypropylene</i>
t	<i>Time</i>

$\tan \delta$	<i>Dumping factor</i>
T_c	<i>Temperature of crystallization</i>
T_m	<i>Melting temperature</i>
w	<i>Concentration of the matrix</i>
WA	<i>Water absorption</i>
WF	<i>Wood flour</i>
WF/PP	<i>Wood flour/polypropylene</i>
WPC	<i>Wood-plastic composites</i>
X_c	<i>Crystallinity</i>
X_α	<i>Alfa crystallinity</i>
X_β	<i>Betta crystallinity</i>
δ	<i>Phase angle</i>
η'	<i>Real viscosity component, Dynamic viscosity</i>
η''	<i>Imaginary viscosity component</i>
η^*	<i>Complex viscosity</i>
η_0	<i>Zero shear viscosity</i>
λ_0	<i>Characteristic relaxation time</i>
σ	<i>Shear stress</i>
σ_e	<i>Fold surface energy</i>
ω	<i>Frequency</i>
$\dot{\gamma}$	<i>Shear rate</i>
ΔH_m^0	<i>Enthalpy of theoretical fully crystallized material</i>
T_m^0	<i>Equilibrium melting temperature</i>
ΔH_c	<i>Heat of crystallization</i>
ΔH_m	<i>Heat of fusion</i>
Δh_v	<i>Volumetric heat of fusion</i>

RÉSUMÉ

Ce travail porte sur l'étude des composites à base de polypropylène et de farine de bois. Seuls des composites à base d'une matrice polypropylène et de fibres végétales ont été mis en œuvre sans aucun recours à quelque agent comptabilisant que ce soit. En premier lieu nous avons regardé l'influence de la viscosité initiale de la matrice polypropylène sur la processabilité des biocomposites en utilisant des polymères de grades variés. Puis nous avons étudié l'influence de la nature et de la concentration de la farine en utilisant des farines de pin (bois mou) et de chêne (bois dur). Enfin, une attention spécifique a été portée sur la possibilité de nucléation en phase Beta de la matrice polypropylène en présence de fibres végétales. Des polypropylènes β -nucléés ainsi que des farines ayant subies des extractions par des solvants de leurs composés volatils ont été utilisées. Les mélanges obtenus ont été testés au moyen de la viscoélasticité à l'état fondu pour mettre en évidence les effets d'interaction charges-matrices et par des mesures de diffraction aux rayons X ainsi que d'analyse thermique différentielle pour la caractérisation de leurs morphologies cristallines.

ABSTRAKT

Předložená doktorská práce je zaměřena na kompozity polypropylenu a dřevní moučky. V experimentální části práce jsou připraveny kompozity s různými koncentracemi plniva a izotaktických polypropylenů s různými indexy toku taveniny. Na základě této studie je vybrán jeden konkrétní polypropylen, který může mít v kombinaci s dřevní moučkou i praktické využití. Tento polypropylen je dále zkoumán s různými druhy a koncentracemi dřevní moučky. Pozornost je také kladena na úpravu vlastností izotaktického polypropylenu užitím specifického β -nukleačního činidla. Jsou porovnávány a popisovány rozdíly mezi kompozity s čistým a nukleovaným polypropylenem. Práce se dále zabývá extrakcí dřevní moučky v rozpouštědle. Je studován vliv extrakce a rozpouštědla dřevní moučky na vlastnosti připravených kompozitů. Byly studovány reologické, strukturální a tepelné vlastnosti, které se lišily v závislosti na zvoleném typu plniva, jeho koncentraci a typu polymerní matrice.

ABSTRACT

This doctoral thesis is focused on composites based on polypropylene and wood flour. Firstly, the experimental work deals with preparation of composites based on wood flour with various concentrations and isotactic polypropylene with various melt flow indexes. In terms of this study, one polypropylene, which can have also practical use, was chosen. Further, this polypropylene is investigated with various types and concentrations of wood flour. Also, the attention is devoted to the modification of polypropylene by a specific β -nucleating agent. The differences are compared and described between the composites with neat and nucleated polypropylene. Further, the work is focused on solvent extraction of wood flour. The effect of extraction and solvent of wood flour is also examined in composites with neat and nucleated polypropylene. On prepared composites, the rheological, structural and thermal properties are studied. These properties differ depending on specific type of wood flour, its concentration and specific type of polypropylene.

1 INTRODUCTION

Today's world faces many environmental problems and two of them are plastic waste and excessive felling. The former is connected with tremendous production and use of plastics in practically all areas of everyday living, while the latter should be related to people's demand and desire to be surrounded by natural products, particularly wood. Wood then found use not only in furniture, but also in building industry. [1, 2]

Combination of these materials – synthetic polymer, plastic, and wood, can not only reduce mentioned problems, but also bring another advantages such as low specific weight, higher specific strength or stiffness, when compared to glass reinforced composites. From this point of view, the wood fibers provide safer handling and working conditions and also less abrasive properties to mixing and molding equipment. Still the most interesting aspect about natural fillers is their potentially positive environmental impact. Wood flour is original to plants, such as other cellulose materials, it is thus included in renewable resources which production require minimum of energy. Moreover, they are carbon-dioxide neutral, which means, their contribution to CO₂ concentration in atmosphere after combustion equals to the CO₂ consumption during the wood growth. [3, 4]

In last two decades, the wood-plastic composites (WPC) gained attention of both – scientific centers and industry. Production of WPC has grown significantly. Potential applications are then found primarily in composites for use in automotive, building industry as well as furniture and household equipment industry. [5] However, the limitation is usually low interaction between the filler and matrix. Wood flour (WF) is cellulose, which bears hydroxyl groups, so its surface is hydrophilic, while most of the commodity plastics are hydrophobic, particularly polyolefins. This problem could be handled for example by use of coupling agents or chemical modification of the WF or matrix, but also by effective filling and mixing, which optimizes properties of the composite. [4, 6, 7]

Quality of the composite material depends strongly also on the origin of the wood, which may have different composition and structure of the cellulose fibers. [8] Purity of the material in connection with relatively large amount of possible accompanying substances is even more crucial. [9, 10] In present study, two materials are used – pine and oak, as representatives of softwood and hardwood, respectively. These materials are investigated,

after compounding with polymeric matrices, by means of rheology, X-ray structural analysis and differential scanning calorimetry (DSC). To check possible influence of extractible wood-accompanying low-molecular substances, cyclic washing with ethanol or cyclohexane in Soxhlet apparatus was used to purify the filler.

Isotactic polypropylene (iPP) is used in the present study since it is one of extensively used plastic, which found application in many areas of living including those for which the WPC composites are currently designed – i.e. building, automotive industry etc. iPP is an interesting material from both the scientific and industrial point of view, which is caused by its polymorphism. The strength, toughness and thermal stability is usually connected with monoclinic α phase, while tenacity, drawability, but also decreased thermal stability is typical for trigonal β phase. [11–14] The latter form is usually achieved by introduction of nucleating agent to the material. [15] There were some studies showing practically no impact of cellulose on the crystallization process, particularly α crystallites formation. [16, 17] Concerning the ability of iPP to crystallize in different structures as well as the presence of nucleating substance, one can imagine that the wood may either support or suppress the β phase formation. Both X-ray structural study and DSC were performed with purpose to check possible influence on the amount and composition of the crystalline phase.

2 STATE OF THE ART

2.1 Introduction to Wood-Plastic Composites

Composites are complex materials made from two or more distinct components which once they are combined, produce a structural and a functional new material [18].

Eco-friendly composites are made from natural renewable resources and synthetic polymer matrix. Wood flour (WF) can be considered as an example of natural filler and in combination with a wide variety of polymeric matrices, including polypropylene (PP), can be obtained wood-plastic composites (WPC).

2.1.1 Properties of Wood-Plastic Composites

The WPC are widely used modern materials, due to their environmentally friendly basis. Wood in the WPC represents the natural filler which is both renewable and biodegradable. The mentioned properties of WPC can be influenced by many factors such as concentration of fillers, size and distribution of filler particles, modification of filler or polymer matrix, processing conditions and parameters, all of these have a big impact on the properties of the WPC. Nevertheless, the WPC have some disadvantages. They are highly sensitive to humidity and have tendency to swell. They are also easily attacked by mildew which leads to lose their mechanical properties. [4, 6]

Mechanical Properties

Content of WF in WPC has significant impact on the mechanical properties. Bouafif et al. [8] found that the best mechanical properties were obtained with composites with a high WF content. Mechanical properties, namely tensile modulus of elasticity and maximum tensile strength, increase with the average particle size. This behavior is shown in the Figure 1 (65 mesh \approx 230 μm , 24 mesh \approx 710 μm). [8]

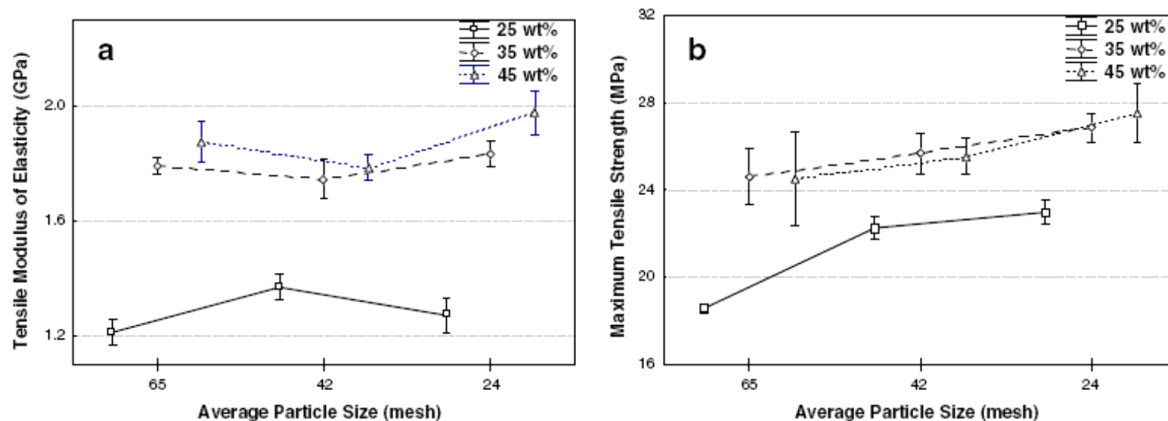


Figure 1 Effect of wood particle size with various filler content on tensile modulus (a) and maximum tensile strength (b) [8]

Bledzki et al. [4] studied the effect of compounding method on mechanical properties. They investigated, that addition of maleic anhydride (MA) to PP/WF composites during compounding process improves the tensile modulus and strength while the flexural modulus and strength of composites is not changed. Composites were compounded with twin-screw extruder, two-roll mill and agglomerator. Composites with maleated PP prepared on twin-screw extruder showed better mechanical properties thanks to both better dispersion of WF in PP matrix and better adhesion between matrix and filler. [4] This finding was confirmed by Yang et al. [19] who published, that the composites prepared on twin screw extruder have better tensile properties. Ashori and Nourbakhsh [20] studied tensile strength and modulus of composites as a function of maleated polypropylene (MAPP) and fiber content. They found, that composites with MAPP exhibit improved strength since the interaction of MAPP-filler causes strong interfacial bonding. They also found, that the tensile strength and modulus decrease with higher WF content. This was explained by poor adhesion between filler and matrix and by the fact, that higher concentrations need more coupling agents. [20]

Water Absorption

The ability of wood to absorb water may cause problems in certain applications. Chemical modification of wood can decrease significantly the water absorption (WA) which was studied by Dányádi et al. [21]. Izacho et al. [22] focused on the influence of WF content on the WA. They discovered that WA increases with increasing concentration of WF in composites. This increase is logically explained by hydrophilic character of wood. Mainly

the concentration of particles and their chemical modification have an influence on WA on the other hand the size of the particles does not influence WA essentially. When the amount of WF was increased, the polar character was higher and hence the WA increased. [22]

2.1.2 Processing of Wood-Plastic Composites

The WPC are commonly produced by mixing of polymer matrix and wood as filler. Some additives (colorants, stabilizers, blowing and coupling agents) can be incorporated to the composite [23]. Modification of the wood can help to obtain required properties of the WPC, as well as the modification of polymer matrix can. The most often method of matrix modification in case of PP is grafting it with MA or acrylic acid [24, 25].

The most used methods of goods and semi-finished goods production are extrusion and injection molding. However, thermoforming can also be used for processing of the WPC [26]. Extrusion is a method which is used for production of profiles, such as decks and handrails. On the other hand, goods with more complicated shape can be made by injection molding. Extrusion as well as injection molding includes the same processing steps: compounding, melting, shaping and cooling. During these various methods of manufacturing processing factors have to be kept strictly.

Two types of extrusion can be employed for production of the WPC. Single screw extruder and twin co-rotating screw are usually used. The single screw extruder does not have a mixing part and can only feed the melted mixture to the die, thus the pre-blending is required before extrusion. On the other hand, the twin screw extruder provides feeding and mixing together. In this system, the screw has a multiplex shape and therefore the fillers and polymer matrix are blended very well. [19]

2.1.3 Applications of Wood-Plastic Composites

The WPC was proposed as good candidate for many applications in various industry sectors as shown in Figure 2. In the year 2008, the automotive industry made use of a significant percentage of the WPC substituting glass fiber with plant fiber. [23] Mechanical strength, lower production cost, passenger safety and shatterproof performance under extreme temperature changes are provided by the WPC for the interior parts in automotive industry. [23]

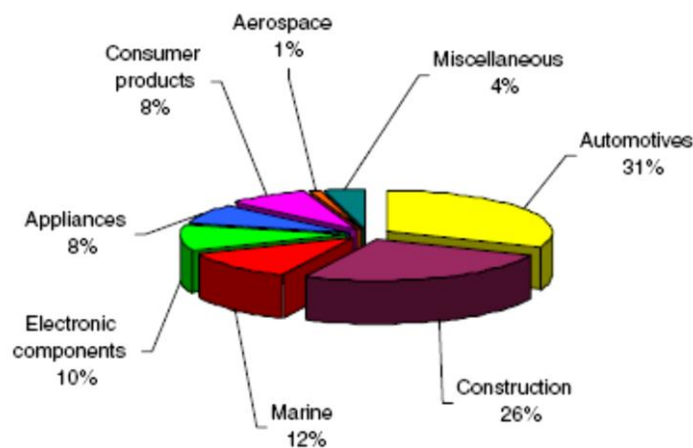


Figure 2 Wood-plastic composites used worldwide in 2002 [23]

The second biggest sector regarding the use of the WPC is building industry. For example, in the United States softwoods and hardwoods are widely used for various applications. The WPC with softwood (in the form of lumbers or plywood) are applied in constructions for decking, forms, scaffolding, framing, sheathing, flooring, molding, paneling, cabinets, poles and piles, and many other building components. Hardwoods are used in the WPC for constructions of architectural woodwork, interior woodwork (flooring, furniture), and paneling. [27] Applications of WPC are as well actual in Asia, Australia, and Europe. In Germany the main areas for the application of WPC are in the automotive industry for car interiors and also in decking (floor coverings, used mainly in outdoor areas, such as terraces and public places) [28].

The impressive growth of WPC leading up to 2010, had been followed by stagnation in 2011 to 2012, but growth is now expected to resume, North America has been the biggest inventor and producer of WPC in the world. Still Europe lags far behind North America where usage is around twice as high. However, in Europe decking continues to be the dominant application for WPC. [29]

In 2012, more than 1.5 million tons of WPC were produced worldwide, especially in North America (about 1 million tons), China (200,000 tons) and Japan (100,000 tons). Germany was the European leader with more than 70,000 tons. Nowadays, the road furniture has been studied by Muszynski who examines the possible replacement of currently used materials in many of highway applications of WPC. These street furniture products are manufactured in Australia and rarely in Europe and Asia [28-30].

2.2 Wood

Wood is a stiff tissue of coniferous and broadleaved species which is grouped among the renewable resources. It has been used since ancient times with outstanding availability. Wood can be recycled and when it reaches the end of its life it can be disposed of with minimal impact to the environment.

2.2.1 Chemical Structure of Wood

From the chemical point of view, wood is composed from 49.5 wt. % of carbon, 44.2 wt. % of oxygen, and 6.3 wt. % of hydrogen. Wood is composed primarily of organic compounds such as macromolecular components (90–98 %) which form a structure of cell wall: cellulose, hemicellulose, and lignin. [27, 31] The typical composition of wood is in Table 1.

Table 1 Typical chemical compositions of wood [31, 32]

Main components 90–98 %	Polysaccharides 70 %	Cellulose Hemicellulose	
	Aromatic parts 25 %	Lignin	
Minor components 2–10 %	Organic	Polymers Low-molecular substances	
	Anorganic	Salts Ca, K, Mg, Na, Mn	

Cellulose

Cellulose (Figure 3), which is the main component of wood, is a linear homopolymer which consists of repeating β -D-glucopyranose units. These units are bonded by 1,4-glycosidic bonds. Each of the unit contains three hydroxyl groups, which play an important role in physical properties of cellulose. The length of the cellulosic chain varies considerably. The average polymeric degree of cellulose is between 8 000 and 10 000. [3, 31, 33, 34]

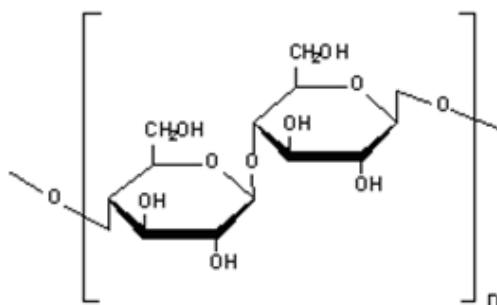


Figure 3 Structure of cellulose monomer [32]

Cellulosic fibers could be used, for example, in the paper making industry. One of the most important characteristic is their natural origin. The reason of the growing interest in these fibers is that they are non-polluting, safe to use, and energy efficient. [33, 35]

Hemicellulose

Hemicellulose is a linear polysaccharide with short side chains (Figure 4) and has lower molecular weight than cellulose. The average degree of polymerization of hemicelluloses is approximately 150. Hemicellulose is less chemical resistant and easily hydrolyzed. [3, 31]

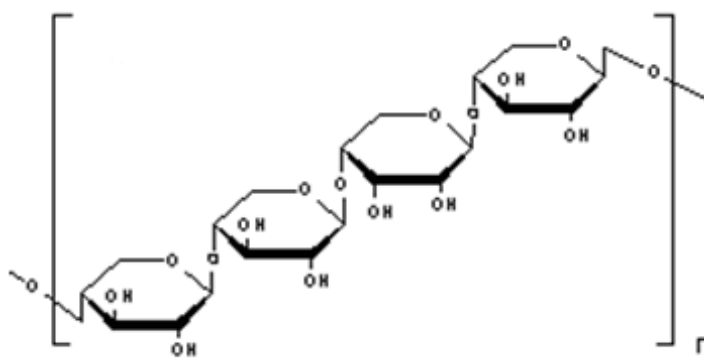


Figure 4 Structure of hemicellulose [32]

Lignin

Lignin is an amorphous polymer, which has a three-dimensional structure (Figure 5). This structure consists of phenylpropane units, which are variously substituted mainly with hydroxyl and methoxyl groups on the benzene ring of side chains. [31] One of the characteristics of lignin is a strong absorption of ultraviolet light. Therefore, radical-induced depolymerization of both lignin and cellulose can occur. [36]

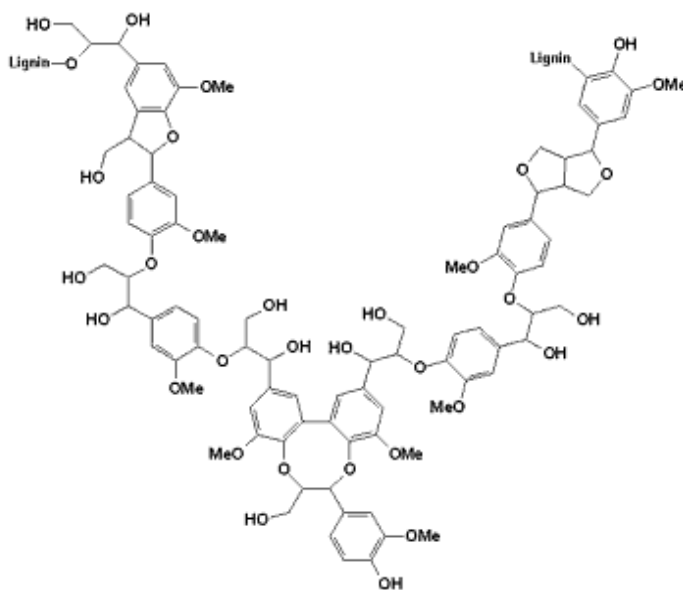


Figure 5 Structure of lignin [37]

2.2.2 Properties of Wood

Differences in the characteristic compositions of wood make material with various properties. It can be heavy or light, stiff or flexible. Particular pieces have essentially the same properties as the whole wood. However, an attention on selection of wood with respect to applications must be paid. [27]

Wood can differ in many properties accordingly to the age of tree, portion, mechanical properties and others. In literature earlywood and latewood, sapwood and heartwood, softwood and hardwood are recognized. Hardness is from practical point of view the most important criterion for selection the right wood for the final product. [38, 39] Wood is classified as hardwood or softwood accordingly to their mechanical properties, but not all softwoods have soft and lightweight wood, nor do all hardwoods have hard, heavy wood. Botanically these woods can be defined by name of their origin. Softwood comes from

gymnosperms, which usually are conifers, whereas hardwood comes from angiosperms, so called flowering plants. [27, 39] Softwood is non-porous, whereas hardwood is porous material, which consists of vessel elements. These two different kinds of wood differ in their anatomy. Vessel elements have open ends of cell and thus can transport water or sap in the tree. Hardwood is oak, maple, ash, elm, chestnut, locust, hickory, poplar, alder etc. and softwood is pine, fir, spruce, cedar, larch etc. [27, 39] The main properties, which limit the use of wood in some application, are density, porosity, and moisture content. Density of wood varies around 1.5 g/cm^3 , depending on the wood species. Wood with thin walls and small lumen volumes has high density whereas thin walls with large lumen volumes are ascribed to wood with low density. The magnitude which is related with density is strength. Cells with thick wall endure greater stress than cells with thin wall. These cells serve as interphasing region and it is necessary to ensure strong adhesive bond as strong as the wood. [40]

The porosity of wood system influences a direction of adhesive flow and amount. Softwood does not have pores; there are pits between fibers that let and keep lateral transfer of fluids in tree, this makes complex capillary system in tree. In the capillary system it is easy to deeply penetrate adhesives. On the other hand, because of the large vessel with no end walls in hardwood, it is not possible to penetrate deeply to the grain. In hardwood, few pits for lateral transfer of adhesive can be found. [40]

Large quantity of water is contained in a tree. The residual moisture content in wood is influenced by relative humidity of the surrounding air. Water is removed by drying. Quality of wood is anisotropic, which means that its properties vary according to direction in which they are measured. Both mentioned phenomenon must be taken into account when measuring and assessing its mechanical, thermal and other properties. [41, 42]

2.2.3 Modification of Wood

It is well known, that polymers especially non-polar have hydrophobic character, whereas bio-based fillers are usually hydrophilic. Because of these opposite characters, it is uneasy to get composite with good compatibility. Modification of wood seems to be a possible method to obtain a good interfacial connection of the polymer matrix and the filler. The incorporation of coupling agents or compatibilizers can also create a good connection

between wood fibers, flours, or ligno-cellulosic materials with the non-polar used polymer matrix. [40–45]

Chemical Modification

The properties of wood are determined by cell wall components. Chemical modification of cell wall can influence basic properties of wood. Modifiers or coupling agents are chosen on the basis of final required properties. Usually the main aim of this modification is to get a good interfacial linkage (Figure 6), an improved adhesion between the polymer matrix and the filler (decrease of wood hydrophilicity), and thereby certain mechanical and physical properties, fire retardancy, and weathering resistance [4, 21, 22, 44–46].

The most applied coupling agents are anhydrides such as phthalic, succinic, maleic, propionic, and butyric; acid chlorides; ketene carboxylic acids; many different types of isocyanates; formaldehyde; acetaldehyde; difunctional aldehydes; epoxides, such as ethylene, propylene, and butylene oxide; and difunctional epoxides etc. [5, 22, 47–49].

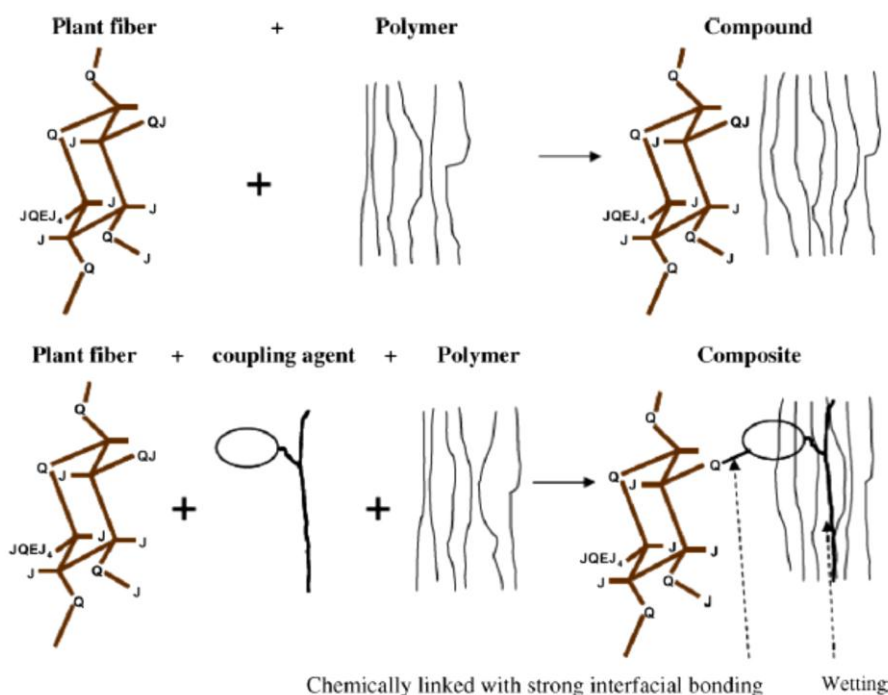


Figure 6 Mechanism of coupling agent activity between hydrophilic fiber and hydrophobic polymer matrix [23]

Physical Modification

Physical modification consists in the removal of water from wood by heating in dry air. This process can take several hours and it is necessary to decrease water content under 3 %. Thermal treatment of wood changes chemical and physical properties and also its structure, which is caused primarily by degradation of hemicellulose. The changes are as high as the temperature is increased [50].

2.2.4 Different Particles of Wood for WPC

Different types (shapes) of filler particles are used for WPC production. The choice of wood source depends on desired properties of final products. Wood particles differ in size, shape and hence influence the properties of composites. Different kinds of wood elements are showed in Figure 7.

Cellulose fibers are used in composites because of good reinforcement. Sometimes white color of fibers could be an advantage for special applications. However, WF is used as reinforcement rather than separated wood fibers. Isolation process of wood fibers is more expensive than get WF. [51]

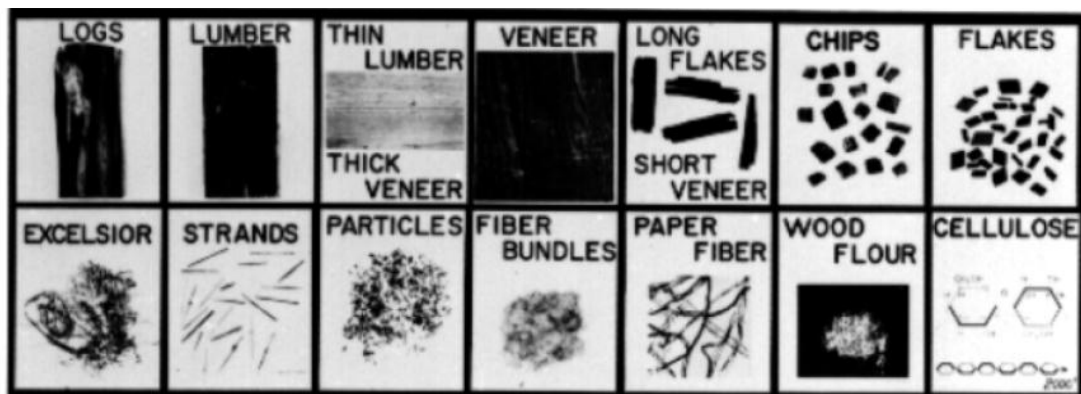


Figure 7 Basic wood elements (largest → smallest) [52]

2.3 Polypropylene

Polypropylene (PP) is a linear polymer consisting of only two elements – carbon and hydrogen; and together with polyethylene or poly(1-butene) it is a part of the polyolefins or saturated polymers. The PP possesses an excellent resistance to organic solvents. PP generally has higher tensile, flexural, and compressive strength and higher moduli than PE. This is due to the steric interaction of the pendant methyl groups, which can result in a more rigid and stiff polymer chain than in PE. [53]

2.3.1 Synthesis

In 1869, the French chemist Marcellin Pierre Berthelot performed the first experiment of PP polymerization with sulfuric acid. The result of this experiment was viscous oil, however did not find utilization in industry. The next important step in evolution of PP was the year 1954, when Giulio Natta used organometallic catalyst based on titanium and aluminum to produce semi-crystalline polymer [54]. Further development of catalysts for PP polymerization (in the 1950's) made the production of stereospecific PP easier and led to the growing annual production that remains until today. [53]

Catalysts are substances that decrease activation energy of particular reaction and make reaction possible to run under given conditions, whilst their composition remains untouched. [53] Ziegler-Natta or metallocene catalysts are used for preparation of PP. Ziegler-Natta catalysts are the most common commercial catalysts. Karl Ziegler and Giulio Natta received the Nobel Prize in 1963 for the development of polyolefin polymerization catalysts with high yield and high degree of stereospecificity. Metallocene catalysts have recently been developed for industrial use, and metallocene-produced PP is now available. [53]

2.3.2 Structures of Polypropylene

The polymerization reaction is highly stereospecific. Propylene molecules are connected to the main polymer chain, increasing the chain length, and not to one of the methyl groups attached to alternating carbon atoms (the pendant methyl groups), which would result in branching [53]. Polymerization of the non-symmetrical propylene molecules can lead to three possible sequences (Figure 8): head-to-tail, tail-to-tail or head-to-head [53, 55].

The structure and stereochemistry of PP affect its properties, because each of this structure is a part of new produced PP and their relative ratio influences the condition of polymerization. From the practical point of view, it is important to get the highest ratio of isotactic PP (higher than 90 %) and equally the lowest ratio of atactic PP, since this is source of decrease in mechanical properties. [53]

The most common commercial form of PP is isotactic polypropylene (iPP) in which all pendant methyl groups are in the same configuration and on the same side of the polymer chain. Due to this regular arrangement, iPP achieves high degree of crystallinity. [53, 56]

The syndiotactic PP consist of mers with alternating pendant methyl groups on opposite sides of the polymer backbone, with exactly opposite configurations relative to the polymer chain [53, 56]. In atactic PP, opposite methyl groups have a random orientation with respect to the polymer backbone.

Amounts of isotactic, atactic, and syndiotactic parts are determined by the catalyst used and the polymerization conditions. PP is predominantly isotactic, they however have small amount of atactic polymer. New metallocene catalysts allow other stereochemical configurations, such as hemi-isotactic PP. In this configuration, opposite methyl groups are on the same side of the PP chain, as in iPP; however, other methyl groups are inserted at regular intervals on the pendant side of the chain. [53, 56]

2.3.3 Isotactic Polypropylene

iPP usually achieves high crystallinity, leading to good mechanical properties, especially stiffness and tensile strength [53]. The conformation of chain of iPP is a helix, which has three units and can be right-handed or left-handed with period of 0.65 nm. As written above, methyl groups are always on the same side along the axis of the main chain and this configuration is caused of four different insertions of helix in iPP (these are related to axis) in crystalline state. [53, 56, 57] The crystal lattice of iPP is shown in Figure 10.

iPP is polymorphic material which crystallizes into several crystallographic forms. These differ in crystallographic lattice: α form is monoclinic, β form is trigonal and triclinic γ form, the last crystallographic modification is so-called mesomorphic (smectic) form, which consist of rather small irregular crystallites. The occurrence of particular forms

depends on tacticity and conditions given during crystallization such as temperature, pressure and rate of cooling. [56–58]

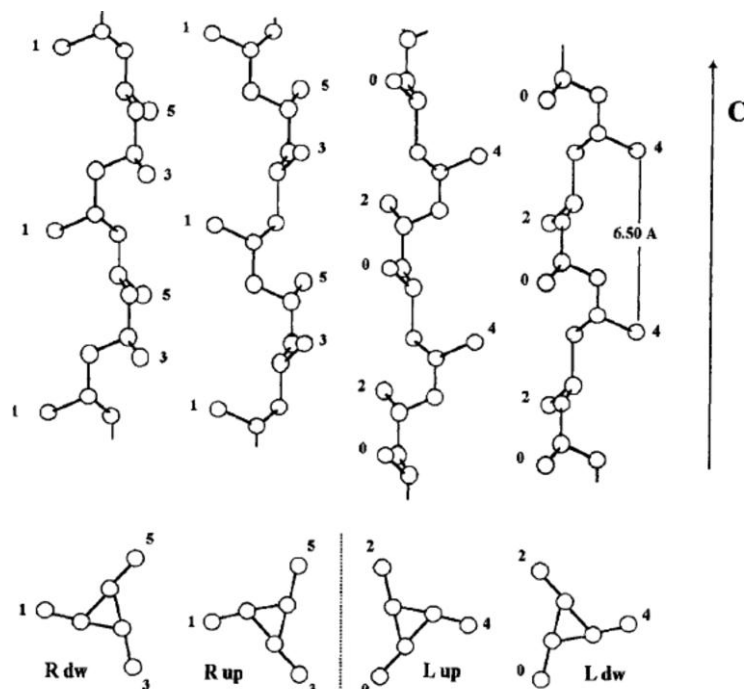


Figure 10 iPP chain in the crystal lattice – the four possible insertions [57]

α form

α form is the predominant structure of iPP and the most important modification for practical purposes [57, 59]. The α form in iPP (α -iPP) is characterized by thermodynamic stability and has good mechanical and other working characteristics. The α form is obtained from the melt cooling or solution crystallization at the atmospheric or slightly increased pressure [59].

This crystallographic modification consists of four helices, which create monoclinic lattice with dimensions: $a = 0.666 \text{ nm}$, $b = 2.078 \text{ nm}$, $c = 0.6495 \text{ nm}$ and angles $\alpha = \gamma = 90^\circ$, $\beta = 99.62^\circ$. The density of α form is 0.946 g.cm^{-3} [56, 57, 60].

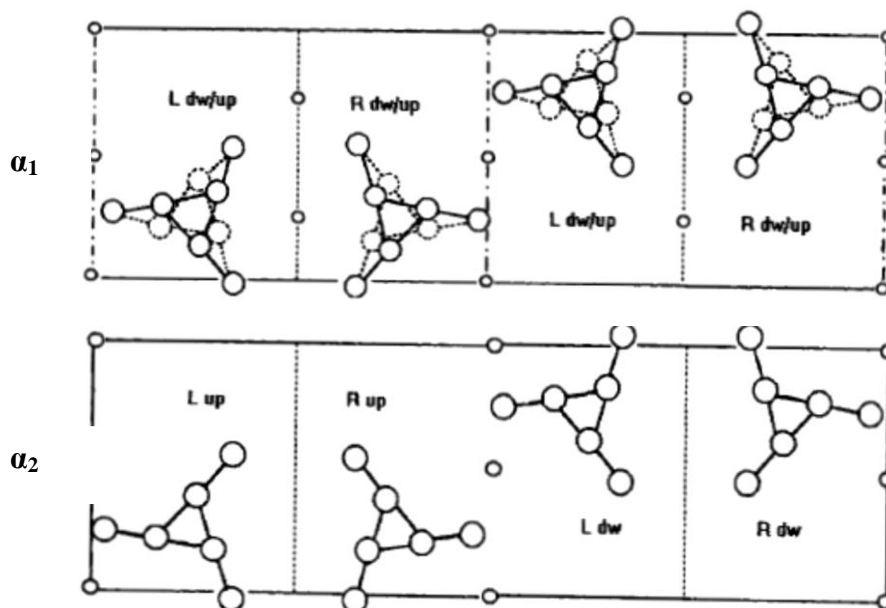


Figure 11 The crystalline structure of α form [57]

Spherulites of α form of iPP are spherical formations of lamellae, which show typical cross structure when observed in polarized light microscope. α -iPP can crystallize from less ordered α_1 form to more ordered α_2 (Figure 11). α_1 form was found by Natta and Corradini. This structure is monoclinic with random distribution of *up* and down (*dw*) chain packing methyl groups, while L and R helices occupy well-defined positions. The second structure, α_2 was investigated by Mencik, it is a monoclinic symmetry caused by a reduction of disorder of the local *up* and down (*dw*) helices in the crystal unit cell. It is a process, which is never complete, making α_2 only a limit situation. [57, 60]

β form

β form is a trigonal (in older literature sometimes also described as hexagonal), which was identified in 1959 by Keith et al. [57, 60]. iPP containing β form (β -iPP) is characterized by density of 0.921 g/cm^3 . In comparison of α -iPP, β -iPP is metastable with melting temperature $150 \text{ }^\circ\text{C}$ versus $180 \text{ }^\circ\text{C}$ and is unstable upon stretching, which can lead in a transition to α -iPP or to the smectic form. This depends on the processing conditions. Transition of the β -iPP to α -iPP can occur via a melting-recrystallization process or at high temperatures, whereas transition of β form to smectic form at low temperature occurs. [57, 60, 61]

The trigonal lattice can possess a unit cell of $a = 0.636 \text{ nm}$, $b = 0.635 \text{ nm}$, $\gamma = 120^\circ$ and $\alpha = \beta = 90^\circ$ [20]. The three isochiral helices with up-down statics are contained in the trigonal unit cell of β -iPP (Figure 12).

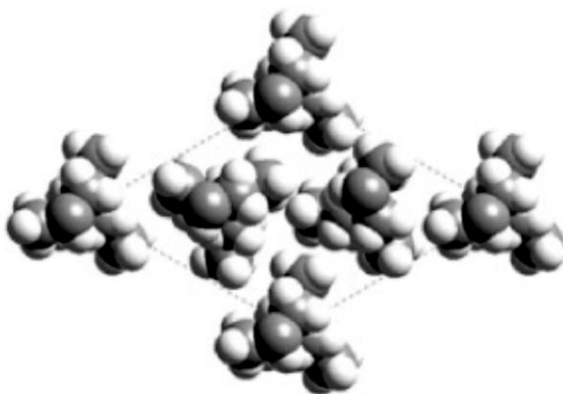


Figure 12 Structural model of β -iPP as determined by electron crystallography [58, 62]

β spherulites, which have strong negative birefringence, can be obtained by crystallization at 128–132 °C, on the other hand pure β form can be obtained with the aid of nucleating agents. Tensile properties of β -iPP generally show lower elastic modulus, yield strength at a given strain rate and higher impact strength and breaking strain values if compared with α -iPP. [57]

γ form

γ form was found by Addink and Beitema in 1961 as the most peculiar crystallographic modification with short chains. Density of iPP with γ form (γ -iPP) is equal to α -iPP (0.954 g/cm^3) and γ -iPP is as stable as the α -iPP is. [53, 57, 60] The main procedure of preparation of γ -iPP is crystallization under high pressure or by addition of small amount of comonomer (ethylene, 1-butene, 1-hexene). Through the same conditions α and γ form in iPP are simultaneously obtained. With increasing pressure their ratio is changed in favor of γ form. If the critical pressure (200 MPa) is exceeded, the γ form becomes to be predominant. Similarly as β form, this modification is unstable upon stretching. [53, 57]

The structure of γ form (Figure 13) is a triclinic lattice with parameters of unit cell: $a = 0.654 \text{ nm}$, $b = 2.14$, $c = 0.650$, $\alpha = 89^\circ$, $\beta = 99.6^\circ$ and $\gamma = 99^\circ$. This structure is unique in

the field of synthetic polymers since non-parallel polymer chains coexist in the same crystal lattice. [53, 60]

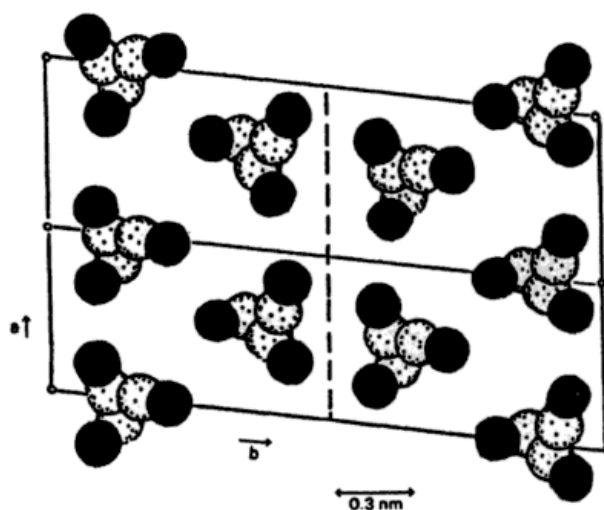


Figure 13 The crystal unit cell of the γ form on the ab plane [60]

Mesomorphic Form

The mesomorphic or smectic form was first mentioned in 1958 by Slichter and Mandell. This form of PP is non-crystalline, which is characterized by intermediate order between crystalline and amorphous phase. The smectic form has low density (0.88 g/cm^3) and is metastable since annealing at temperatures higher than $70 \text{ }^\circ\text{C}$ leads to the transformation into the α -iPP. [53, 57]

In the first studies this form was called paracrystalline, which came from its deformed or disordered lattice structure. The lack of lamellar order in addition to a low density and small size of ordered structures were recorded. Therefore this form has high clarity and is useful in quenched film applications. [53]

3 AIMS OF THE WORK

Several PP with different MFI were selected for the study. These materials were filled with various concentrations and types of WF. Prepared composites should show number of attractive properties, which can offer wide range of applications. A fundamental presumption for use of composites is a need to understand interrelations between processing, structure, and properties.

Thus, the main goal of the study is experimental determination of the interrelations between processing, structure and properties of composites based on PP and WF.

These factors are studied by various experimental devices and methods such as oscillatory rheometry, wide-angle X-ray scattering (WAXS), and DSC.

Subsequently, the main attention in this work is dedicated to following points:

- to prepare PP/WF composites with various concentrations of filler in PP with various MFI,
- to compare the properties of composites with different types of wood,
- to evaluate the influence of various concentrations of wood and various MFI on structural, thermal and processing properties of final composites and increase an amount of renewable carbon.

4 EXPERIMENTAL PART

4.1 Materials

Five various PP homopolymers were selected as a matrix in this study. The materials were provided by Borealis group – exact name is in Table 2. Weight average molecular weight (M_w), number average molecular weight (M_n), polydispersity index (PDI) and melt flow index (MFI) of used materials are summarized also in Table 2. The molecular characteristics were obtained from gel permeation chromatography equipped with a light-scattering detector. The MFI values were measured at temperature of 230 °C with load of 2.16 kg according to ISO 1133. [15]

Table 2 Characteristics of PP samples [15]

Material	M_w	M_n	PDI	MFI [g/10min]
HB205TF	830 000	300 000	2.8	1
HE125MO	490 000	130 000	3.8	12
HF136MO	410 000	170 000	2.5	20
HG455FB	360 000	150 000	2.4	27

The β -specific nucleating agent *N,N'*-dicyclohexylnaphthalene-2,6-dicarboxamide was provided by Rika Int., Manchester, Great Britain, under commercial name NJ Star NU 100. The nucleating agent (NA) concentration was set to 0.03 wt. % by dispersing of solution of the NA in paraffin oil. NA and 0.3 wt. % of paraffin oil was properly immixed into PP. The technique is described by Chvatalova et al. and Obadal et al. [15, 63, 64].

These PPs were filled with three different WF:

- Industrial French pine (*Pinus Sylvestris* - natural)
- Czech pine (*Pinus Sylvestris*) as an alternative to French pine
- Czech oak (*Quercus Robur*) as a representative of hardwood group.

French pine was already obtained as a powder with mean particle size of 0.25 mm. The other two materials were prepared from Czech local sources by milling. Obtained flour was

subsequently dried at 90 °C in vacuum for 24 hours and sieved. Particles size fractions smaller than 0.63 mm (mesh-size) were used as filler after additional drying.

To remove soluble accompanying substances a Soxhlet extraction was done with cyclohexane and ethanol as solvents. About 100 ml of the liquid was immersed into flask and heated. About 10 g of wood flour was inserted into the apparatus in which it was cyclically washed by the condensing solvent for 4 hours in case of cyclohexane and 7 hours in case of ethanol. Wet material was finally removed from the apparatus and let air-dried to evaporate excess solvent. Subsequently, vacuum drying at 80 °C for 1 hour was done. The goal of the solvent extraction process is to remove more or less polar molecules and to render the internal structure more accessible. PP is mainly a polar hydrophobic molecule and wood is a polar hydrophilic material, this results then incompatibility between both. It has been clearly done the choice, for formulation simplification and also for cost considerations, to not add a third component (compatibilizer) as up to now no specific compatibilizer is specially designed for specific lignocellulosic compatibilizer with organic olefinic molecules. All the published papers use maleic anhydride based compatibilizers classically used for PP glass fibers composites. The objective of this work, is to have a first evaluation of non compatibilized WPC or of improved interactions WF-PP (solvent extraction) composites properties.

4.2 Preparation of Composites

Composites were prepared by using Haake MiniLab Rheomex CTW5 twin screw extruder, which was filled by manually pre-mixed wood flour and polypropylene granulate. The extruder was heated to 180 °C and screw rotation was set to 80 rpm. After about 10 minutes of mixing, the machine was set to extrusion mode and molten composite was discharged.

It can be pointed out, that the mixing process is often hardly to proceed. It is known, that in any mixing processing equipment some filler can stay at the entrance (just down the hopper). The consequence is that it is very difficult to know with a high precision the exact final concentration. Moreover, in the case of natural fillers composites, it is not possible to perform thermogravimetric analysis as in the case of inorganic fillers to know the final

content of the filler after pyrolysis of the organic phase. Then in the following, the concentration of our composites is the initial content of WF.

Denotation of prepared composites follows this pattern: “PP” is the matrix and is followed by number in brackets indicating its MFI. This root is prefixed with “nu-” in case of β -nucleated material and followed with the filler denotation. The filler origin is then named “FrPine”, “CzPine”, and “CzOak” for French or Czech pine, and Czech oak, respectively. This denomination is prefixed by weight percent of the filler concentration and followed by suffix “-hex” or “-eth” for cyclohexane- or ethanol-extracted materials, respectively. A model is then:

$$nu-PP(27)-10CzOak-hex$$

which should be decoded as “nucleated PP of MFI = 27, which is filled with 10 wt.% of Czech oak, which was extracted with cyclohexane”.

4.3 Experimental Methods – Rheological Characterization

4.3.1 Backgrounds of Rheology

Rheology is a science discipline which studies deformation and flow of matter [65]. Rheology can study materials in the form of liquids or solids and describe their elasticity and viscosity. Rheology says: “Every material can flow, if the material has enough of time.”

Polymer melts exhibit viscoelastic behavior, which is described in real systems by mathematical models. The basic one is by Maxwell model (1), proposed by J.C. Maxwell in 1867, constitutes from spring and dashpot in series. [66]

$$\tau_{ij} + \lambda \dot{\tau}_{ij} = 2\eta D_{ij} \quad (1)$$

The spring and dashpot represent two extreme. Ideally elastic system, representing by spring, equals elastic modulus with ration of applied stress and created deformation. In case of simple liquids, their shear flow – internal stress by flow is defined by Newton’s law (2), which defines applied stress directly proportional to viscosity and the strain rate tensor [65, 67]:

$$\tau_{ij} = 2\eta D_{ij} \quad (2)$$

Dynamic Shear Flow

Fluid deformation under dynamic simple shear flow can be described considering the fluid within a small gap between two parallel plates. The upper plate is then usually taken as oscillating with defined frequency (ω) and small amplitude ($\dot{\gamma}_0$). Since the $\dot{\gamma}$ is not constant as in steady simple shear and varies as sinusoidal curve, one can write [67]:

$$\dot{\gamma}(t) = \dot{\gamma}_0 \cos \omega t \quad (3)$$

The shear stress in simple dynamic shear flow can be expressed by the amplitude and phase shift function of the frequency:

$$\tau_{21}(t) = \dot{\gamma}_0 [G'(\omega) \sin \omega t + G''(\omega) \cos \omega t] = \tau_{21}^0 \sin[\omega t + \delta] \quad (4)$$

In the equation, the δ is the phase angle, $\dot{\gamma}_0$ and τ_{21}^0 is amplitude of the strain and stress, respectively, G' and G'' are then linear viscoelastic material characteristics: dynamic storage modulus and dynamic loss modulus. The former is defined by relation:

$$G'(\omega) = \frac{\tau_{21}^0}{\dot{\gamma}_0} \cos \delta \quad (5)$$

the latter is given by:

$$G''(\omega) = \frac{\tau_{21}^0}{\dot{\gamma}_0} \sin \delta \quad (6)$$

The values of G' and G'' are obtained from measurements together with damping factor (loss tangent), which is defined as their ratio:

$$\tan \delta = \frac{G''(\omega)}{G'(\omega)} \quad (7)$$

A dynamic complex viscosity can be also defined in terms of G' and G'' :

$$\eta^*(i\omega) = \eta'(\omega) - i\eta''(\omega) \quad (8)$$

Dynamic viscosity is then given by ratio:

$$\eta'(\omega) = \frac{G'(\omega)}{\omega} \quad (9)$$

and the imaginary viscosity component is defined with:

$$\eta''(\omega) = \frac{G'(\omega)}{\omega} \quad (10)$$

The storage modulus (G') and the imaginary part of the complex viscosity (η'') are considered as the elastic parts of the complex functions. Their meaning is amount of energy storage. On the other hand, the loss modulus (G'') and the dynamic viscosity (η') are the viscous parts that define energy dissipation [67].

Cole-Cole Plot

The Cole-Cole plot, or spectrum, was extended to the linear viscoelastic mechanical properties of polymer blends by Havriliak and Negami [68, 69]. This plot is expressed by complex viscosity (η^*) in following form [69–71]:

$$\eta^*(\omega) = \frac{\eta_0}{1 + (i\omega\lambda_0)^{(1-h)}} \quad (11)$$

where λ_0 is characteristic relaxation time, h stands for dispersion parameter and η_0 represents a zero shear viscosity. The Cole-Cole plot provides direct information on the modality of relaxations as much as the relaxation spectrum does [68]. In the complex plane, this model predicts the variation of the viscosity components (η'' vs. η') and it is illustrated as an arc of circle. From this representation it is possible to determine the parameters η_0 , which is obtained through extrapolation of the arc on the real axis and the dispersion parameter h through the measurement of an angle ($h\pi/2$) given by the real axis and line going from the origin of the axis to the center of the circle, see Figure 14 for illustration.

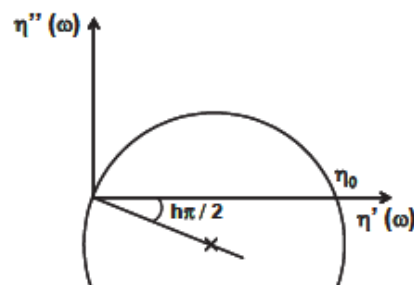


Figure 14 Cole-Cole plot

4.3.2 Rheological Measurements

A mechanical spectrometer Ares (TA Instruments) was employed for measurement of rheological properties. The parallel plate-plate geometry arrangement with the diameter of plates 8 mm was chosen. **For the determination of the linear viscoelasticity, dynamic strain sweep test was performed at first any materials under study (polymers and composites).** After that, frequency sweep test was measured and dependence of both elastic and viscous moduli and dumping factor on frequency were recorded. All measurements were performed at the temperature of 200 °C. Then it means that, all the viscoelastic experiments have been carried anytime in the linear viscoelastic domain.

4.4 Experimental Methods – Structural Characterization

4.4.1 Principles of Wide-Angle X-Ray Scattering

Wide-angle X-ray scattering (WAXS) is an X-ray diffraction technique, which is used to reveal the crystalline structure of materials. In case of bulk polymers, the powder diffraction is usually considered since the crystalline domains in the bulk are statistically oriented in all possible directions. According to Bragg's law, which defines the condition of maximum intensity of scattered radiation, one can recalculate obtained pattern to define crystal lattice dimensions. Bragg's law is usually written in form [72]:

$$n\lambda = 2d \cdot \sin \theta \quad (12)$$

where n is an integer number, d stands for the spacing between diffraction planes, λ is the wavelength of used radiation, and the θ represents the angle of incidence of the radiation. The situation is depicted in Figure 15.

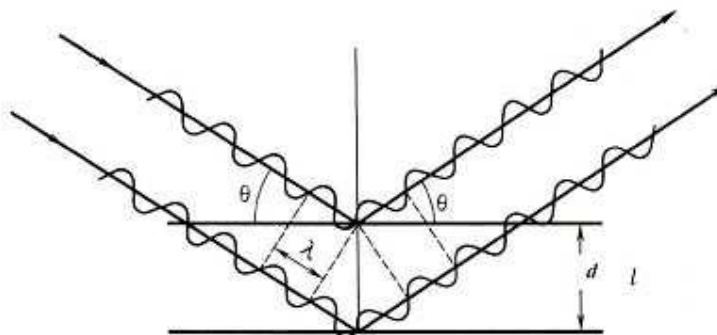


Figure 15 Schematic illustration of Bragg's law

The crystal lattice dimensions are not the only information, which can be obtained from the WAXS spectrum. As it was showed by Turner-Jones et al. [73] the crystallinity (X_c), i.e. the amount of crystalline phase, can be calculated from:

$$X_c = \frac{\sum A_c}{\sum A_c + \sum A_a} \quad (13)$$

where the sum of crystal reflections intensities, represented as an integral area under the curve (A_c), are divided by the sum of this integral intensity and intensity of amorphous halo (A_a). In case of iPP, the considered crystalline reflections are (100), (040) and (130), and in case of β -nucleated material the reflection of (300) plane.

Amount of the β crystallites can be established by another equation also published by Torner-Jones et al. [74], which determine the portion of β phase in the total crystalline phase amount, expressed as K_β :

$$K_\beta = \frac{A_{(300)}^\beta}{A_{(300)}^\beta + A_{(100)}^\alpha + A_{(040)}^\alpha + A_{(130)}^\alpha} \quad (14)$$

The $A_{(300)}^\beta$, $A_{(100)}^\alpha$, $A_{(040)}^\alpha$, $A_{(130)}^\alpha$ are intensities of (hkl) reflections indicated in the subscript, which were obtained by fitting the measured spectra with Pearson VII function. The intensity is in this case integral area of the fit.

The overall crystallinity can be then divided into the β crystals (X_β) and the α crystals (X_α) crystallinity according to:

$$X_\beta = K_\beta \cdot X_c \quad (15)$$

$$X_\alpha = X_c - X_\beta \quad (16)$$

From the fitted functions, the full width in half maximum (FWHM) can be directly recalculated according to Scherrer equation, which gives relation between the peak broadening and mean number of diffracting (hkl) planes. The equation is:

$$L_{(hkl)} = \frac{K \cdot \lambda}{FWHM \cdot \cos \theta} \quad (17)$$

where L_{hkl} is the crystalline domain length. Since the reflection broadening is strongly affected by crystal distortions, the L_{hkl} is rather information about the crystalline structure

perfection, than the information about the crystallite size. K stands for constant which depends on the crystal shape and which can vary typically from 0.8 to 1.2, but in case of polymers K is commonly assigned a value of unity. [72]

4.4.2 Measurement of Wide-Angle X-Ray Scattering

For the WAXS measurement, the prepared composites were compression molded at temperature 220 °C for 1 min and pressure of 10 MPa. In such conditions no preferential orientation of WF particles can be expected. PANalytical X'Pert PRO diffractometer was employed to obtain WAXS pattern in reflection mode. Ni-filtered $\text{CuK}\alpha$ radiation (0.1541874 nm) generated at 40 kV and 30 mA was used. Measurements were performed in the range of angles from 5 to 35 ° (2θ) and step size 0.0525 °, counting time 47 s per step. Each spectrum was decomposed by using a Gaussian peak with fixed maximum at 17° (amorphous halo) [72, 75, 76] and up to 6 individual peaks defined with Pearson VII function (reflections of the crystalline phase).

4.5 Experimental Methods – Thermal Behavior Characterization

4.5.1 Introduction to Differential Scanning Calorimetry

Differential scanning calorimetry (DSC) is an analytical technique which is used to measure difference in heat flow between sample and empty reference. Commonly, two main types are recognized: power-compensated system which consists of two separate cells, and heat flux DSC, in which both sample and reference are placed in one cell.

Two main effects could be observed in case of polymers in the DSC record. A step in the heat flow, or thermal capacity, is ascribed to glass transition temperature, while peak means latent heat of melting, crystallization or in extreme it can be also oxidation. The peaks can be then analyzed – maximum (sometimes onset) is considered as the transition temperature (melting temperature, T_m , or temperature of crystallization, T_c), the integral area of the peak is then evolved or consumed energy, i.e. enthalpy of the transition – heat of fusion (ΔH_m) or heat of crystallization (ΔH_c). A model curve is depicted in Figure 16, to illustrate all the thermal effects. [77]

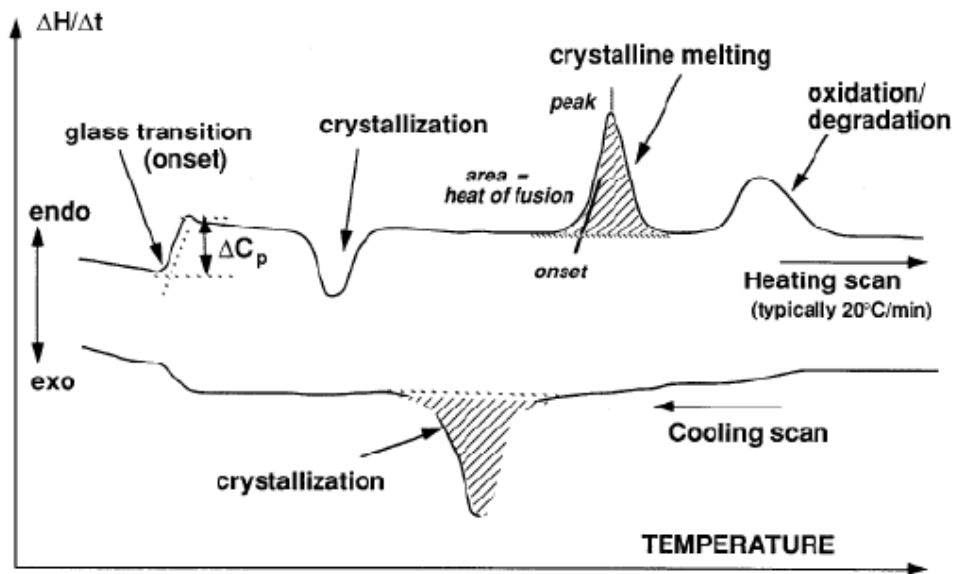


Figure 16 Illustration of the polymer DSC thermograms [77]

According to polymer nucleation theory [78], the peak position – i.e. value of T_m , one can calculate the apparent crystallite thickness (fold length, l_c) with Thomson-Gibbs equation:

$$T_m = T_m^0 \left(1 - \frac{2\sigma_e}{\Delta h_v \cdot l_c} \right) \quad (18)$$

where T_m^0 , Δh_v and σ_e are equilibrium melting temperature, volumetric heat of fusion and fold surface energy, respectively, which are usually found in literature.

Finally, the crystalline phase amount can be estimated by division of measured enthalpy with enthalpy of theoretical fully crystallized material:

$$x_c = \frac{\Delta H_m}{\Delta H_m^0} \cdot 100[\%] \quad (19)$$

Since the ΔH_m is usually related to the whole sample mass, in case of composites in which, the matrix concentration is equal to w , previous equation is modified to:

$$x_c = \frac{\Delta H_m}{w \cdot \Delta H_m^0} \cdot 100[\%] \quad (20)$$

4.5.2 Differential Scanning Calorimetry

Mettler Toledo DSC 1 calorimeter was used to measure thermal behavior of prepared composites. About 10 mg of each material was closed in an aluminum pan and measured with an empty pan as a reference. Each measurement was started with rapid heating (200 K/min) from 25 °C to 200 °C at which the sample was kept isothermally for 3 min to erase any possible thermal history. Subsequently, the sample was cooled down to 25 °C with rate of 10 K/min. At this temperature, the sample was hold isothermally 2 min and heated again with the same rate up to 200 °C.

Obtained records were evaluated by using software provided with the instrument. Crystallinity of the composites and lamellar thickness were subsequently calculated from the evaluation with constants found in [79–81], here summarized in Table 3.

Table 3 Constants used for calculation of lamellar thickness

<i>Name</i>	<i>Symbol</i>	<i>α crystallites</i>	<i>β crystallites</i>	<i>Unit</i>
Specific heat of fusion of fully crystallized iPP	ΔH_m^0	146	113	J/g
Equilibrium melting temperature	T_m^0	481	449	K
Volumetric enthalpy of fusion	Δh_v	1.96×10^8	1.77×10^8	J/m ³
Fold surface energy	σ_e	0.122	0.052	J/m ²

5 RESULTS AND DISCUSSION

5.1 Rheological Characterization

5.1.1 Effect of Melt Flow Index on Viscoelastic Behavior

Viscoelastic behavior of various PP matrices was examined. For uncrosslinked polymer melts with monomodal distribution, Cole-Cole plot gives an arc of circle. Its extrapolation to the real axis gives zero shear viscosity η_0 (the classical power law: $\eta_0 = K.M_w^a$ is exemplified on this figure with a power law index value $a = 3.5$) that is proportional to M_w . All the samples exhibit the same range of values for the distributions times relaxation parameter h ($0.38 < h < 0.46$). They are classified in the range of polydispersity indexes what is in good agreement with what is expected. Their rheological parameters are reported in Table 4. The variation of the Newtonian viscosity vs. the average weight molecular weight is reported in Figure 17.

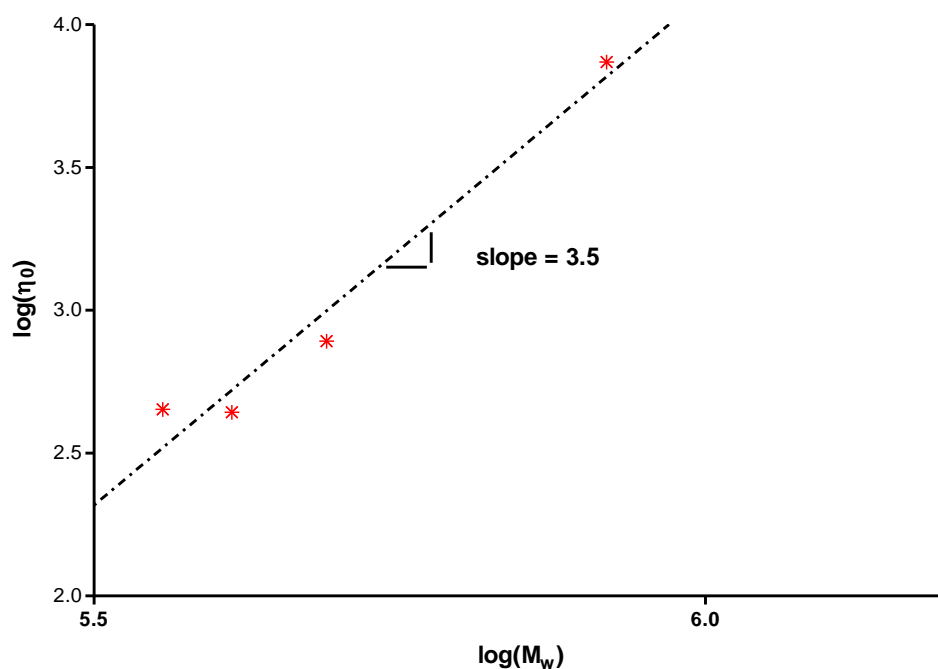


Figure 17 The variation of the Newtonian viscosity vs. the average molecular weight

Table 4 Rheological parameters for used polymer matrix

Reference	η_0 (Pa.s)	λ_0 (s)	h
PP(1)	7400	0.35	0.42
PP(12)	780	0.15	0.46
PP(20)	440	0.031	0.39
PP(27)	450	0.02	0.38
nu-PP(27)	214	0.01	0.39

The comparison of Cole-Cole plots for PP with various MFI is reported in Figure 18. The decrease of arc of circles confirms the fact that PP with increasing MFI material flows better.

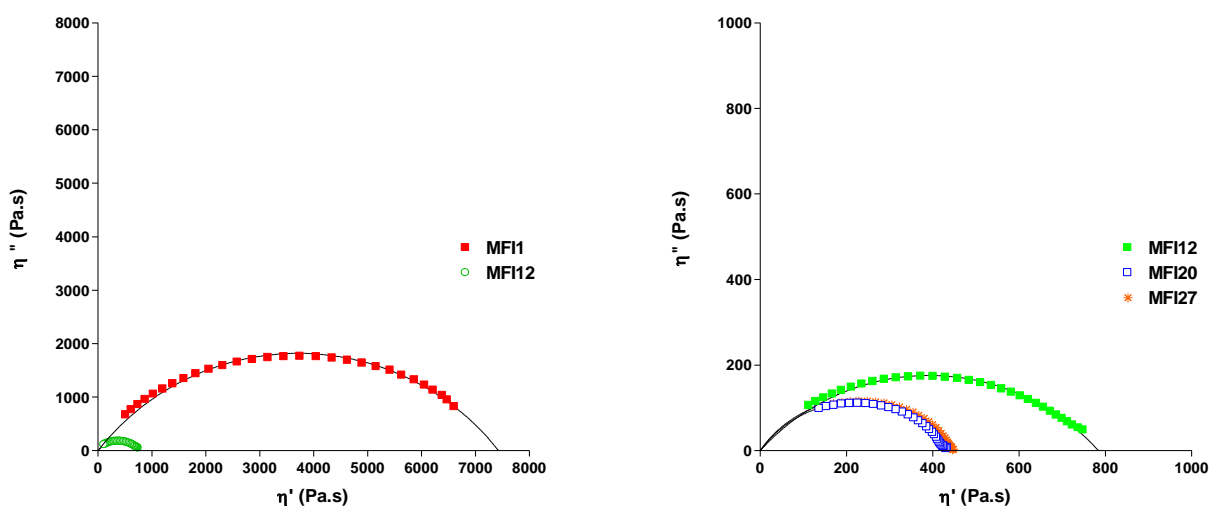


Figure 18 Illustration of Cole-Cole plots for PP(1, 12, 20, 27)

Viscoelasticity of composites with four various MFI and seven concentration of WF, in this case - French pine, are illustrated in following figures. The relation of η' and frequency was used to describe viscosity of composites. In Figures 19-22 viscosity decreases with the increase in frequency in all cases. The viscosity of the most filled PP is virtually the same regardless the MFI of the matrix. Concentration of WF does not influence the viscosity of composites with PP(1) considerably (Figure 19). The composites with lower concentrations exhibit lower values of η' than PP(1). However, the high concentration of

WF does not show higher viscosity than PP(1) as it could be expect. The viscosity of composites with 30 and 50 % is slightly higher than PP(1), nevertheless the decrease of viscosity in all the composites is noted in higher frequencies.

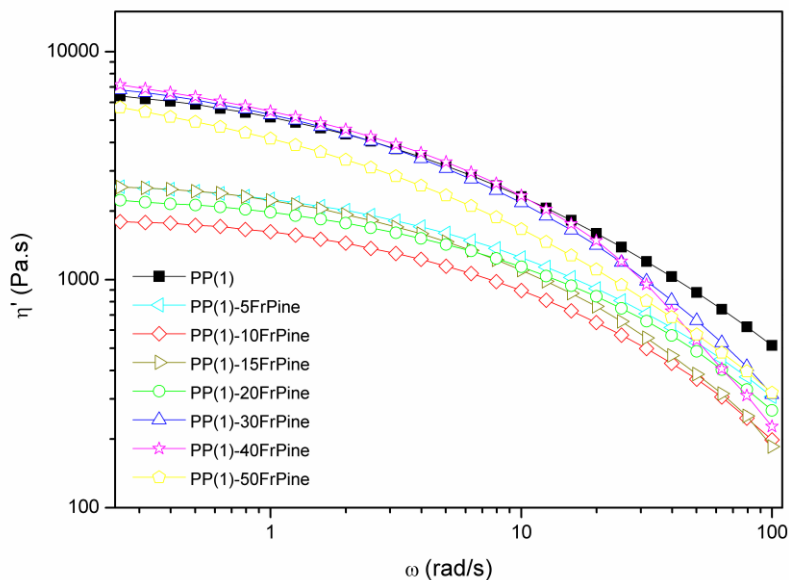


Figure 19 Dependence of viscous dissipation (η') on frequency in composites with PP(1)

The viscosity of composites is dramatically changed in the case of PP(12) (Figure 20). The composites with concentrations 10, 15 and 20 % exhibited lower viscosity in the region of lower frequencies. Except the composite with 10 % the viscosity of all composites is higher than PP(12) at frequencies higher than about 8 rad/s. The impact of polymer matrix is obvious.

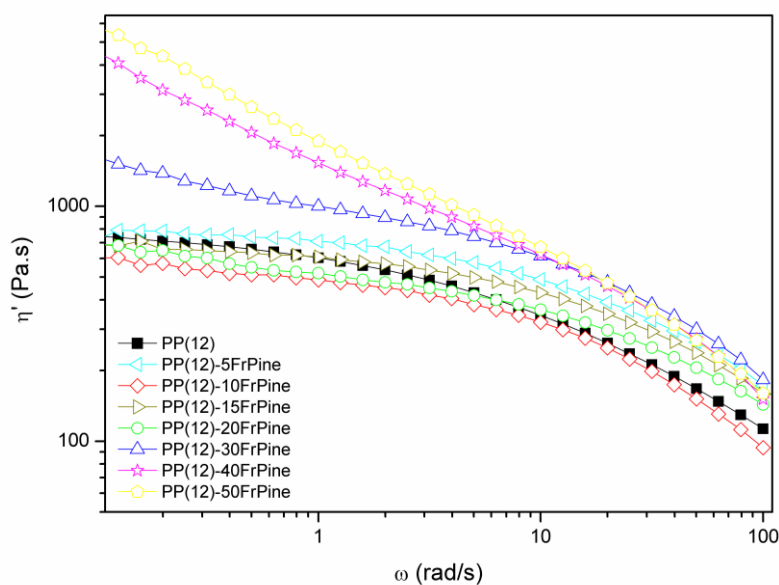


Figure 20 Dependence of viscous dissipation (η') on frequency in composites with PP(12). The composites with PP(20) are widely influenced by concentration of WF. The viscosity increases rapidly with concentration from 30 %. The composites with lower concentrations approximate to curve of PP(20). The effect of WF concentration is obvious in the Figure 21. The incorporation of higher content of WF to the polymer structure increases the viscosity. Although the viscosity of composites with PP(27) seems to be conformable to composites with PP(20), the composites with PP(27) and lower concentrations exhibit unlike extent of viscosity.

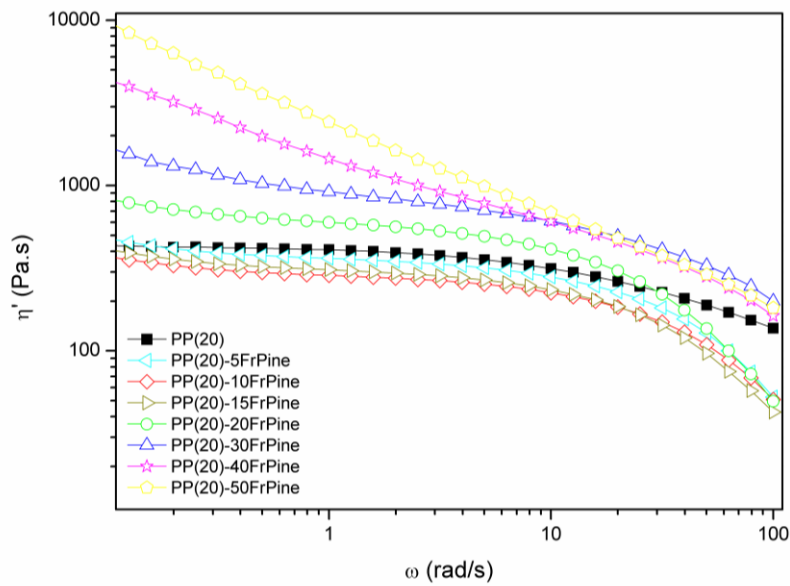


Figure 21 Dependence of viscous dissipation (η') on frequency in composites with PP(20)

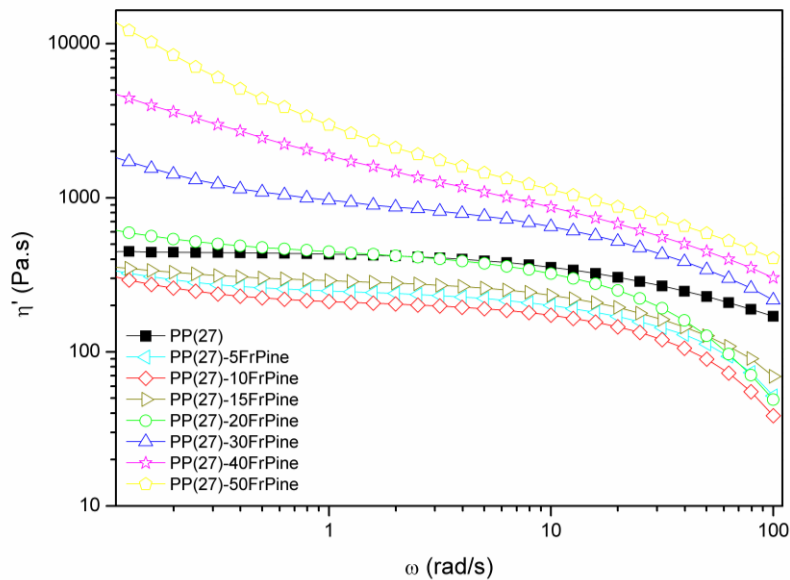


Figure 22 Dependence of viscous dissipation (η') on frequency in composites with PP(27)

The polymer matrix strongly influences the viscosity of composites as it is obvious from previous Figures (19–22). However, the viscosity of low-filled composites is permanently lower than the viscosity of PP. Nevertheless, the polymer with higher MFI can influence the flow of composites and thus the viscosity starts to increase and to be close to PP. In this case, the occurrence of curves of low-filled composites under PP could mean lower interaction between filler and matrix. However, it should be considered that filled systems have certain critical amount of filling. These low concentrations are not able to overcome the flow of polymer matrix and composites are more viscous than un-filled polymer matrix. Also it is important to note that no filler modification was carried out on samples and thus the lower filler-polymer interaction can cause decrease of viscosity in composites with lower concentrations.

The viscoelasticity of composites is presented by relation of η'' and frequency. The effect of MFI and concentration of WF is obvious in Figures 23-28, respectively. The composites with PP(1) show markedly different behavior than others melt flow indexes. The concentration of WF does not influence the evolution of η'' of PP(1) substantially (Figure 23). The values of η'' of composites with low concentrations is much lower than PP(1) and moreover the concentration 30–50 % feature approximately the same elastic viscosity as the PP(1). The values at frequency of 0.2 rad/s of η'' of PP(1) and composites are plotted in Figure 24. This plot shows that the elasticity at frequency of 0.2 rad/s is lower for composites with concentrations of 5–20 % and higher for composites with concentration of 30–50 %.

Elasticity of PP(1) and PP(12) increases in lower frequencies and decrease in higher frequencies, on the other hand PP(20) and PP(27) exhibit increasing trend of elasticity with higher frequencies. While composites with PP(1) show parallel trend to PP(1), composites with PP(12-27) exhibit opposite trend in lower frequencies. In addition, in Figure 28, it is clear to see that the elasticity is as high as high is the concentration of composites with PP(27). Here, the influence of polymer matrix on elasticity is evident.

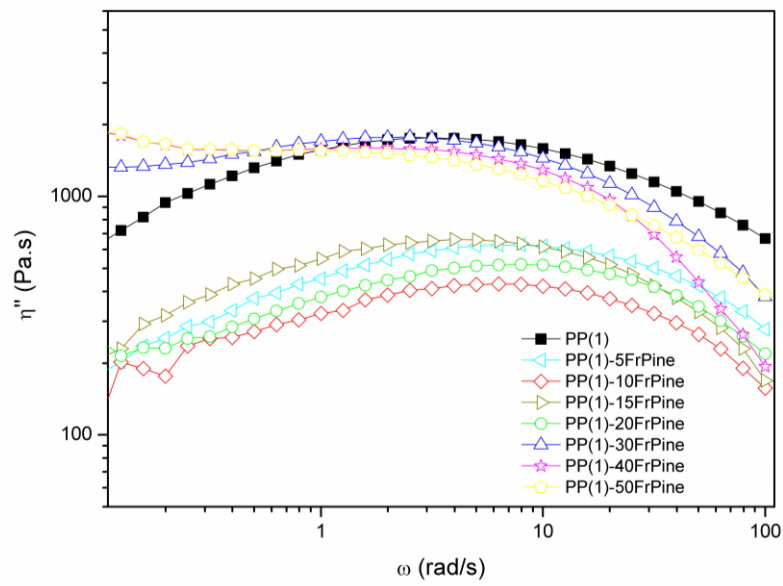


Figure 23 Dependence of η'' on frequency in composites with PP(1)

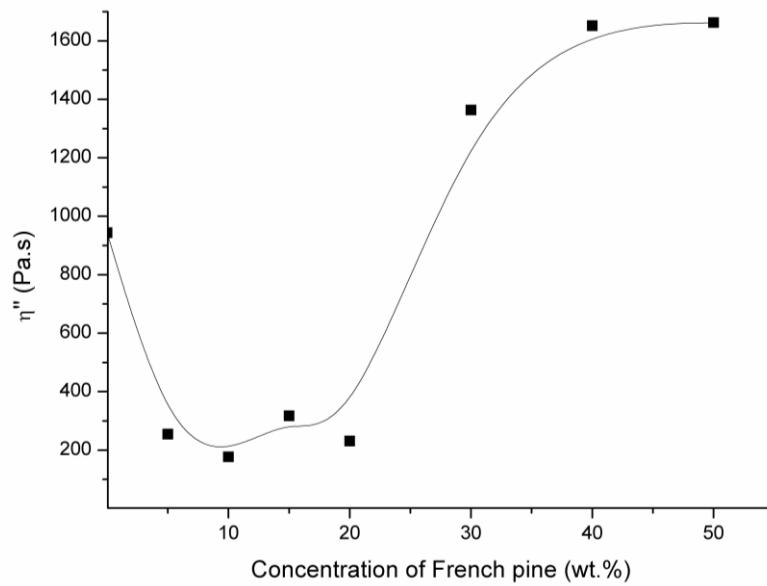


Figure 24 Ratio of η'' of PP(1) and composites in function of the amount of WF at $\omega=0.2$ rad/s

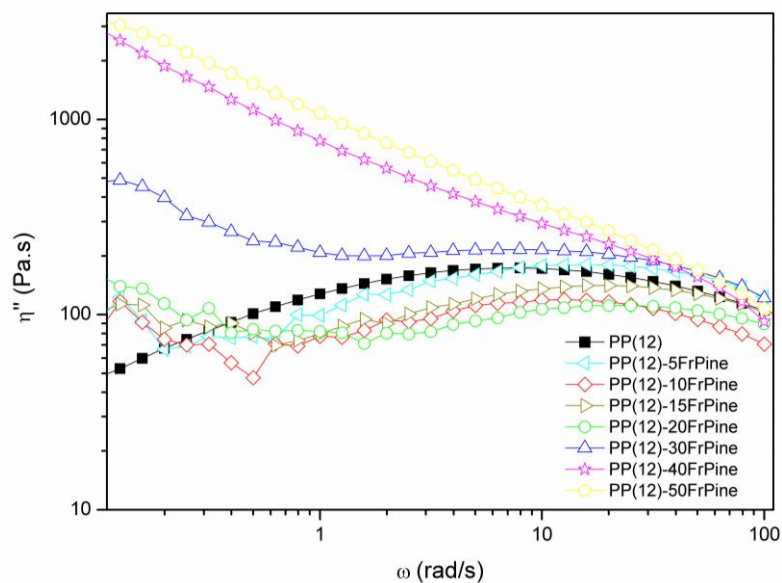


Figure 25 Dependence of η'' on frequency in composites with PP(12)

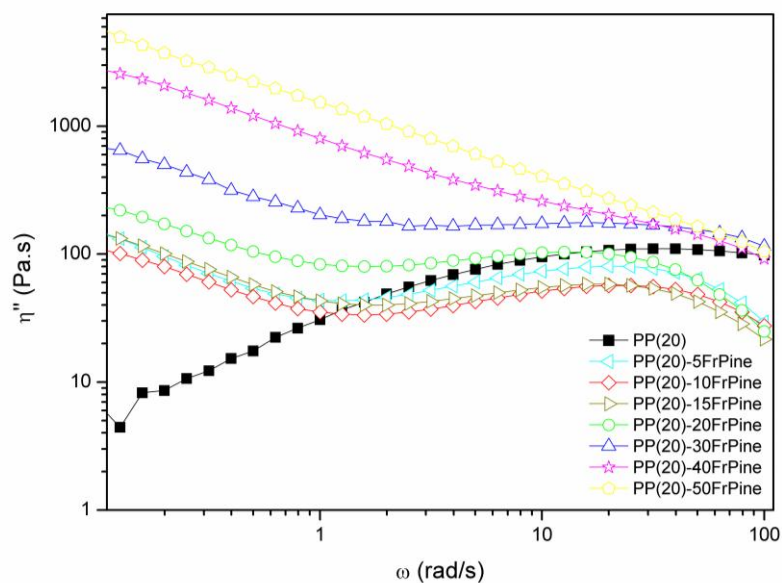


Figure 26 Dependence of η'' on frequency in composites with PP(20)

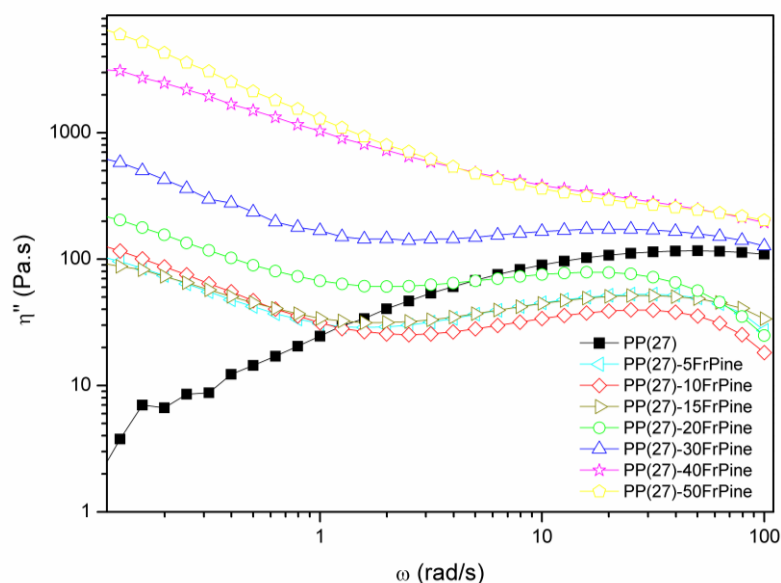


Figure 27 Dependence of η'' on frequency in composites with PP(27)

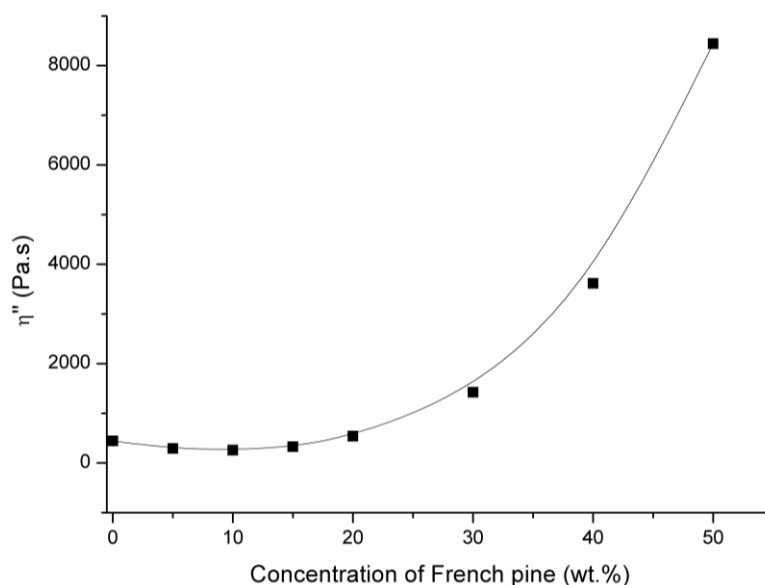


Figure 28 Ratio of η'' of PP(27) and composites in function of the amount of WF at $\omega=0.2$ rad/s

Further, complex viscosity of WF composites was examined in a Cole-Cole plot, which shows plot of the imaginary and real viscosity. The Cole-Cole plots of all the composites and PP are evaluated in Figures 29–32. It can be seen that for PP the curve is a semicircle while, for composites, the shape of curve changes with higher content of WF. It seems that with high WF content, the composite behaves more as a solid material. The change of the shape means that there is a higher interaction between the polymer matrix and the filler.

Nevertheless, curves of composites with PP(1) (Figure 29) show different behavior in comparison with composites with PP(12, 20, 27). The curves of composites with PP(1) with higher concentration of WF do not change the shape from semicircle except higher composites with high concentration. Composites with PP(1) exhibit a low interaction. This can be explained by the shape of the curves of composites, which copy the curve of the PP(1). In this case, the particles are more organized and create themselves the network, which means that the composites behave as gel and not solid. The change from viscous to gel behavior depends on MFI of PP. The composites start to show different evolution of Cole-Cole plots with higher MFI. In composites with PP(12, 20, 27) the double distribution occurs, it is given by higher restriction of molecules. However, the shape of the curves results from the summary of small arc of circle and a straight line. These results correspond to the strong interaction between the WF and PP.

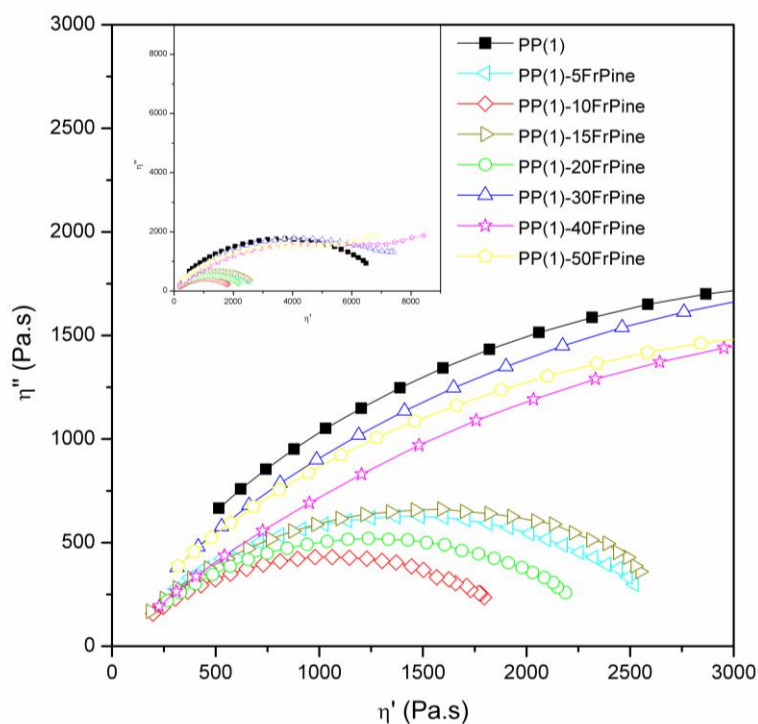


Figure 29 Cole-Cole plot of composites with PP(1)

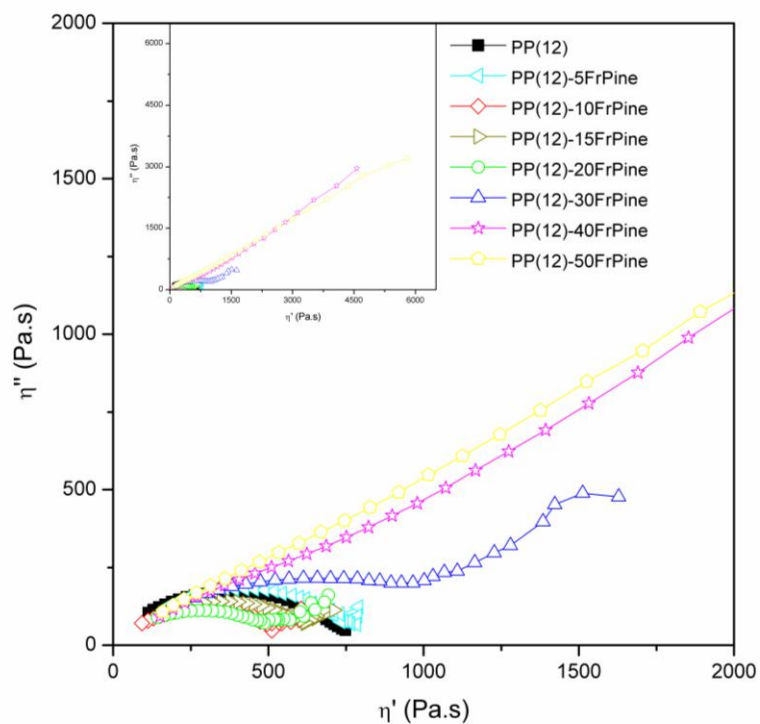


Figure 30 Cole-Cole plot of composites with PP(12)

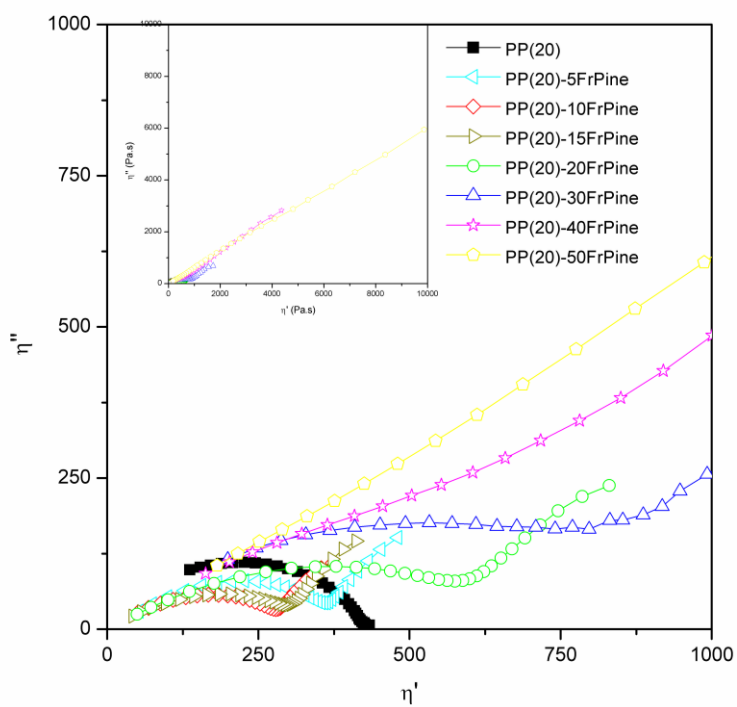


Figure 31 Cole-Cole plot of composites with PP(20)

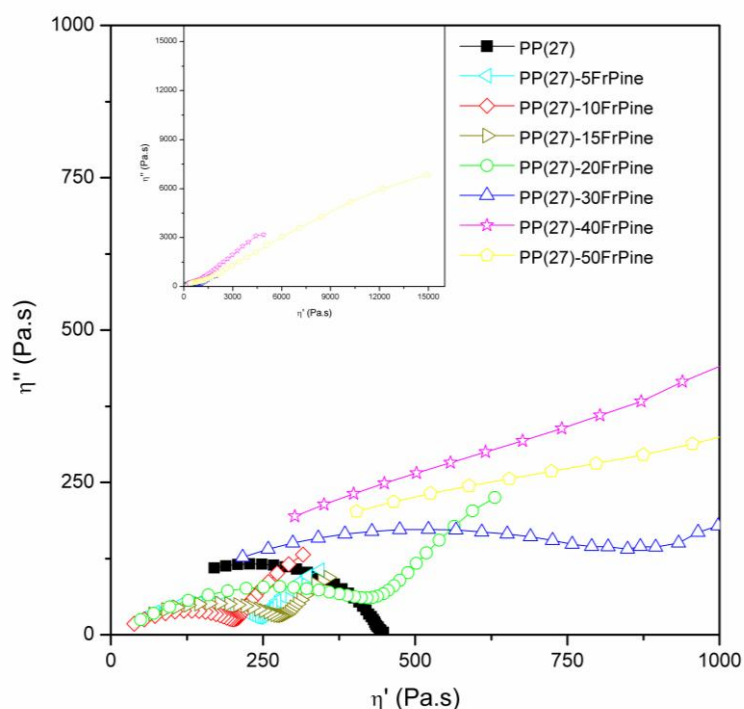


Figure 32 Cole-Cole plot of composites with PP(27)

The results say that PP(12) has a strong reinforcement effect in combination with WF. For $PP < PP(12)$, WF disturbs the chain friction movements and acts more as a lubricating agent, which confirm the decrease of viscosity. For $PP > PP(12)$ WF acts as a reinforcement agent, which promotes the chain interaction. This is described by increasing viscosity and low frequency elastic relaxation.

Finally, these results suggest that the molecular dynamic of polypropylene macromolecular chains is obviously strongly disturbed by the wood fillers depending on their initial macromolecular mobility. However, strong interactions (gel behavior) as well lubricating process (viscosity reduction) can be observed and more generally a mix of both phenomena can be exemplified.

5.1.2 Effect of Wood Flour Origin and Filler Size

Viscoelasticity of compounds from 3 various fillers and PP(27) is described by relationship of real (η') and imaginary part (η'') of complex viscosity (η^*) and frequency (Figures 33–34). In lower frequencies, the expecting order of curves is observed. The values of η' of composites decrease with increasing frequency. The curves of composites with low concentrations of WF occur under the curve of PP(27), while the curves of

composites with higher concentrations of WF appear above the curve of PP(27). There are recorded no differences in the type of the filler except in the size of filler particles. Size of French pine is 250 mm whereas Czech pine and oak have the size of 630 mm. It is known that orientation of larger fibers is worse than short fibers. The large particles are heavier to align in the direction of flow [82]. However, this fact is not confirmed by our findings. Composites with Czech pine exhibit similar behavior as French pine.

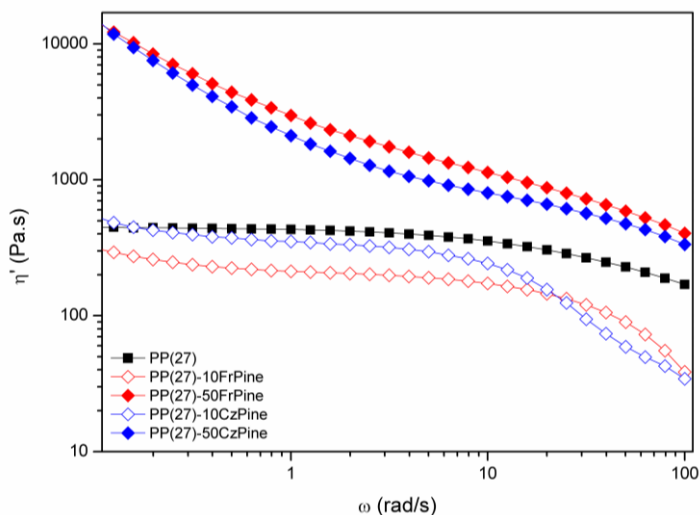


Figure 33 Dependence of viscous dissipation (η') on frequency in composites with pine and PP(27)

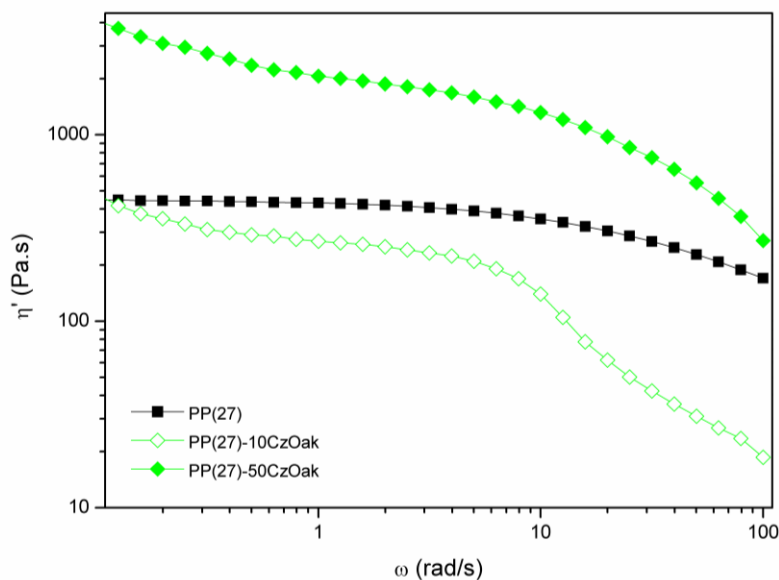


Figure 34 Dependence of viscous dissipation (η') on frequency in composites with oak and PP(27)

5.1.3 Effect of Polymer Matrix

The curve of nu-PP(27) copy the shape of the curve of PP(27) (Figure 35). The elasticity of PP(27) increases with increasing frequency and viscosity decreases with increasing frequency. However, the viscosity and similarly the elasticity of nu-PP(27) are lower than for nu-PP(27). This could be written multiple extrusion, which is additional process for granulation of nu-PP(27). Cole-Cole plots of both PP are illustrated in Figure 36. The arc of circle of nu-PP(27) is smaller than PP(27).

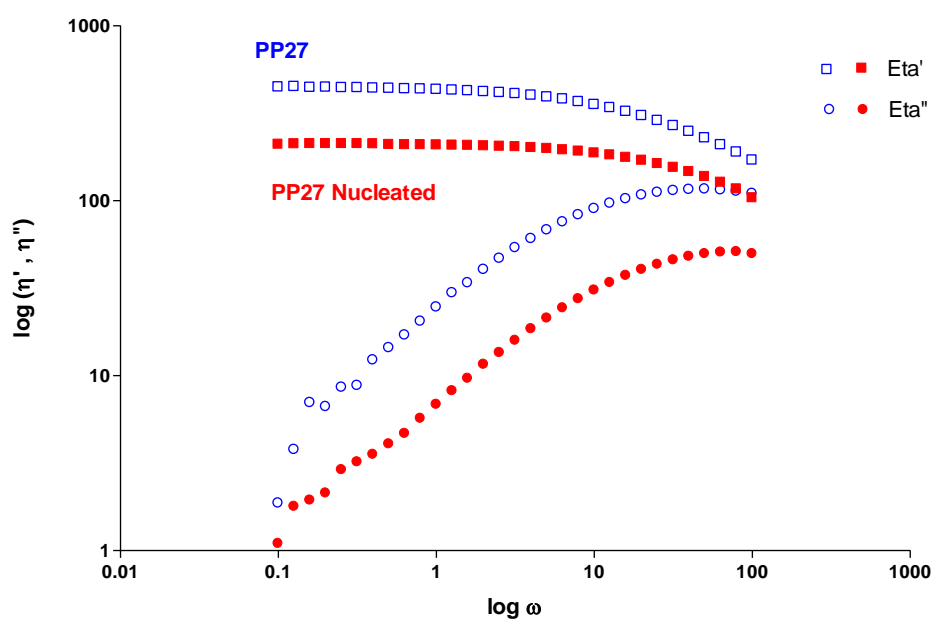


Figure 35 Viscosity of PP(27) and nu-PP(27)

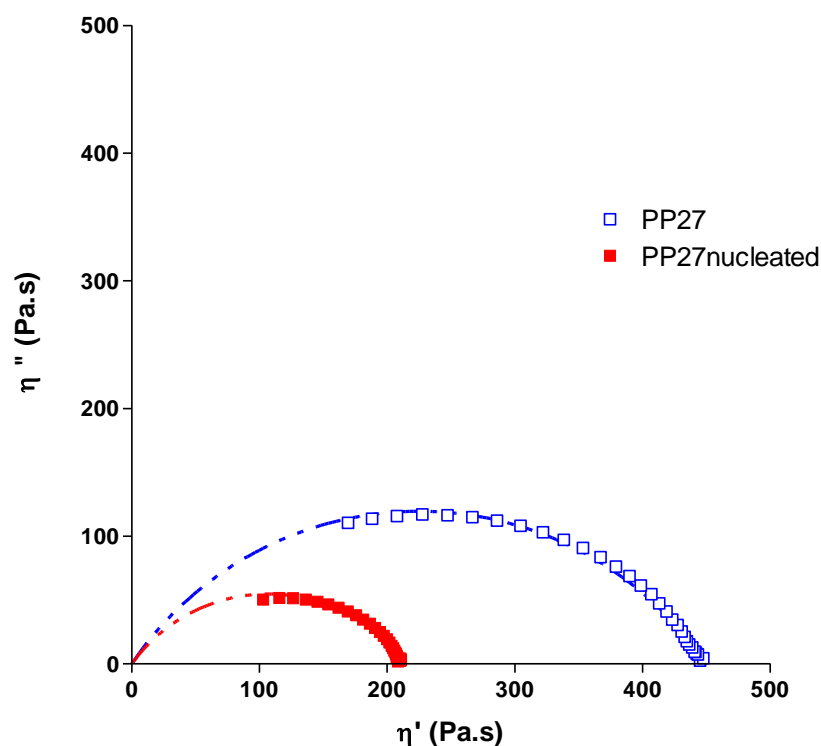


Figure 36 Comparison of Cole-Cole plots of PP(27) and nu-PP(27)

Some differences can be observed in composites with PP(27) (Figures 37) and nu-PP(27) (Figures 38) as a polymer matrix. The relation of η' and frequency is shown. It is obvious that values of η' of PP(27) are higher than for nu-PP(27). Composites with 10 % of WF and PP(27) occur under the curve of PP(27). This behavior was also observed in composites with nu-PP(27), but since lower frequencies. Composites with 50 % of WF show higher values than PP(27) and nu-PP(27). However, composites with pine and oak indicate similar behavior in both polymers.

In Figures 39 and 40, the elasticity of composites with PP(27) and nu-PP(27) is illustrated. In both types of PP, the curves of composites indicate different evolution of elasticity than PP(27) and nu-PP(27). The decrease of elasticity is noted in both cases of composites in comparison to non-filled PP. The elasticity of composites with 50 % of WF does not change considerably, therefore we can maintain, that the polymer matrix does not have any influence on composites with 50 % of WF.

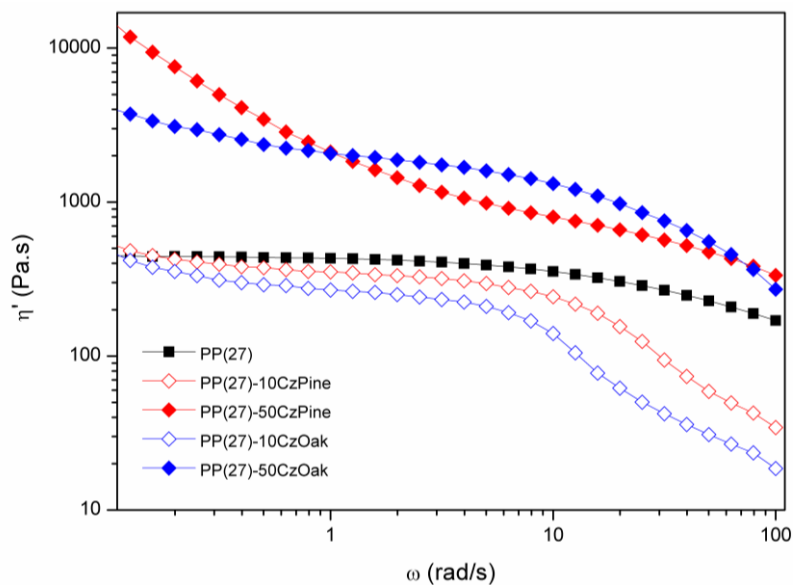


Figure 37 Dependence of viscous dissipation (η') on frequency in composites with pine and oak and PP(27)

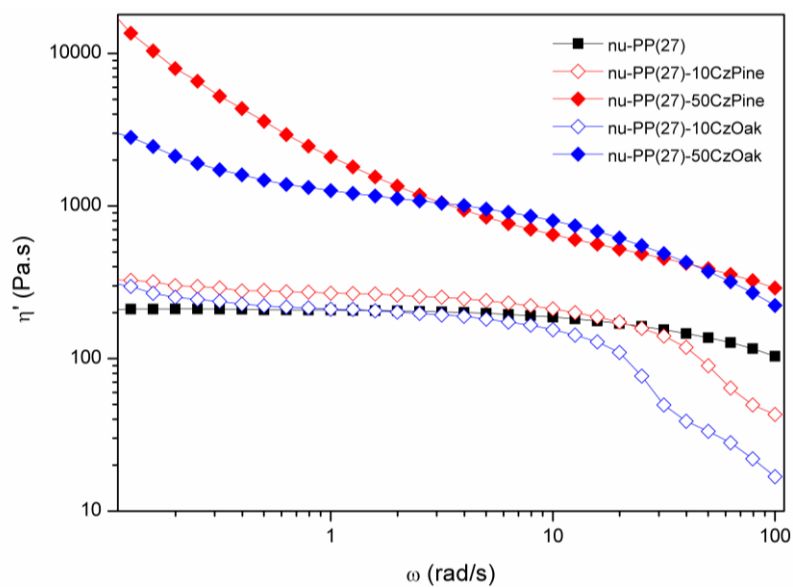


Figure 38 Dependence of viscous dissipation (η') on frequency in composites with pine and oak and nu-PP(27)

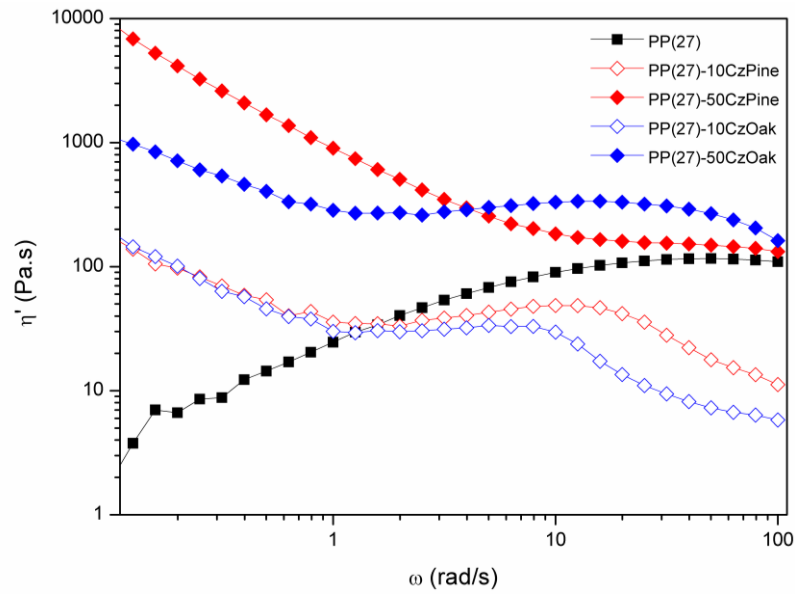


Figure 39 Dependence of η' on frequency in composites with pine and oak and PP(27)

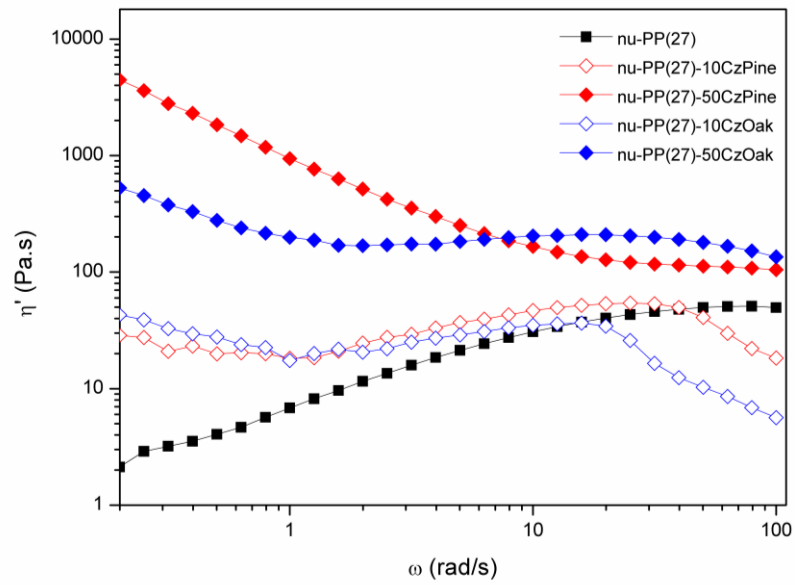


Figure 40 Dependence of η'' on frequency in composites with pine and oak and nu-PP(27)

In Figures 41 and 42, the Cole-Cole plots of composites with PP(27) and nu-PP(27) are displayed. It is obvious that the behavior of composites change dramatically with increasing concentration of the filler. Where the plot of PP(27) is almost a semicircle, the composites with 10 and 50 % signify a different shape of the curve. The arc of circle characterizes an un-crosslinked system and the straight line is typical for crosslinked materials. In composites a double distribution occurs, it is given by higher restriction of molecules. However the shape of the curves results from the summary of small arc of circle and a straight line. These results correspond to the strong interaction between the WF and PP.

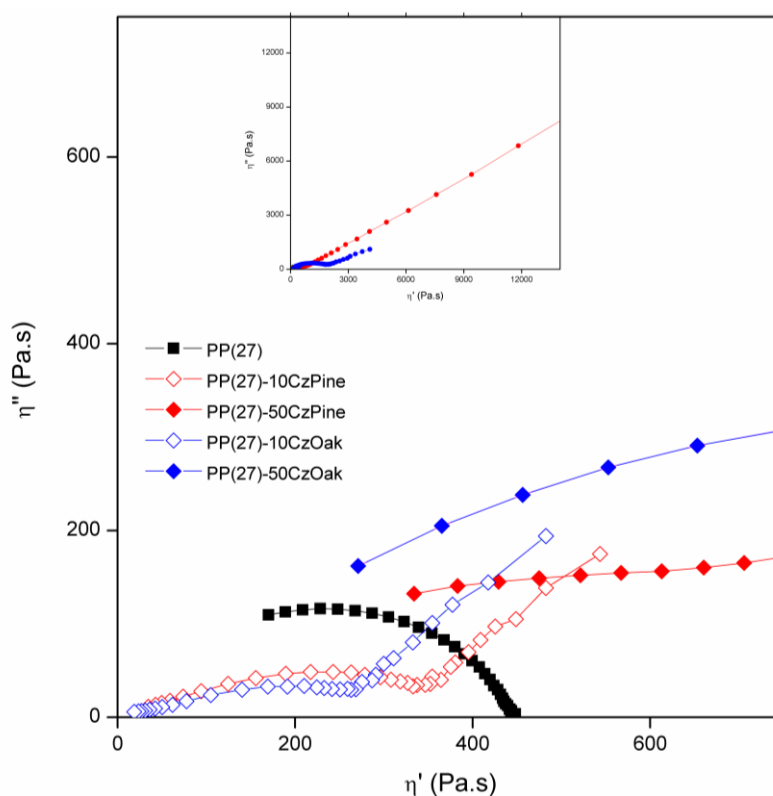


Figure 41 Cole-Cole plots with pine and oak and PP(27)

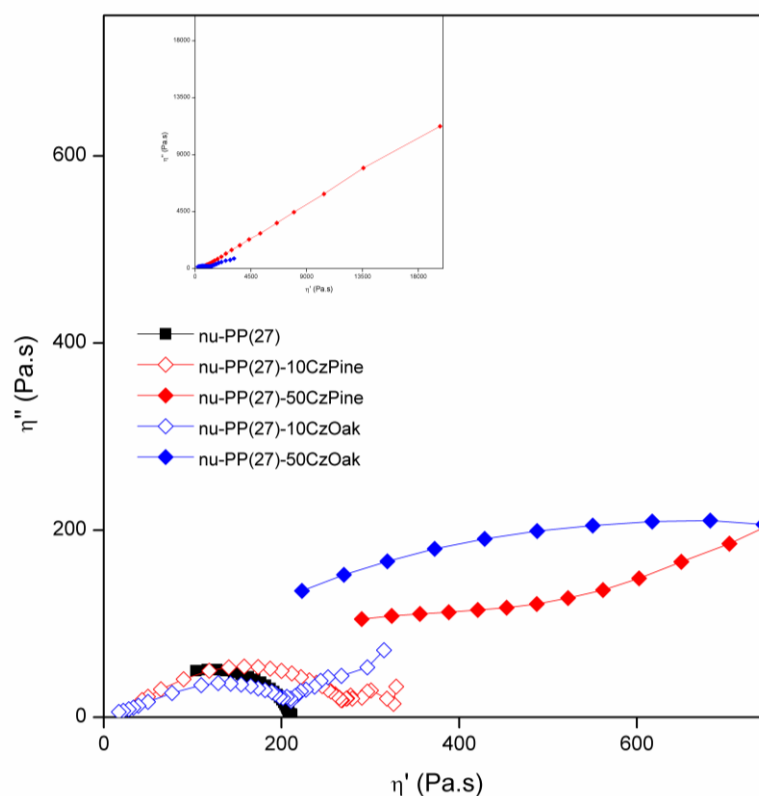


Figure 42 Cole-Cole plots with pine and oak and nu-PP(27)

5.1.4 Effect of Wood Flour Extraction

The influence of WF extraction on viscoelastic properties of composites, which consist of PP(27)/extracted WF and nu-PP(27)/extracted WF, is illustrated in Figures 43–50. Czech pine and oak were extracted in cyclohexane and ethanol.

The real component of the complex viscosity, eta prime (η') describes the viscous dissipation in the sample. In Figures 43 and 44 it is possible to observe that η' decreases with increasing frequency. The curve of PP(27) seems to be linear, however the η' starts to decrease with increasing frequencies. Similar behavior is presented in composites with 10 % of WF. According to knowledges in full-filled systems, the filled materials should exhibit higher values of η' than the neat material. Neverthelless, both types of WF with 10 % show lower values than PP(27). By contrast, the curves of composites with 50 % of WF appear above the curve of PP(27). In the case of wood with concentration 10 %, we can imagine that incorporation of the filler did not create so strong network or this behavior can be also explained by the flow of the matrix and this is so that 10 % of WF is small amount and the distrubution has not to be uniform, also such a few amount of WF can

accelerate the flow of PP(27) and this causes the lower values of η' in higher frequencies for lower concentrations of filler.

The eta double prime (η'') is an imaginary component of complex viscosity and represents the stored elastic energy. In Figures 45 and 46 it is shown, as the elasticity is changed in the relation to concentration and solvent extraction of WF. The curve of PP(27) behaves as an exponential function, whereas composites display some peaks with increasing frequency. We can observe as the filler concentration influence the elasticity of composites. Composites with 10 % of WF show substantially opposite trend than composites with 50 % of WF.

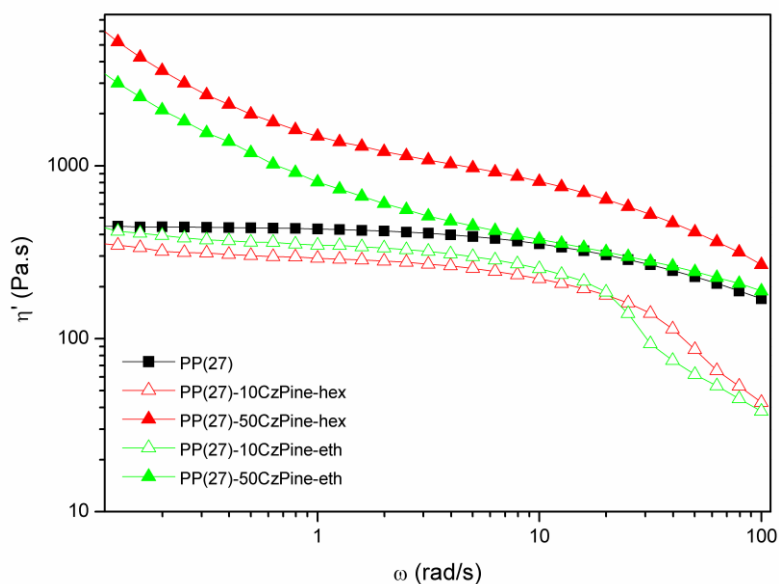


Figure 43 Dependence of viscous dissipation (η') on frequency in composites after various solvent extraction of pine with PP(27)

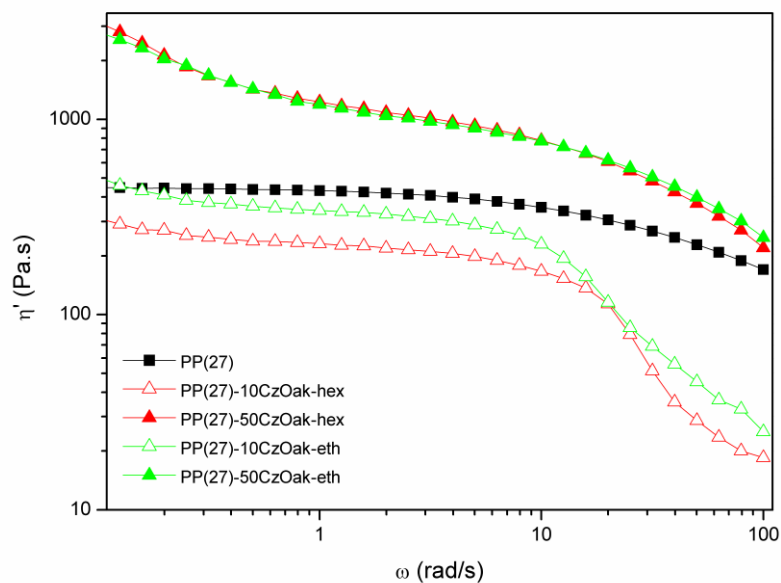


Figure 44 Dependence of viscous dissipation (η') on frequency in composites after various solvent extraction of oak with PP(27)

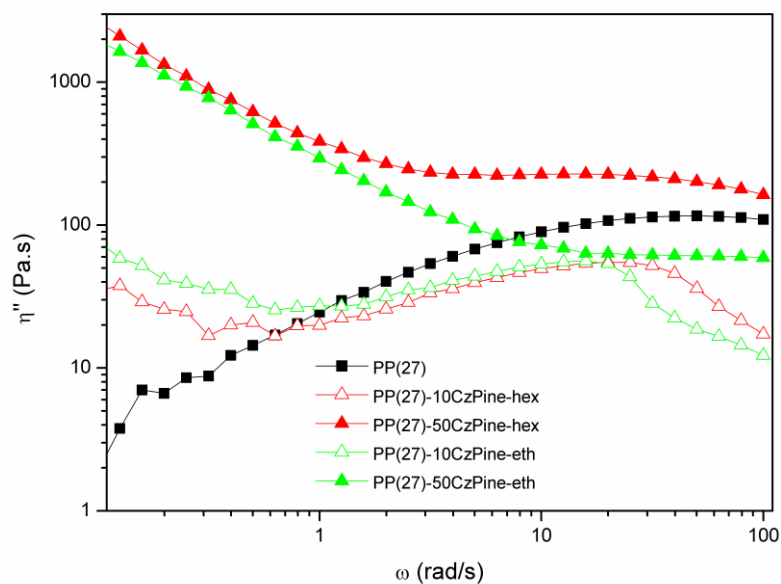
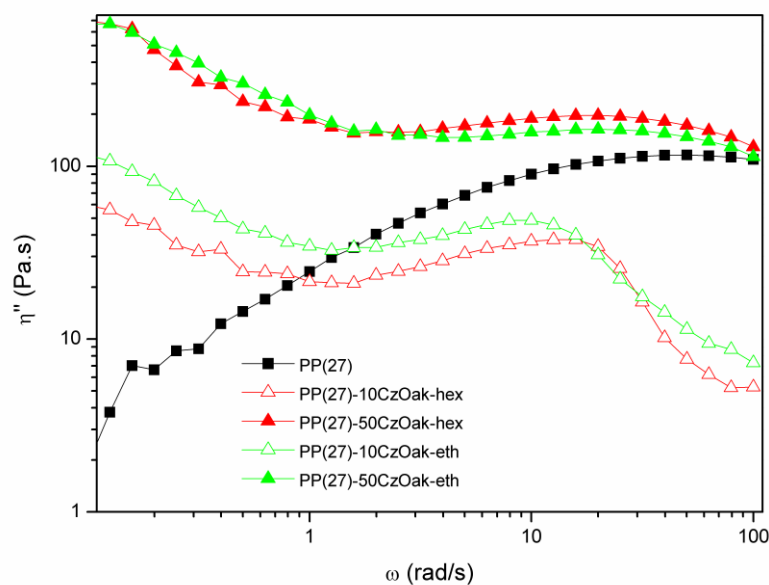


Figure 45 Dependence of η'' on frequency in composites after various solvent extraction of pine with PP(27)



*Figure 46 Dependence of η'' on frequency
in composites after various solvent extraction of oak with PP(27)*

In Figures 47 and 48, the plots of dependence of η' on frequency are illustrated composites with nu-(27) and its combination with two various concentrations of WF and extracted oak and pine, respectively. Eta prime increases with increasing WF content. This is valid for composites with pine. The curves almost copy the shape of nu-PP(27) and fluently decrease with increasing frequency. This expected behavior (Figure 47) can be written to the formation of stronger network of nuPP(27)-WF, which was achieved due to the solvent extraction in cyclohexane and ethanol and thus interaction between nu-PP(27). On the contrary, the composites with oak do not display this unique behavior (Figure 48). Although η' decreases slightly in the highest frequencies in composites with 10 % of oak, during almost whole measurement these composites show higher values of η' than nu-PP(27). In the case of oak 50 % extracted in cyclohexane the same trend as by pine was recorded.

If the composites with the extracted pine and oak are compared we could conclude that the solvent extraction has a big influence on the structure of pine and the compatibility of the composites with nu-PP(27) was the strongest, this can be seen in the Figure 47.

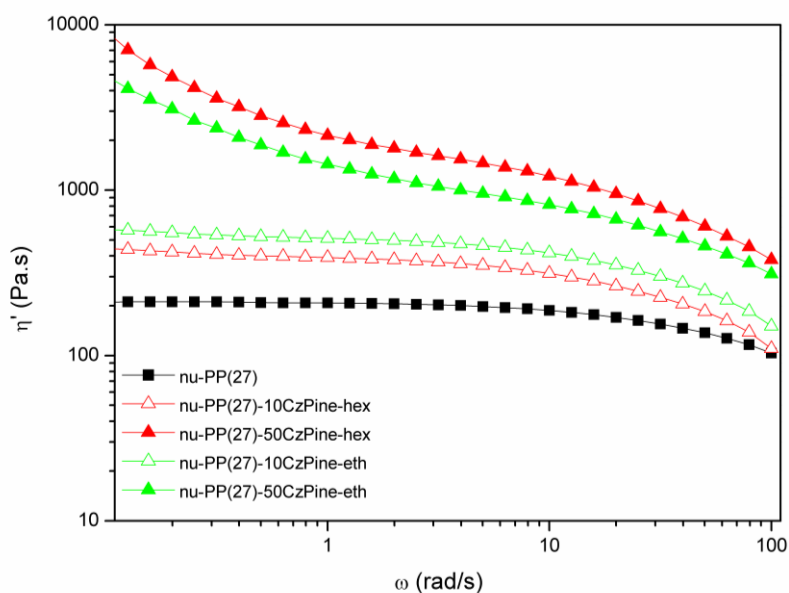


Figure 47 Dependence of viscous dissipation (η') on frequency in composites after various solvent extraction of pine with nu-PP(27)

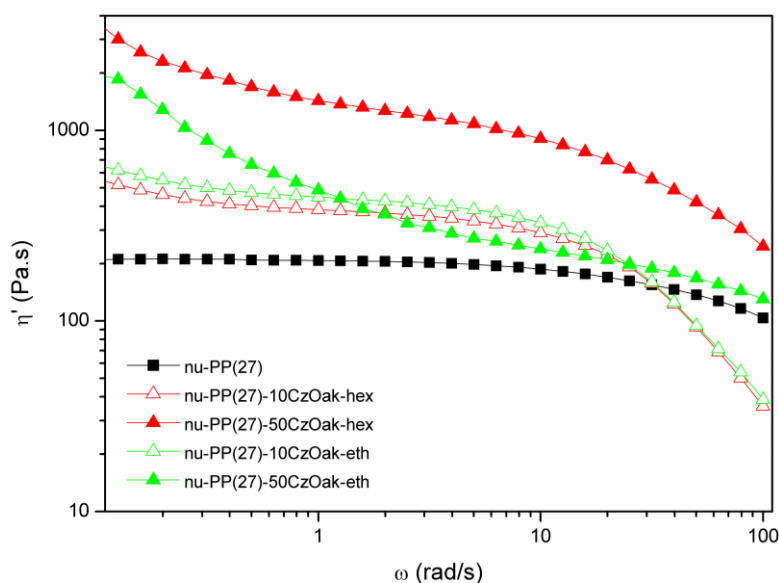


Figure 48 Dependence of viscous dissipation (η') on frequency in composites after various solvent extraction of oak with nu-PP(27)

The elasticity of composites with nu-PP(27) is shown in Figures 49 and 50. While the elasticity of nu-PP(27) increases with increasing frequency, the elasticity of the composites decreases with increasing frequency and start increase in higher frequency. Composites with 10 % of pine approximate to nu-PP(27) however, in lower frequency show higher

values of η'' . In composites with oak, the crossing of curves is noted. Higher elasticity is obvious only the case of oak with 50 % extracted in cyclohexane. The extraction of WF does not show any influence on composites with 10 % of WF.

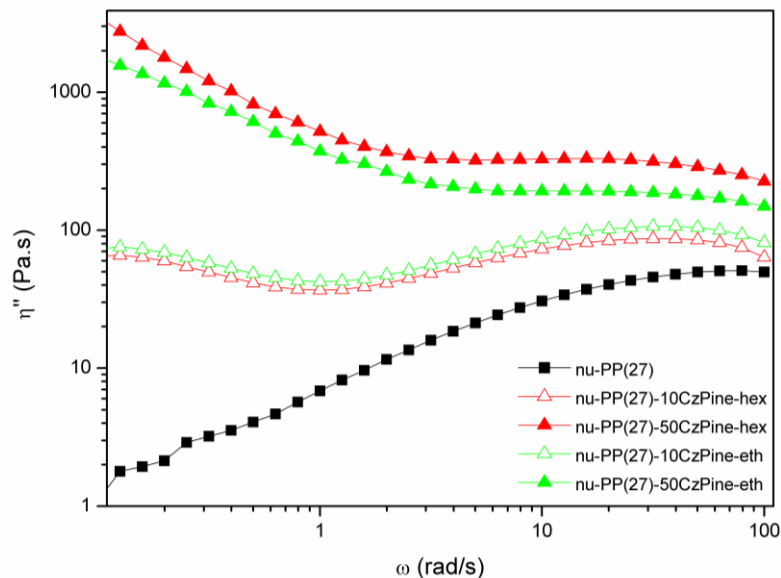


Figure 49 Dependence of η'' on frequency in composites after various solvent extraction of pine with nu-PP(27)

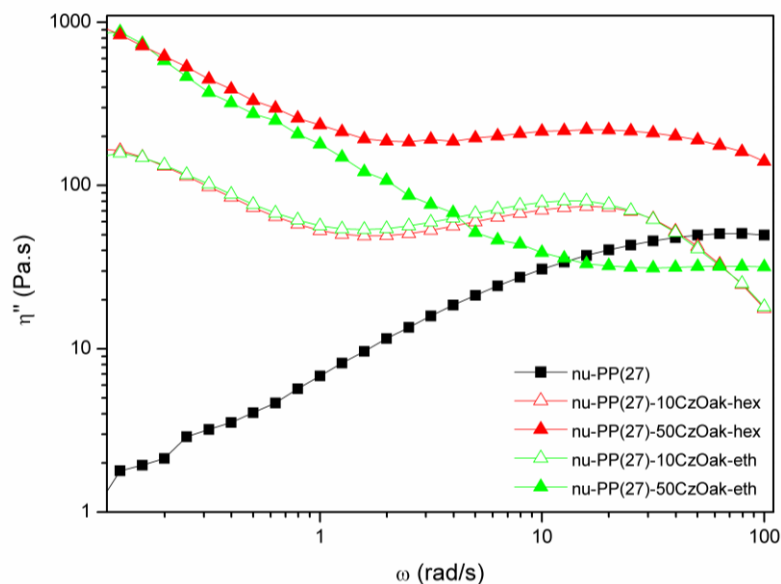


Figure 50 Dependence of η'' on frequency in composites after various solvent extraction of oak with nu-PP(27)

The evaluation of the influence of polymer matrix and solvent extraction of wood on Cole-Cole plots are illustrated in Figures 51–54. For PP(27), the Cole-Cole diagram is almost a semi-circle, while for composites with increasing WF content, the Cole-Cole diagram changes to an irregular shape (Figures 51–52). In composites, a double distribution occurs, it is given by higher restriction of molecules. The composites with 10 % of WF behave as viscous materials and exhibit a lubricating effect. However the shape of the curves results from the summary of small arc of circle and a straight line. The arc of circle characterizes an un-crosslinked system and the straight line is typical for crosslinked materials. These results correspond to the strong interactions between the extracted wood and polypropylene matrix. This fact is valid as for PP(27) as well as for nu-PP(27). In the case of nu-PP(27) (Figures 53–54), the curve of composites does not finish with a straight line but start to create a new circle. This can indicate stronger interactions between the filler and matrix.

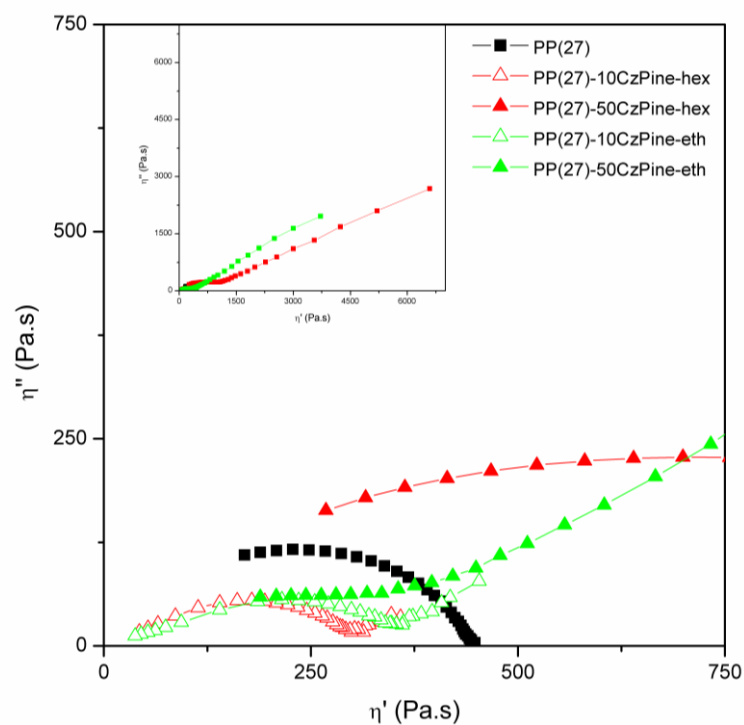


Figure 51 Cole-Cole plot for PP(27)/pine composites

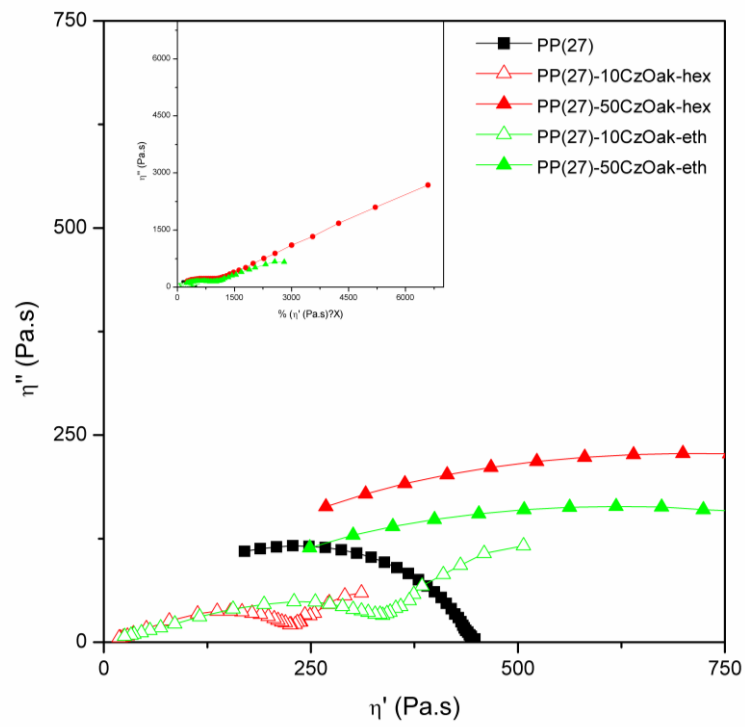


Figure 52 Cole-Cole plot for PP(27)/oak composites

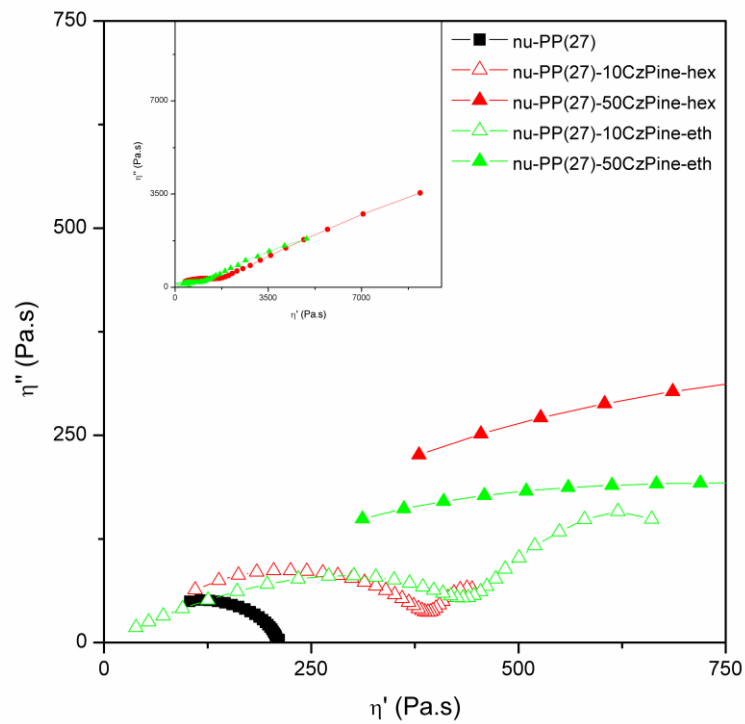


Figure 53 Cole-Cole plot for nu-PP(27)/pine composites

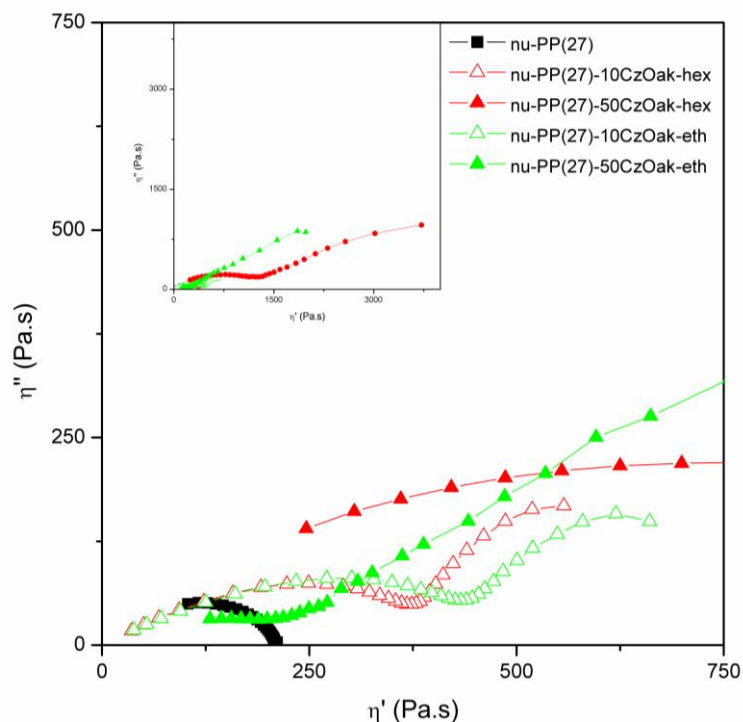


Figure 54 Cole-Cole plot for nu-PP(27)/oak composites

We can conclude that the solvent extraction process modifies greatly the interactions between the WF and the polymer matrix. From a general trend, ethanol which is a more polar molecule extracts quantitatively more compounds than cyclohexane. Then we can imagine that the more polar molecules have been extracted from the lignocellulosic structure and then the compatibility must be improved in the case of composites. This is obvious in the case of pine composites where the Cole-Cole representation exemplifies a gel tendency with these composites. It is less clear with oak and pine/nu-PP(27) composites. In any cases a vegetal oily liquids are obtained after solvent extraction. It is composed of a great variety of different chemical functional molecules (mainly phenolic compounds). Then it should be necessary to check the exact composition in any case to go further in the physical chemical interpretation of these phenomena what is out of the scope of this work. From this preliminary approach it is convenient to show that some chemical treatments onto the WF can change a lot the interfaces properties and then the viscoelastic behavior and probably the final properties of the natural filler composites.

5.2 Structural Characterization

Structure of neat and WF-filled PP was investigated with WAXS. Obtained spectra were decomposed with several peaks, which number was selected according to apparent reflection. Gaussian peak with fixed position at 17° was used to model amorphous halo [69, 70], while rest of the reflections were fitted with Pearson VII function:

$$I(2\theta) = I_{\max} \frac{w^{2m}}{\left[w^2 + (2^{1/m} - 1)(2\theta - 2\theta_0)^2 \right]^m} \quad (21)$$

where w means half width at half maximum, m is the shape factor and 2θ is the independent variable. I_{\max} and $2\theta_0$ are the peak coordinates.

In case of WPC, a problem of the 1D spectra decomposition is two overlapping phenomena – the first one is the PP amorphous halo, which was modeled as described above, the second one is signal of the filler. It was found from decomposition of spectrum of pure wood flour that the shape can be described with a sum of two peaks. A model situation is here presented in Figure 55.

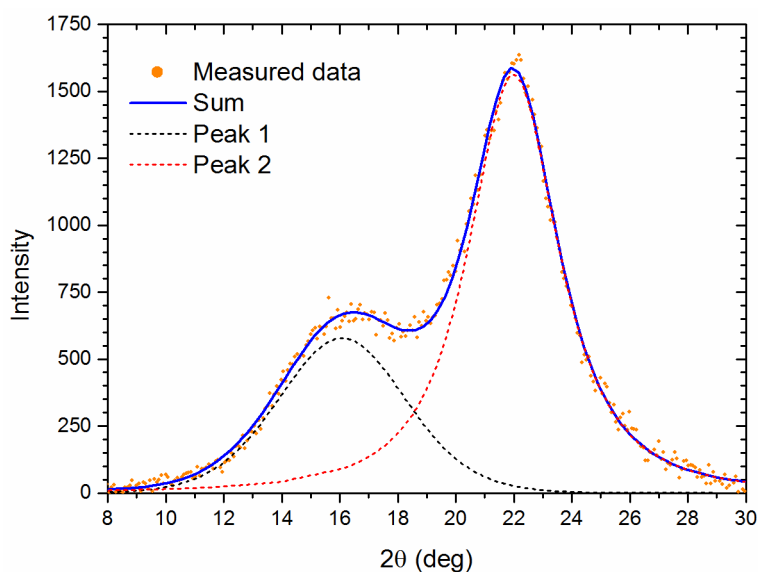


Figure 55 Decomposition of experimental data with two Pearson VII peaks

To check validity and possibility of generalization in the first approximation, both pine and oak WF were fitted in the same manner. In addition, a sawdust (mixture of unidentified woods) from our joiner's workshop was measured with WAXS instrument and the signal

was decomposed as well (see Figure 56). Peak parameters are summarized in Table 5 together with their differences.

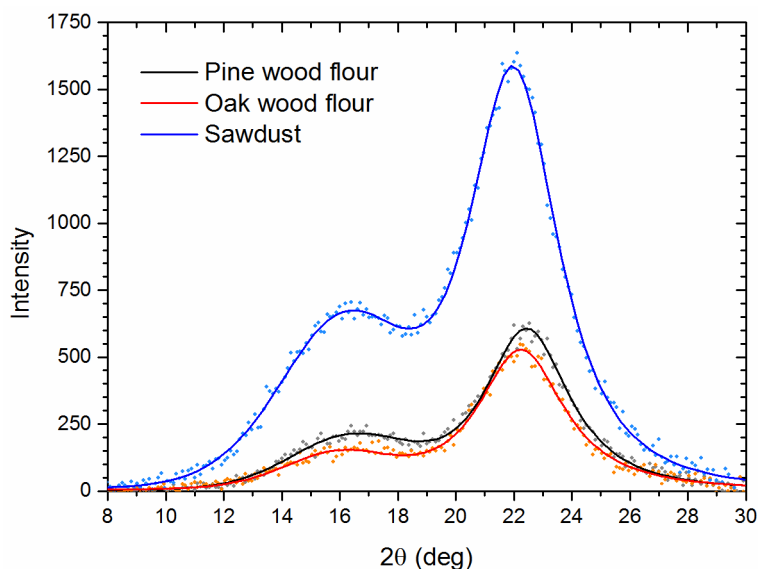


Figure 56 Decomposition of experimental data with two Pearson VII peaks

Table 5 Calculated peak parameters and their mutual difference

	<i>Pine WF</i>			<i>Oak WF</i>			<i>Sawdust</i>		
	<i>Peak 1</i>	<i>Peak 2</i>	<i>Diff.</i>	<i>Peak 1</i>	<i>Peak 2</i>	<i>Diff.</i>	<i>Peak 1</i>	<i>Peak 2</i>	<i>Diff.</i>
$2\theta_0$	16.30	22.45	+6.15	16.02	22.27	+6.25	16.06	21.98	+5.92
I_{max}	186.71	602.8	×3.23	142.22	501.13	×3.52	569.00	1580.90	×2.80
w	4.89	3.45	×0.71	4.92	3.43	×0.70	5.13	3.70	×0.72
m	5.12	1.25	×0.24	1.04	1.60	×1.54	14.05	1.30	×0.09

From comparison of the differences, one can find their apparent proximity, except the shape factor values. Eventhough it could be rough approximation, the wood signal can be then modelled with a sum of two Pearson VII functions in this form:

$$\begin{aligned}
 I(2\theta) = I_{max} \cdot \frac{w^{2m}}{\left[w^2 + (2^{1/m} - 1)(2\theta - 2\theta_0)^2 \right]^m} + \\
 + (3.18 \cdot I_{max}) \cdot \frac{(0.71 \cdot w)^{2M}}{\left[(0.71 \cdot w)^2 + (2^{1/M} - 1)(2\theta - (2\theta_0 + 6.11))^2 \right]^M}
 \end{aligned}
 \tag{22}$$

where the constants of the second peak (second addend) are substituted by the constants valid for the first peak (first addend) with differences, which come from average of calculated differences between first and second peak (see Table 5). Since the shape factor value significantly vary, the parameter of the second peak (M in eq. 22) was left so the fitting program was able to optimize it. Position ($2\theta_0$) then can be set equal to 16.12° , which is again average position of first peak, or optimization may be enabled in terms of $16.12 \pm 0.2^\circ$ in the process of data fitting, which takes into account possible error caused during WAXS measurement. The former option was applied in this study.

Spectra decomposition was done with nonlinear curve fitting program Fityk [83], which is freely available under GNU licence. A typical decomposition is depicted in Figure 57.

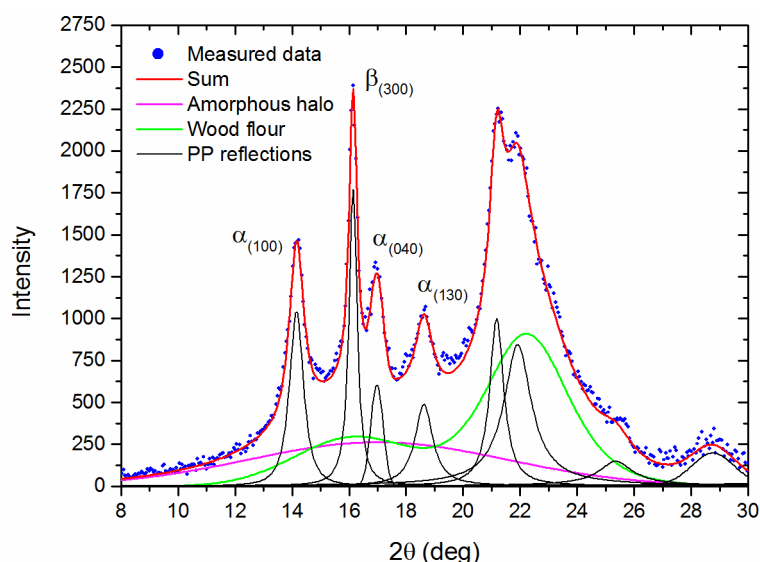


Figure 57 Example of WF/PP spectrum decomposition (nu-PP(27)-50CzOak-eth)

Obtained data (Figure 58 and 59) were analyzed to calculate peak areas and widths at half maximum ($\text{FWHM} = 2w$). From these values one can easily calculate morphological characteristic, which are summarized in Table 6 and graphically presented in Figure 60. As expected, the β -nucleated materials exhibited reflection at 16.2° , which is related to (300) crystallographic plane, while the non-nucleated materials did not. This implies, the wood is not nucleating trigonal morphology ascribed to β crystallites. Moreover, in high concentrations (materials: nu-PP(27)-50FrPine, nu-PP(27)-50CzPine, nu-PP(27)-50CzOak) WF is inhibiting the nucleating agent in that extend so spectrum decomposition in case of nu-PP(27)-50CzPine was done with total omission of peak at (300) position, hence the K_β is zero. In the other cases, the (300) reflection was incorporated by the Fityk algorithm to

the fit of experimental data, but still the (300) peak was weak enough to achieve very low K_{β} , considering nucleating agent presence, which imply high K_{β} values. Two main phenomena may occurred – the nucleating agent is adsorbed on the wood surface, where it is disabled for nucleation, or some of the wood low-molecular accompanying substances may be dissolved in the matrix, during melt mixing. The dissolved substances then could react with the nucleating agent and disable it.

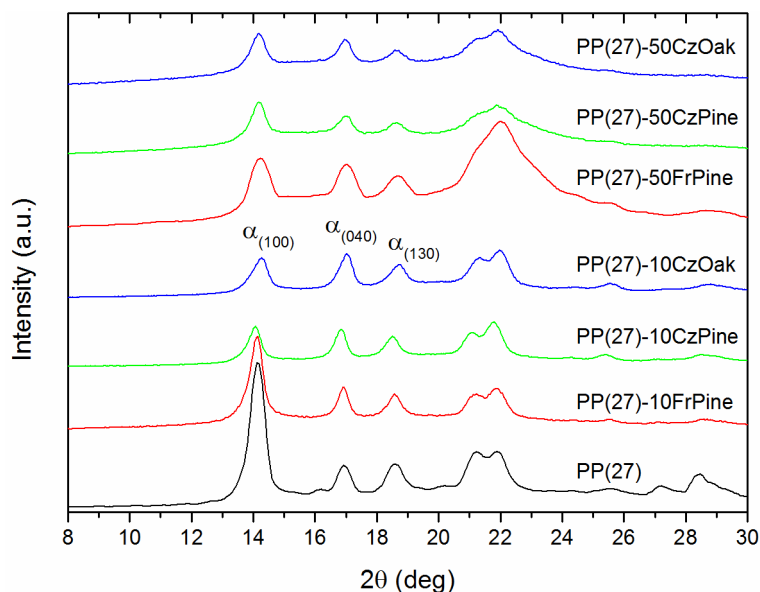


Figure 58 X-ray diffraction patterns of composites with PP(27)

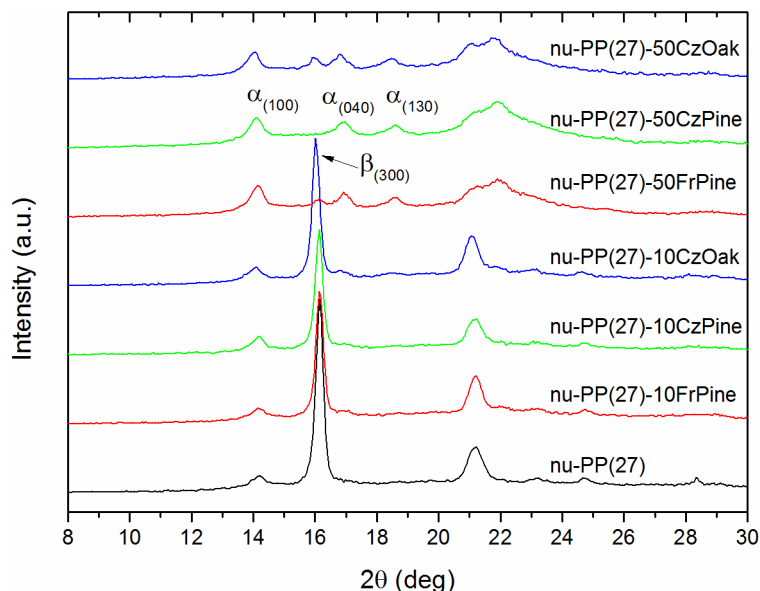


Figure 59 X-ray diffraction patterns of composites with nu-PP(27)

Table 6 Calculated characteristic of PP and composites with unextracted woods

	K_{β}	X_c	$L_{(100)}$	$L_{(040)}$	$L_{(130)}$	$L_{(300)}$
	[-]	[%]	[nm]	[nm]	[nm]	[nm]
PP(27)	—	52.85	18.37	20.92	14.08	—
PP(27)-10FrPine	—	49.56	17.30	21.36	16.02	—
PP(27)-10CzPine	—	69.46	16.67	19.45	15.56	—
PP(27)-10CzOak	—	83.34	13.07	16.19	10.35	—
PP(27)-50FrPine	—	50.26	16.31	20.82	13.80	—
PP(27)-50CzPine	—	29.65	15.31	17.08	13.11	—
PP(27)-50CzOak	—	27.77	14.92	17.76	13.98	—
nu-PP(27)	0.897	60.48	15.74	—	—	30.87
nu-PP(27)-10FrPine	0.848	63.27	16.87	21.68	—	31.28
nu-PP(27)-10CzPine	0.868	68.38	16.20	16.39	4.85	31.20
nu-PP(27)-10CzOak	0.836	59.76	14.78	17.97	9.78	31.50
nu-PP(27)-50FrPine	0.071	58.06	16.30	19.83	13.43	25.45
nu-PP(27)-50CzPine	—	32.39	15.71	16.98	13.67	—
nu-PP(27)-50CzOak	0.108	52.50	16.51	17.66	11.48	26.89

When overall crystallinity (X_c) is compared, in case of non-nucleated material, WF original to Czech location may have some nucleating ability in low concentration of the filler, while high concentration reduce crystalline content. It is worth to mention, the French pine WF had practically no influence on the final crystalline phase amount. French pine behaved similarly in nucleated matrix, where both low and high concentration of Czech oak also made no evident change in overall crystallinity of the matrix. On the other hand, the Czech pine rose the value in case of 10 wt. % filling, and decrease the crystalline amount when the matrix is filled with 50 wt. %. Concerning this fact together with literature [84, 85], which ascribes to cellulose some α -nucleating ability, it is possible to assume, the natural wood may contain some accompanying substances, which disturb β -phase crystallization – particularly in case of Czech pine and high filler content. Extraction then may eliminate this phenomenon, which will be discussed below.

Regarding lengths of crystalline domains, $L_{(hkl)}$, calculated according to Scherrer equation, which should be related to crystall perfection, values for the non-nucleated materials are

ambiguous. Comparing pure matrix (PP(27)) data with composites of low filling, the PP(27)-10CzOak shows the lowest dimensions of „perfect“ crystalline domain, on the other hand, when filler content is raised to 50 wt. % (PP(27)-50CzOak) the values are higher. This may imply the crystalline domains are bigger and/or less distorted. Logically, one would expect at least preserving or deterioration, regarding the material with 10 wt. %. Similar ambiguity is seen also in case of β -nucleated materials, in which the low filling is virtually improving the crystal perfection, while high filler content is decreasing β phase content, yet preserving the α -crystallites perfection. Unfortunately, only the $L_{(100)}$ could be compared.

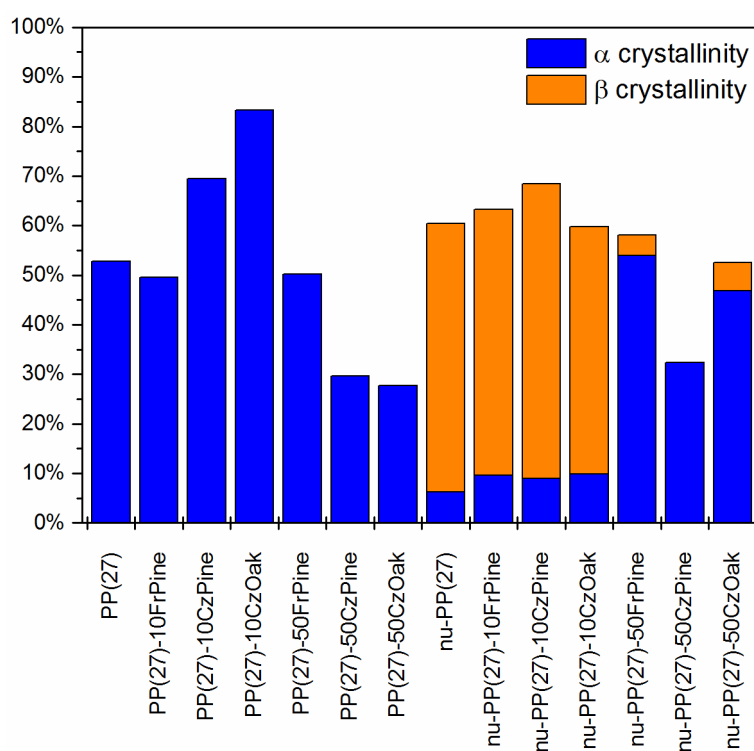


Figure 60 Crystalline phase amount and composition in studied composites

To check the possible effect of low-molecular wood accompanying substances on matrix crystallization and morphology, fillers were extracted with ethanol and cyclohexane to remove extractables prior to composite mixing. The measured WAXS spectra are here presented as Figure 61 and 62. Obtained patterns were again decomposed to assess the crystalline structure – calculated data are summarized in Table 7 for the non-nucleated PP, with graphical comparison in Figure 63, and Table 8 for the β -nucleated matrix and graphically in Figure 64.

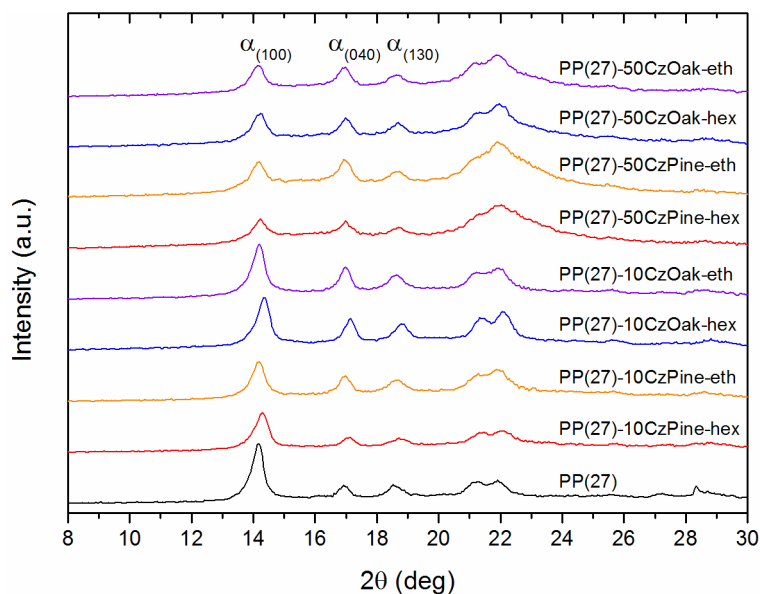


Figure 61 X-ray diffraction patterns of extracted wood flour composites with PP(27)

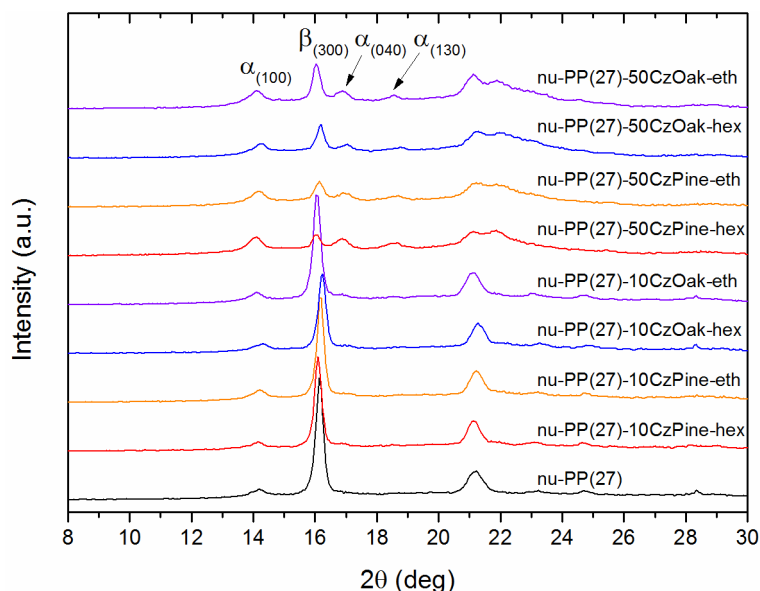


Figure 62 X-ray diffraction patterns of extracted wood flour composites with nu-PP(27)

Regarding crystallinities of non-nucleated composites with low filling, all the X_c values are higher than the value of PP(27) indicating slight nucleating activity of extracted WF. In comparison with non-extracted materials (see Table 7) the crystalline phase content is lower, particularly in case of oak WF. On the other hand, filling of 50 wt. % in both cases – the original and extracted WF composites caused decrease in crystalline phase content, yet the drop is less intensive for the extracted WF and particularly in case of ethanol-extracted materials. Even though the effects of wood particles presence are ambiguous in case of low filling, it is possible to assume, the low-molecular accompanying substances in

the filler may disturb crystallization. This assumption could be supported by the fact that after the extraction the crystalline phase content increased. From this point of view, extraction with ethanol was more efficient than the cyclohexane – the very same statement could be pronounced also in case of nucleated matrix as discussed below.

Phase composition of WF and β -nucleated composites is more complex, as it is illustrated in Figure 64 and summarized in Table 8. In case of low filled materials, the overall crystallinity is higher for cyclohexane-extracted WF, while the values of ethanol-extracted materials are close to the crystallinity of unfilled nu-PP(27). Regarding the β phase content, the presence of pine WF decreases K_β – only 53 % or 66 % of the crystals are trigonal in comparison to 90% content of unfilled PP. On the other hand, oak WF made practically no change of the K_β value. Further decrease of the β phase content is seen when matrix holds 50 % of WF, yet the drop of overall crystallinity is not seen in case of pine WF and the value in case of oak-filled composites is comparable with composite with ethanol-extracted oak WF. Unfortunately, the missing drop in X_c value of pine WF may not be ascribed to increased α -nucleation, since no similar phenomenon can be found in non-nucleated PP (c.f. Table 6)

Table 7 Calculated characteristic of PP and composites with extracted woods

	X_c	$L_{(100)}$	$L_{(040)}$	$L_{(130)}$
	[%]	[nm]	[nm]	[nm]
PP(27)	52.85	18.37	20.92	14.08
PP(27)-10CzPine-hex	58.43	15.96	18.65	12.00
PP(27)-10CzPine-eth	63.76	16.57	18.80	11.01
PP(27)-10CzOak-hex	42.31	17.02	20.54	15.21
PP(27)-10CzOak-eth	53.82	17.11	20.88	13.31
PP(27)-50CzPine-hex	31.53	14.38	20.18	10.57
PP(27)-50CzPine-eth	34.68	14.95	18.36	11.14
PP(27)-50CzOak-hex	40.49	15.99	19.39	14.07
PP(27)-50CzOak-eth	48.71	16.19	17.99	12.12

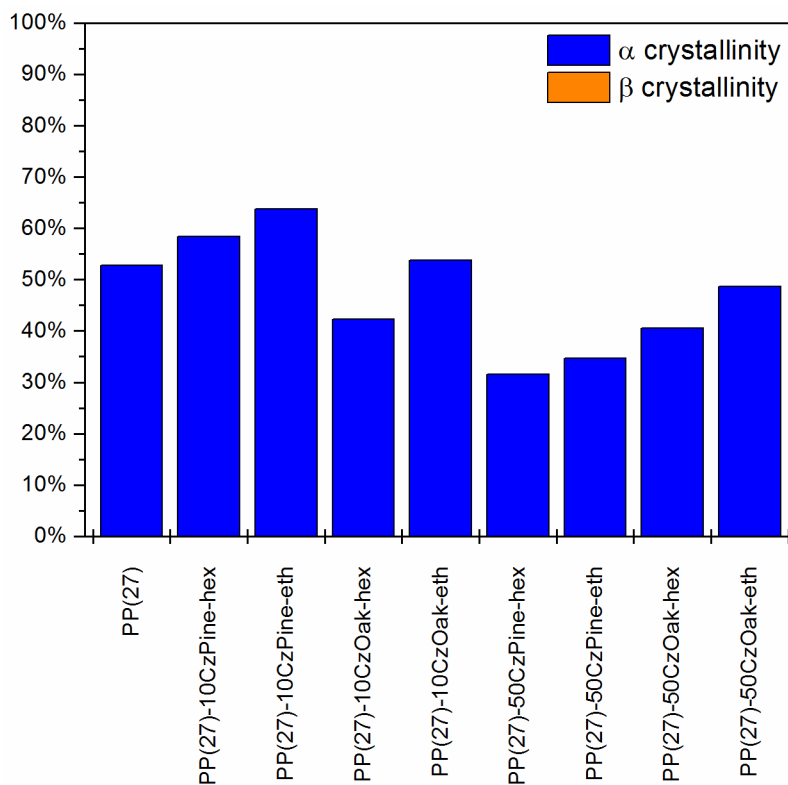


Figure 63 Decomposition of experimental data with two Pearson VII peaks

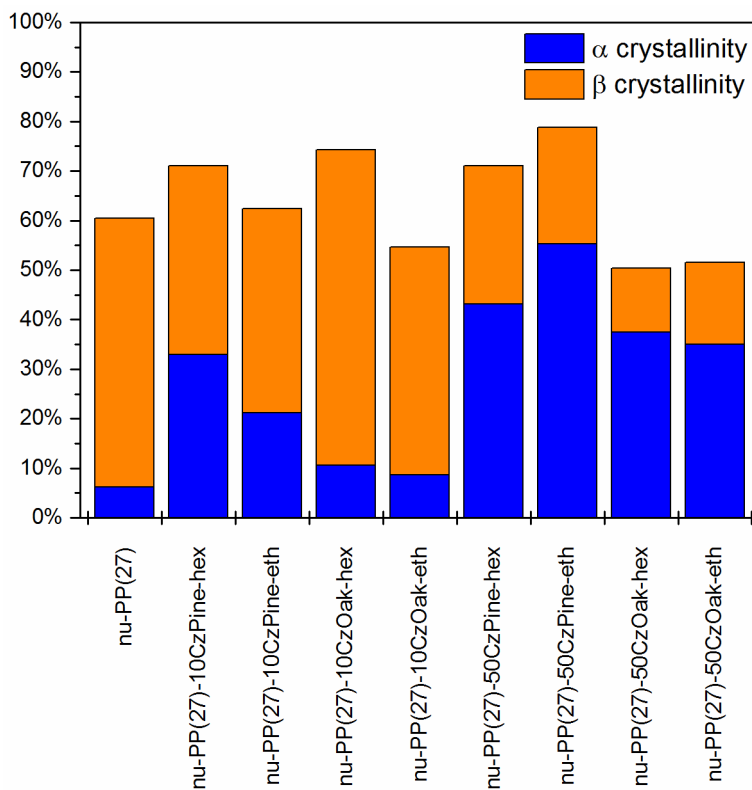


Figure 64 Decomposition of experimental data with two Pearson VII peaks

Table 8 Calculated characteristic of nu-PP(27)composites with extracted woods

	K_{β}	X_c	$L_{(100)}$	$L_{(130)}$	$L_{(040)}$	$L_{(300)}$
	[-]	[%]	[nm]	[nm]	[nm]	[nm]
nu-PP(27)	0.897	60.48	15.74	—	—	30.87
nu-PP(27)-10CzPine-hex	0.536	71.05	13.55	16.99	9.91	29.99
nu-PP(27)-10CzPine-eth	0.661	62.37	16.19	23.72	—	30.87
nu-PP(27)-10CzOak-hex	0.858	74.25	14.94	—	—	33.54
nu-PP(27)-10CzOak-eth	0.840	54.66	16.19	23.12	—	33.58
nu-PP(27)-50CzPine-hex	0.392	71.00	14.04	20.68	10.61	31.38
nu-PP(27)-50CzPine-eth	0.299	78.81	13.02	19.67	14.23	30.01
nu-PP(27)-50CzOak-hex	0.257	50.43	15.27	17.02	12.82	29.71
nu-PP(27)-50CzOak-eth	0.320	51.53	14.63	16.52	11.20	25.08

Regarding the $L_{(hkl)}$, i.e. the lamella perfection, of the extracted-WF composites, in case of non-nucleated matrix, the values are slightly lower than the values neat PP. When nucleated matrix composites are compared, one can see slight variation of the $L_{(300)}$ related to β crystallites, as well as in the values of $L_{(100)}$ and $L_{(130)}$ which are related to α crystallites. Unfortunately, these data provided no unambiguous information on growth or perfection of crystalline domains.

5.3 Thermal Behavior Characterization

Thermal behavior of composites prepared from neat PP is shown in Figures 65 and 66, while the records in Figures 67 and 68 are related to nucleated matrix. From the cooling scans (Figures 65 and 67) it is evident, the behavior, shape of the curve, is practically identical with neat and nucleated PP, respectively, in case of 10 % filling, while the increase in WF content influences the process. The most significant change can be found in case of composites with oak WF, which shifts crystallization towards higher temperatures.

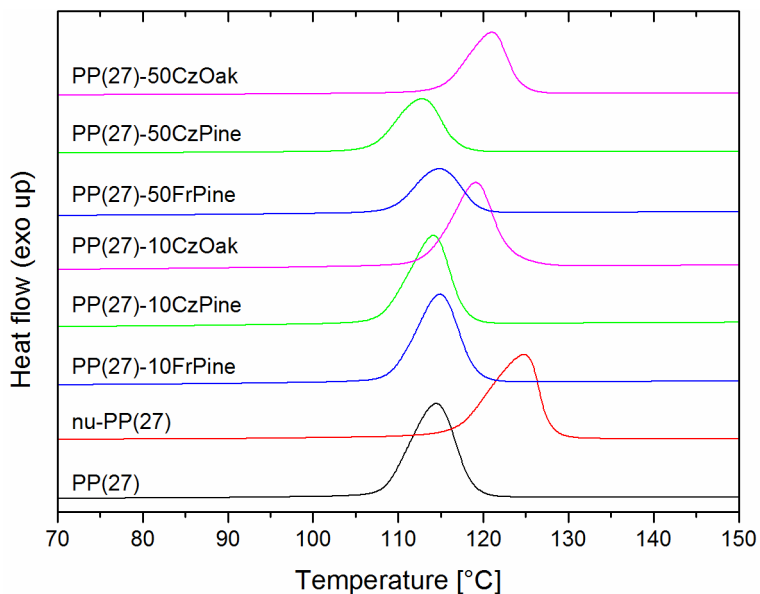


Figure 65 Crystallization thermograms of composites with PP(27)

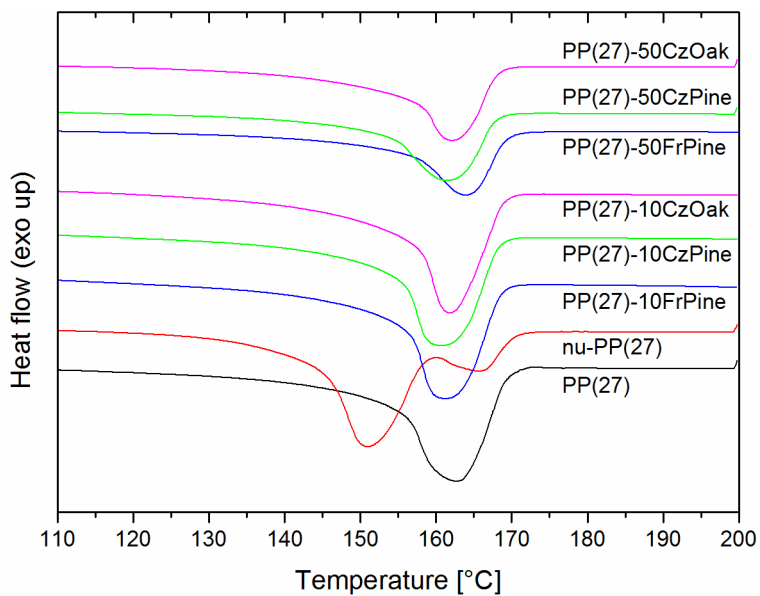


Figure 66 Melting thermograms of composites with PP(27)

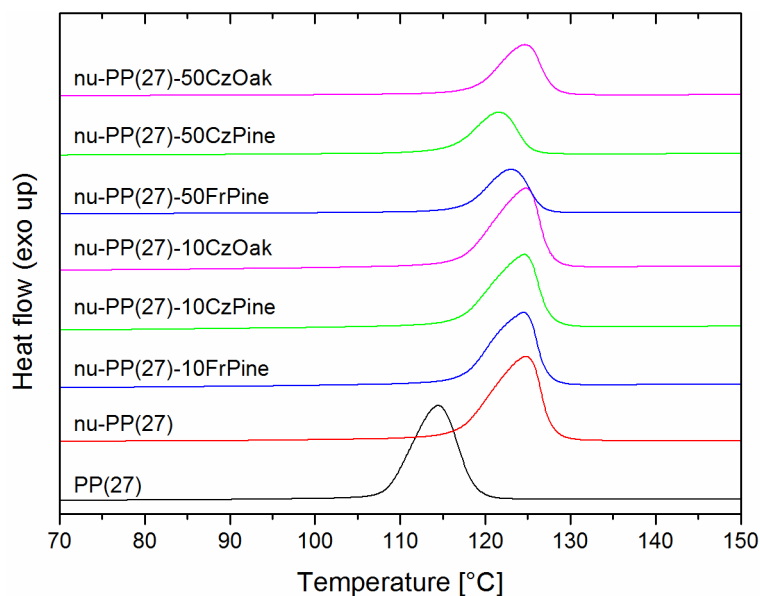


Figure 67 Crystallization thermograms of composites with nu-PP(27)

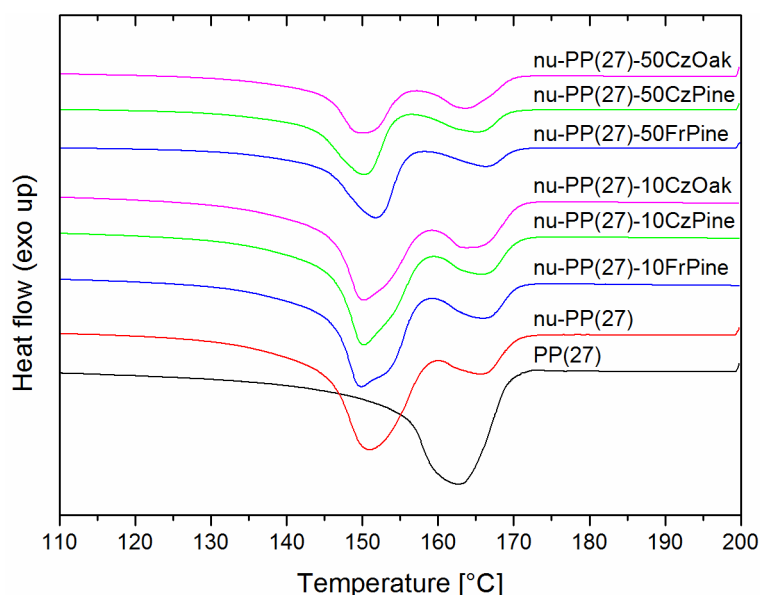


Figure 68 Melting thermograms of composites with nu-PP(27)

Table 9 summarizes measured characteristics – temperature of crystallization (T_c , graphically then in Figure 69), temperature of melting, $T_{m,\beta}$ and $T_{m,\alpha}$, of β and α crystallites, respectively, and corresponding lamellar thicknesses (according to eq. 18). Measured heat of fusion is here not presented, however, crystallinity, calculated with eq. 20, is included in the table and graphically compared in Figure 70. It is worth to note, the crystallinities differ from those obtained from WAXS diffraction analysis. This discrepancy is caused by different thermal history of the specimens, since those analyzed in DSC were quickly melted and then cooled as described above in methods section. Regarding the peak of

crystallization process in DSC thermograms, the low filler concentration made virtually no change, except the oak-filled composite, which crystallizes at higher temperature than the neat PP (about 5 °C) and even higher in case of highly filled PP(27)-50CzOak. On the other hand, the composite with pine harvested in Czech Republic decreased the T_c value of both the non-nucleated and β -nucleated matrices, of about 2 °C in the former and 3 °C in the latter case. Since these WF were not extracted, it can be assumed, that some of the low-molecular accompanying substances infused into the matrix during melt mixing causing obstructions in crystallization.

Table 9 Calculated characteristic of composites PP and wood flour without extraction

	T_c	$T_{m,\beta}$	$T_{m,\alpha}$	$x_{c,\beta}$	$x_{c,\alpha}$	$l_{c,\beta}$	$l_{c,\alpha}$
	[°C]	[°C]	[°C]	[%]	[%]	[nm]	[nm]
PP(27)	114.5	—	162.7	—	69.7	—	13.3
PP(27)-10FrPine	114.9	—	161.2	—	67.0	—	12.8
PP(27)-10CzPine	114.1	—	160.8	—	62.0	—	12.7
PP(27)-10CzOak	119.0	—	161.8	—	66.2	—	13.0
PP(27)-50FrPine	114.8	—	164.0	—	65.2	—	13.6
PP(27)-50CzPine	112.8	—	161.4	—	74.2	—	12.9
PP(27)-50CzOak	121.0	—	162.1	—	80.1	—	13.1
nu-PP(27)	124.8	151.0	165.7	75.8	12.0	10.6	14.2
nu-PP(27)-10FrPine	124.7	149.8	165.9	68.3	12.2	10.1	14.3
nu-PP(27)-10CzPine	124.6	150.2	165.7	67.1	13.1	10.3	14.2
nu-PP(27)-10CzOak	124.4	150.1	163.7	68.9	17.5	10.3	13.6
nu-PP(27)-50FrPine	123.0	151.8	166.2	69.7	10.3	11.0	14.4
nu-PP(27)-50CzPine	121.6	150.2	165.1	65.3	14.1	10.3	14.0
nu-PP(27)-50CzOak	124.7	150.0	163.6	65.0	21.7	10.2	13.5

When crystallinity is compared (Figure 70), only PP(27)-50CzPine and PP(27)-50CzOak showed higher amount of crystalline phase, which may point the fact, the filler is supporting crystallization process – at least in case of oak. PP(27)-50CzOak also exhibited shift of the crystallization as mentioned above, which also increased time of crystallite existence at elevated temperature, hence enabled improvement of the structure. This phenomenon was not observed in case of nucleated matrix. All the composite crystallinity

is lower than the value of nu-PP(27) and the lowest are in case of highly filled materials, which correspond to values derived from WAXS analysis. It is worth to note, the amount of the α crystallites ($x_{c,\alpha}$) in the case of nucleated PP matrix is probably not the real amount of α phase in the material, it is rather original to recrystallization processes which happens during slow and mid-rate heating and consequent melting of β crystallites.

Finally, comparison of lamellar thicknesses, which meaning is the macromolecule chain fold length, revealed no unambiguous trend. The high values of $l_{c,\alpha}$ in case of nucleated materials are caused by the recrystallization at elevated temperatures at which, according to generally accepted models [86], thicker lamellae should arise to decrease specific surface of the crystallites, which is connected with addition of energy (i.e. surface energy) to the crystalline system. From this point of view, the low values in case of both oak-filled nucleated PP signalize possible nucleation activity. The heterogeneous nucleation decreases surface energy, hence the lamellae need not to be thick to overcome nucleation barrier driven, primarily, by the surface.

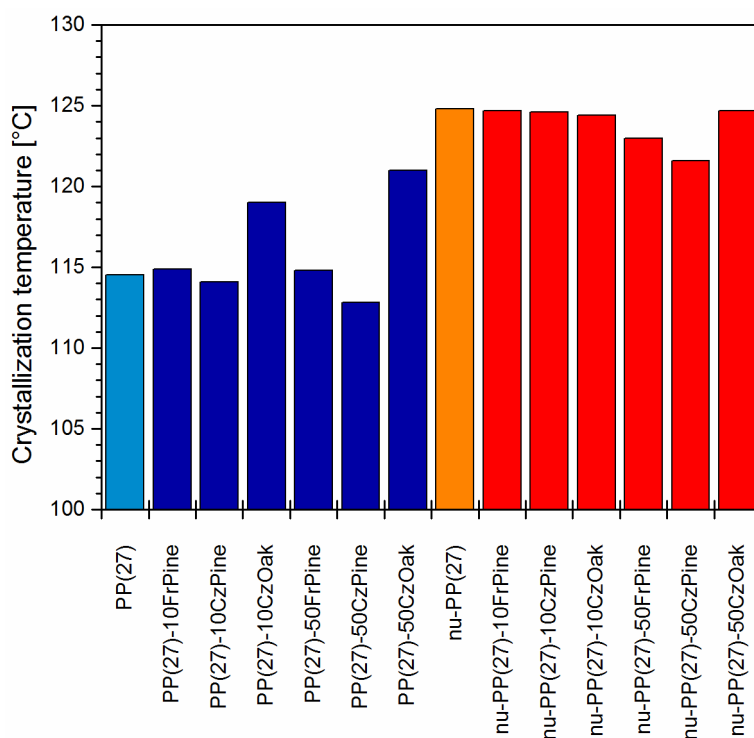


Figure 69 Comparison of crystallization temperatures

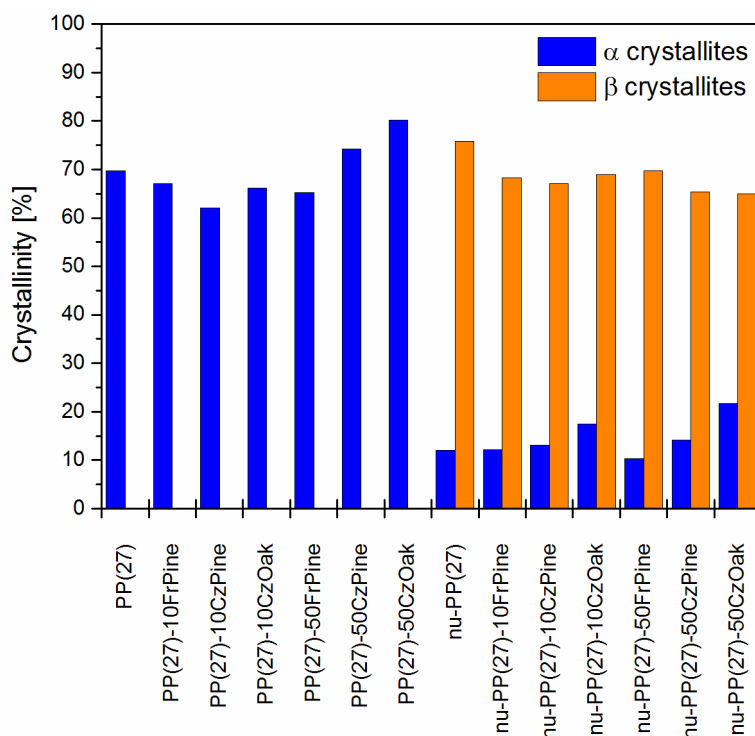


Figure 70 Comparison of crystalline phase amount in each material

Unfortunately, the hypothesis of nucleation activity is in contradiction with the WAXS derived data. Yet the nucleation could also happen during the compression molding of the sheets which were subjected to WAXS measurements. The process of cooling was in this case quick in comparison to cooling rate -10 K/min which was programmed during the DSC scan. Further investigation then should take into account speed of cooling as well as the analysis of the wood accompanying substances – both may be antagonistic factor in the crystallization processes.

Concerning extracted WF, the thermograms are here presented as Figure 71–74 for the non-nucleated PP and Figures 77–80 for the β-nucleated matrix. Summarization of recorded and calculated characteristic is then given in Table 10 and 11 and graphically in Figures 75 and 76. When crystallization temperature is compared with the neat matrix, it can be seen in Figure 75, all the temperatures are higher than the value of unfilled polymer. This could be explained again with the nucleation ability of the wood particle surface, which is free of low-molecular accompanying substances after the extraction. Higher purity wood then can more effectively act as heterogeneous nucleating agent. Regarding the extraction process, the ethanol should be more effective solvent as all the temperatures are higher than those observed in case of cyclohexane extraction. Unfortunately, pine WF

filled PP with concentration of 50 % did not revealed increase in T_c , which may have been due to bad solvent selection or specific composition of the particular wood, similar effect can be seen in case of nucleated matrix, where again the lowest T_c was measured in case of composite highly filled with cyclohexane pine WF. Regarding the rest of nucleated materials, no significant change in crystallization temperature was observed, which imply that even though the wood can nucleate crystallization in α phase, the β -nucleating agent is still more active and the prevailing crystalline structure comprise of β phase.

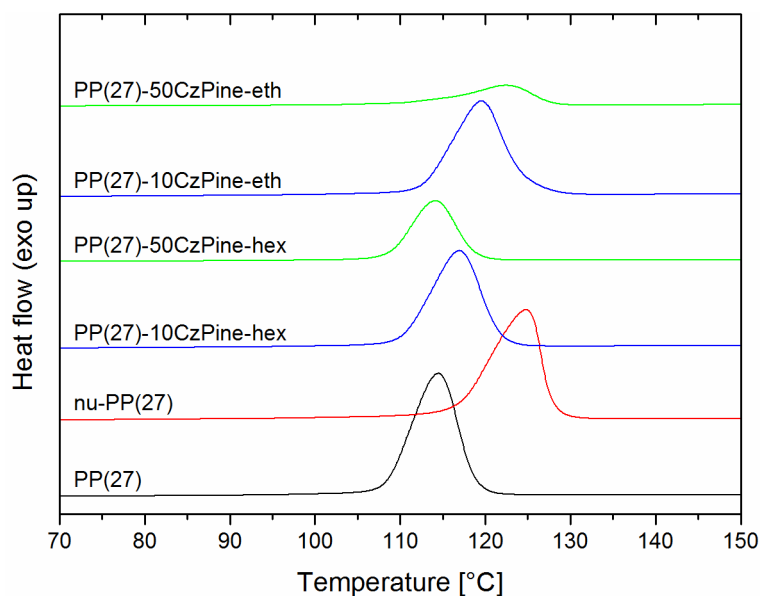


Figure 71 Crystallization thermograms of composites with PP(27) and extracted pine WF

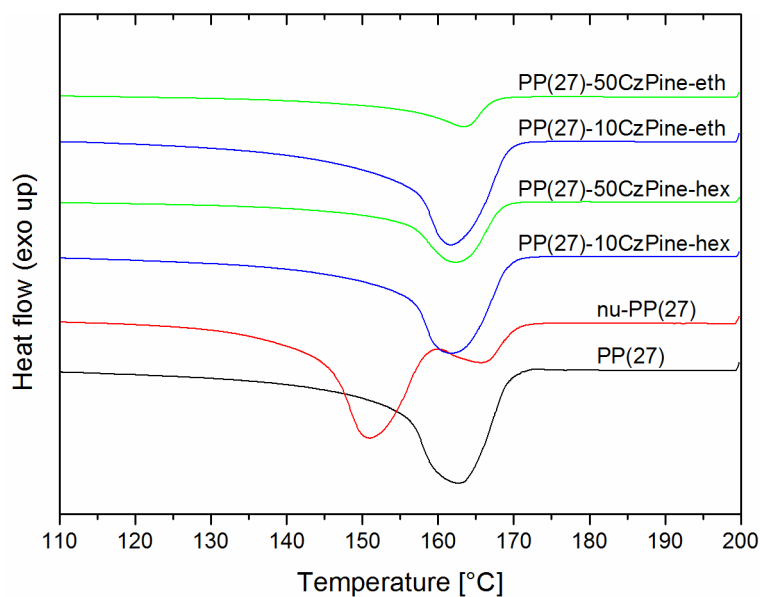


Figure 72 Melting thermograms of composites with PP(27) and extracted pine WF

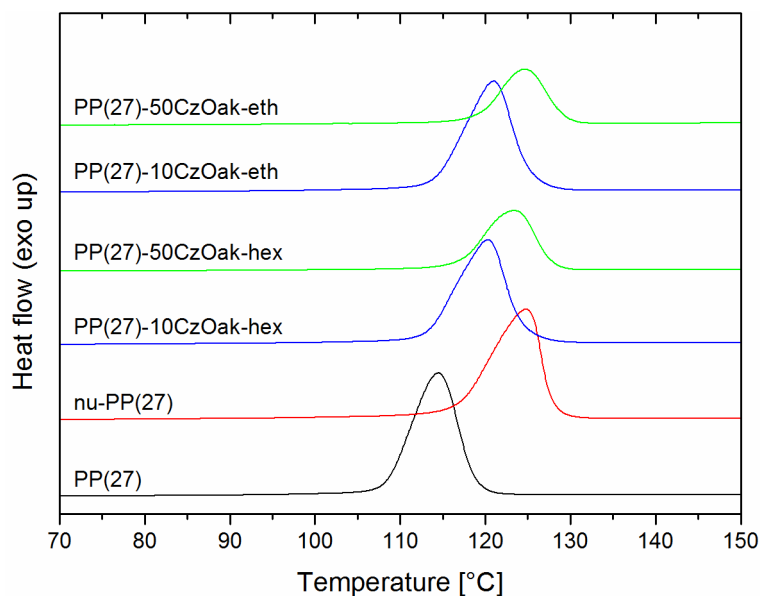


Figure 73 Crystallization thermograms of composites with PP(27) and extracted oak WF

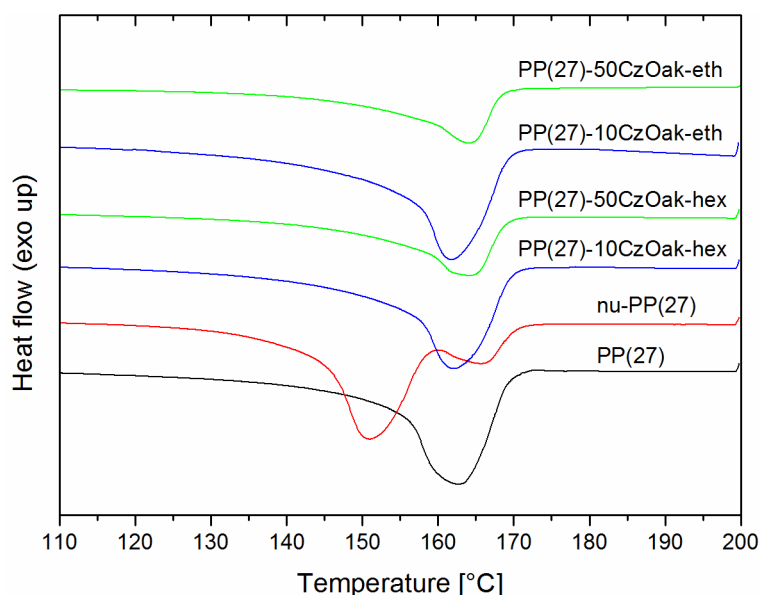


Figure 74 Melting thermograms of composites with PP(27) and extracted oak WF

This is again in contradiction with WAXS derived data, in which the K_{β} – i.e. relative amount of β crystals is significantly low particularly in case of high-filled composites. Unfortunately, peaks related to crystallization of α phase are not visible in the DSC records (Figures 77 and 79), yet the β -phase related peak is slightly deformed and shifted to lower temperature. One can thus presume, the measured peak is a convolution of both β and crystallization. Again, speed of the cooling may have influenced the final composition of compression molded sheets used for X-ray analysis.

Table 10 Calculated characteristic of PP(27) composites with extracted woods

	T_c	$T_{m,a}$	$x_{c,a}$	$l_{c,a}$
	[°C]	[°C]	[%]	[nm]
PP(27)	114.5	162.7	69.7	13.3
PP(27)-10CzPine-hex	117.0	161.8	62.5	13.0
PP(27)-10CzPine-eth	119.5	161.6	67.9	13.0
PP(27)-10CzOak-hex	120.3	162.1	67.2	13.1
PP(27)-10CzOak-eth	121.0	161.8	70.0	13.0
PP(27)-50Czpine-hex	114.1	162.3	64.7	13.1
PP(27)-50CzPine-eth	122.4	163.4	33.0	13.5
PP(27)-50CzOak-hex	123.4	164.2	73.6	13.7
PP(27)-50CzOak-eth	124.6	164.1	64.1	13.7

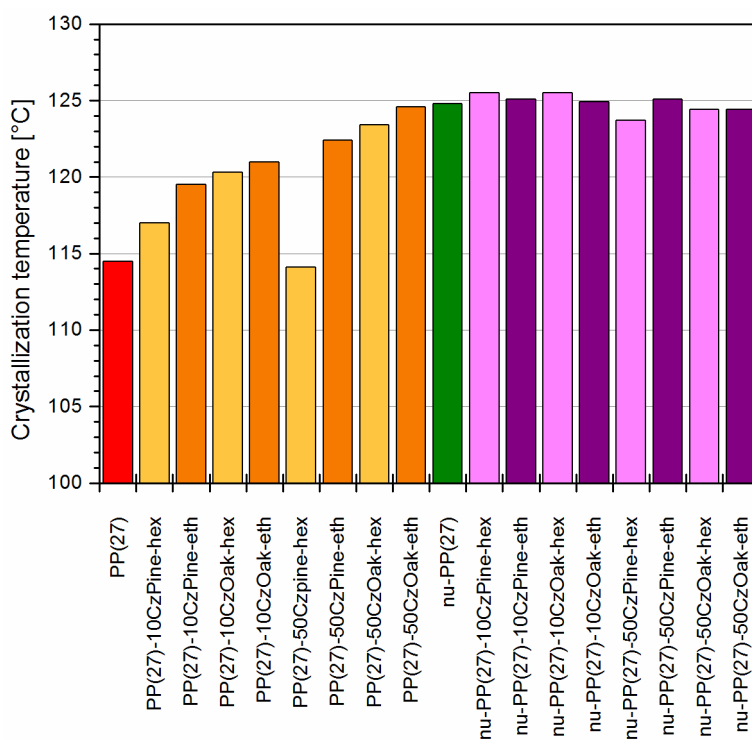


Figure 75 Crystallization temperature comparison of both matrices with extracted WF

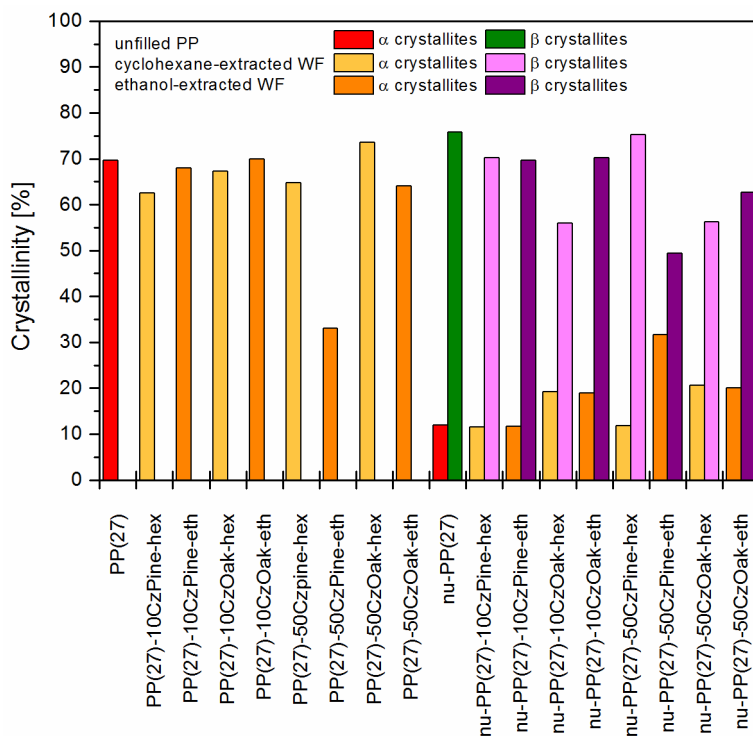


Figure 76 Crystallinity comparison of both matrices with extracted WF

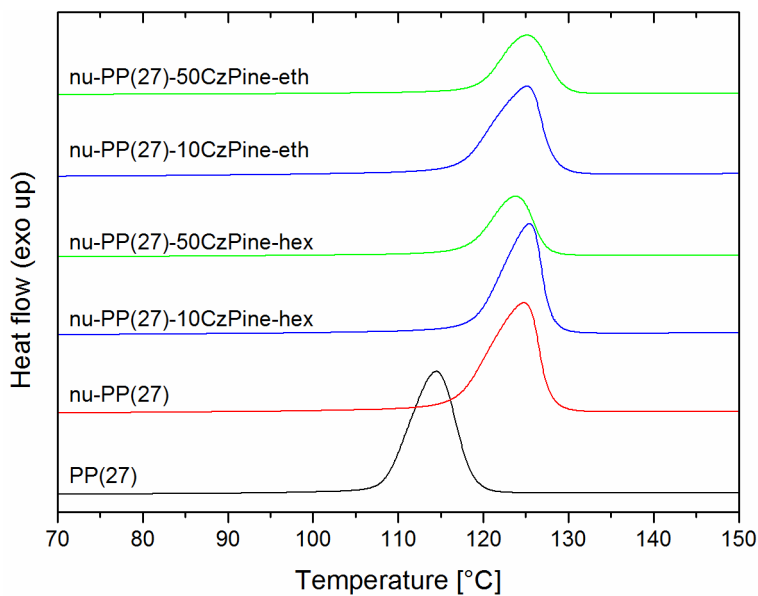


Figure 77 Crystallization thermograms of composites with nu-PP(27) and pine WF after extraction

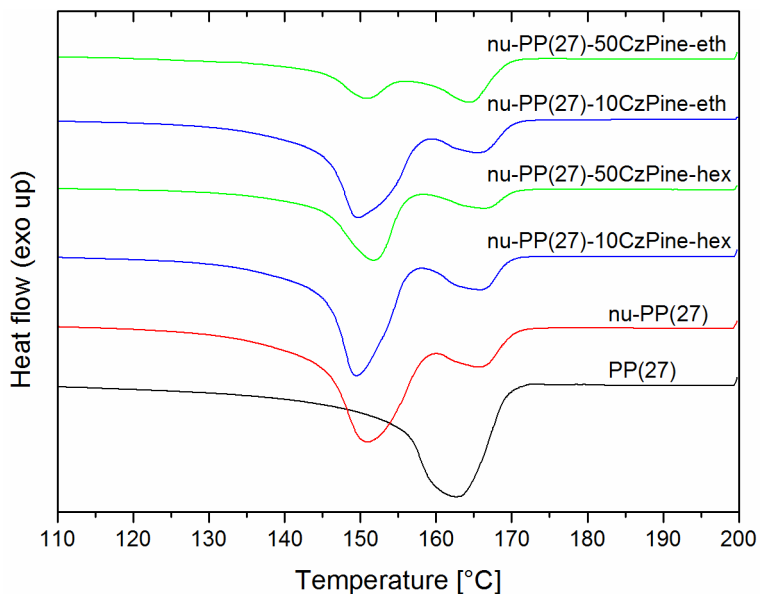


Figure 78 Melting thermograms of composites with nu-PP(27)

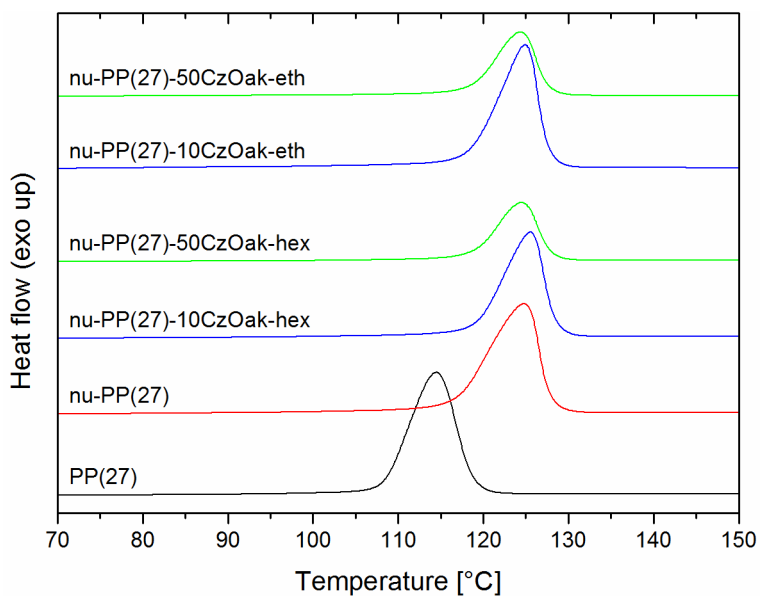


Figure 79 Crystallization thermograms of composites with nu-PP(27) and oak WF after extraction

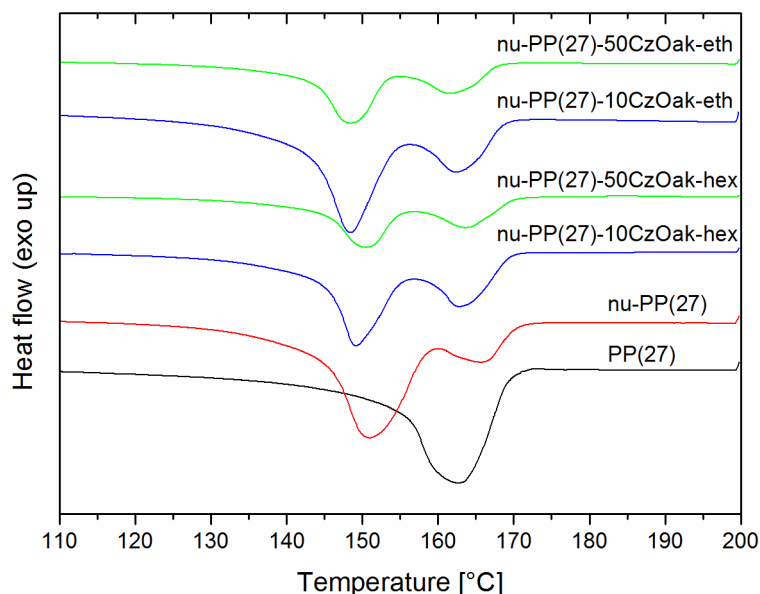


Figure 80 Melting thermograms of composites with nu-PP(27) and oak WF after extraction

Table 11 Calculated characteristic of nu-PP(27) composites with extracted woods

	T_c	$T_{m,\beta}$	$T_{m,\alpha}$	$x_{c,\beta}$	$x_{c,\alpha}$	$l_{c,\beta}$	$l_{c,\alpha}$
	[°C]	[°C]	[°C]	[%]	[%]	[nm]	[nm]
nu-PP(27)	124.8	151.0	165.7	75.8	12.0	10.6	14.2
nu-PP(27)-10CzPine-hex	125.5	149.4	165.7	70.2	11.5	10.0	14.2
nu-PP(27)-10CzPine-eth	125.1	149.6	165.5	69.7	11.7	10.1	14.1
nu-PP(27)-10CzOak-hex	125.5	149.1	162.8	55.9	19.2	9.9	13.3
nu-PP(27)-10CzOak-eth	124.9	148.4	162.4	70.2	19.0	9.6	13.2
nu-PP(27)-50CzPine-hex	123.7	151.7	166.3	75.2	11.8	10.9	14.4
nu-PP(27)-50CzPine-eth	125.1	150.9	164.3	49.4	31.6	10.6	13.8
nu-PP(27)-50CzOak-hex	124.4	150.5	163.7	56.2	20.6	10.4	13.6
nu-PP(27)-50CzOak-eth	124.4	148.4	161.6	62.7	20.1	9.6	12.9

When comparing relative crystalline phase amount (Figure 76), one can see the α crystallinity does not significantly differ from the unfilled PP in case of non-nucleated material, with one exception – the highly filled PP with pine WF. Similarity is found also in WAXS-derived data, where the lowest crystallinity was also in case of pine WF even after the extraction. It was already mentioned above, but for the cyclohexane solvent – the

pine wood may bear some low-molecular substances, which infuse into the matrix and change its properties so both the crystallization temperature and crystalline phase amount is lower than it is in the original unfilled PP. Pine wood is thus the less suitable material in this study, which is also relevant in case of nucleated matrix in which the ethanol-extracted pine WF decreased β -phase crystallinity. In this material, the relatively high amount of α phase was found, which should be, however, ascribed to the recrystallization processes during the heating and melting of thermally less stable β crystallites.

6 CONCLUSIONS

The goal of this work was to investigate, at a molecular scale, the primary physical-chemical interactions of a natural filler (WF) and an polyolefin matrix (PP) without any other chemical molecules. This has been studied by monitoring, through linear small oscillations molten viscoelastic behavior, the changes occurring in the macromolecular mobility of the polymeric chains due to the presence of the fillers and of its interactions with the matrix. A second step has been to look at consequences of these molecular dynamic changes in the melt onto macromolecular reorganization in the solid state.

The first result of this work is to put in evidence the complexity such a dynamic of these systems. Of course, classical parameters such as filler size and concentration are quite yet described in the literature but the influence of the molecular mobility of the matrix and of its consequence onto macromolecular recrystallization is less known.

This work has demonstrated that both gel behavior (expected) as well as viscous reduction (quite unexpected!) can be observed and more generally both processes compete.

Effect of MFI on viscoelastic behavior has been investigated on composites with 7 various concentrations of French pine, which were incorporated into four various PP. It was found that higher concentrations of WF strongly influence η' , η'' , since the lower concentration does not have any influence This behavior of viscosity occurs in relation with frequency in composites. The substantial effect of MFI is observed. It is evident that the influence of WF concentration and evolution of viscosity and elasticity is given by MFI. The increase of values of η' in comparison with neat PP can be caused by worse possibility to order small amounts of WF in the polymer matrix. Nevertheless, the polymers with higher MFI influence the flow of composites and thus the viscosity starts to increase. Indeed, it should be considered that filled systems have certain critical amount of filling. These low concentrations are not able to overcome the flow of polymer matrix and composites are more viscous than un-filled polymer matrices. Also, it is important to note that no filler modification was carried out on these samples and thus the lower filler-polymer interaction can cause decrease of viscosity in composites with lower concentrations. The polymer matrix with higher MFI, which means lower viscosity, brings a superior possibility of incorporation of WF to the matrix. Cole-Cole plots confirm the strong interaction between the WF and PP with highest MFI-PP(27). Influence of WF origin and filler size was examined on composites with PP(27) and two concentrations of French pine, Czech pine,

and Czech oak. The size of the WF did not induce any differences in the viscoelastic behavior. Czech pine and oak influence slightly the viscosity of PP, which is given by the origin. Also the effect of PP(27) and nucleated PP(27) was studied on composites with Czech pine and Czech oak at two concentrations. Nucleated PP(27) without WF behaves more fluid than PP(27). The nucleated PP(27) has a big influence on viscosity and elasticity of composites. In this part of the study, the results showed that composites with low concentrations of WF were able to overcome the flow of nucleated PP(27). The Cole-Cole plots exhibit strong interaction in composites with nucleated PP(27) as well PP(27), which is confirmed by double distribution.

Moreover, the viscoelastic behavior was described on composites with extracted WF in cyclohexane and ethanol and as well PP(27) and nucleated PP(27). Extraction of WF did not have any strong effect on composites with PP(27), on the other hand the extraction of WF influenced strongly the viscosity of composites with nucleated PP(27). It can be concluded that the solvent extraction (especially with ethanol as a benign solvent) has a big influence on the structure of pine and the compatibility of the composites with nucleated PP(27) is the strongest.

Regarding the study of crystalline structure, the results of WAXS analysis showed negligible influence of the French pine WF presence on the overall crystallinity, while the WF original to Czech location decreased the matrix crystallinity, particularly in case of highly filled materials. Both French and Czech wood, when present in high concentration in nucleated matrix, significantly decreases amount of the β phase content. This phenomenon is, however, partly eliminated after extraction of the wood, which implies that the possible disturbance is rather connected with low-molecular accompanying substances. On the other hand, the perfection of crystalline phase (indicated by the length calculated from Scherrer equation) showed ambiguous dependence on both – the filler origin and content.

Furthermore, unextracted woods showed practically no influence on the crystallization temperature with two exceptions – the Czech oak showed slight nucleating activity, since temperature of crystallization is shifted towards higher temperatures, and the Czech pine, which on the other hand decreased the crystallization temperature. The decrease was partly compensated by extraction of the wood. Concerning extraction, ethanol-extracted materials performed the best properties, namely the increase of the temperature of crystallization.

The highest increase was noted in case of highly filled composites what may indicate nucleation activity of the filler.

To sum the findings, the oak wood seems to be more suitable for use in WPC in comparison with the other wood, pine, used in this study. In addition, extraction with ethanol showed better results than the use of cyclohexane.

A prospective development of this work should be to develop the micromolecular-macromolecular interrelations through the mechanical behavior. How the molecular mobility in the melt state and the reorganization in the solid state will influence the static macromechanical properties such as young modulus, elongation at break...? Such analysis and intercorrelation should be of great interest to go further in the description of the state of aggregation and the strength of the interactions between the hydrophobic matrix and the hydrophilic fillers. Solvent extraction can be a tool to take into account this topic. However, it is necessary to develop an exact quantitative and qualitative analysis of the extraction processes what is a huge work.

7 REFERENCES

- [1] GROZDANOV A. et al.; Natural Fiber Eco-Composites, *Polymer Composites*, Vol. 28, **2007**, p. 98–107
- [2] CLEMONS C.; Wood-Plastic Composites in the United States, *Forest Product Journal*, Vol. 52, No. 6, **2002**
- [3] MAYA J. J., SABU T.; Biofibres and Biocomposites, *Carbohydrate polymers*, Vol. 71, 2008, p. 343–364
- [4] BLEDZKI A. K., LETMAN M., VIKSNE A., RENCE L.; A comparison of compounding processes and wood type for wood fibre-PP composites, *Composites*, Vol. 36(6), **2005**, p. 789–97
- [5] DOMINKOVICS Z., DÁNYÁDI L., PUKÁNSZKY B.; Surface modification of wood flour and its effect on the properties of PP/wood composites, *Composites: Part A*, Vol. 38, **2007**, p. 1893–1901
- [6] BOUZA R., MARCO C., NAFFAKH M., BARRAL L., ELLIS G.; Effect of particle size and a processing aid on the crystallization and melting behavior of iPP/red pine wood flour composites, *Composites: Part A*, Vol. 42, **2011**, p. 935–949
- [7] STECKEL V., CLEMONS C.M., THOEMEN H.; Effects of material parameters on the diffusion and sorption properties of wood-flour/polypropylene composites, *Journal of Applied Polymer Science*, Vol. 103, **2007**, p. 752–763
- [8] BOUAFIF H., KOUBAA A., PERRÉ P., CLOUTIER A.; Effect of fiber characteristics on the physical and mechanical properties of wood plastic composites, *Composites: Part A*, Vol. 40, **2009**, p. 1975–1981
- [9] FABIYI J. S., MCDONALD A. G.; Effect of wood species on property and weathering performance of wood plastic composites, *Composites: Part (A)*, Vol. 41, **2010**, p. 1434–1440
- [10] SAPUTRA H., SIMONSEN J., LI K.; Effect of extractives on the flexural properties of wood/plastic composites, *Composite Interfaces*, Vol. 11, **2004**, p. 515–524
- [11] KOTEK J., KELNAR I., BALDRIAN J., RAAB M.; Structural transformations of isotactic PP induced by heating and UV light, *European Polymer Journal*, Vol. 40, **2004**, p. 2731–2738
- [12] VARGA J.; Crystallization, melting and supermolecular structure of isotactic polypropylene in: J. Karger-Kocsis (Ed.), *Polypropylene: structure, blends and composites, Structure and morphology*, Vol. 1, Chapman & Hall, London, **1995**, p. 56–115
- [13] LOTZ B., WITTMANN J. C., LOVINGER A. J.; Structure and morphology of poly(propylenes): A molecular analysis. *Polymer*, Vol. 37, **1996**, p. 4979–4992
- [14] LOTZ B.; Molecular aspects of structure and morphology of isotactic polypropylene. *J Macromol Sci Phys*, Vol. 41, **2002**, p. 685–709

- [15] CHVATALOVA L., NAVRATILOVA J., ČERMÁK R., RAAB M., OBADAL M.; Join effects of molecular structure and processing history on specific nucleation of isotactic polypropylene, *Macromolecules*, Vol. 42, **2009**, p. 7413–7417
- [16] HARPER D., WOLCOTT M.; Interaction between coupling agent and lubricants in wood-polypropylene composites, *Composites: Part (A)*, Vol. 35, **2004**, p. 385–394
- [17] SHEBANI A. N., VAN REENEN A. J., MEINCKEN M.; The effect of wood extractives on the thermal stability of different wood species, *Thermochimica Acta*, Vol. 471, **2008**, p. 43–50
- [18] BERGLUND L., ROWEL R. M.; Wood Composites in Handbook of wood chemistry and wood composites, Edited by Roger M. Rowell, **2005**, ISBN: 978-0-203-49243-7
- [19] YANG H. S., WOLCOTT M. P., KIM H. S., KIM S., KIM H. J.; Properties of lignocellulosic material filled polypropylene bio-composites made with different manufacturing processes, *Polymer Testing*, Vol. 25, **2006**, p. 668–676
- [20] ASHORI A., NOURBAKHS A.; Characteristics of wood-fiber plastic composites made of recycled materials, *Waste Management*, Vol. 29, **2009**, p. 1291–1295
- [21] DÁNYÁDI L., MÓCZÓ J., PUKÁNSZKY B.; Effect of various surface modifications of wood flour on the properties of PP/wood composites, *Composites: Part A*, Vol. 41, **2010**, p. 199–206
- [22] ICHAZO M. N., ALBANO C., et al.; Polypropylene/wood flour composites: treatments and properties, *Composite Structures*, Vol. 54, **2001**, 207–214
- [23] ASHORI A.; Wood-plastic composites as promising green-composites for automotive industries!, *Biosource Technology*, Vol. 99, **2008**, p. 4661–4667
- [24] PRITCHARD G.; Two technologies merge: wood plastic composites, *Plastic Additives & Compounding*, Vol. 6 (4), **2004**, p. 18–21
- [25] DÁNYÁDI L., JANECSKA T., SZABÓ Z., NAGY G., MÓCZÓ J., PUKÁNSZKY B.; Wood-flour filled PP composites: Compatibilization and adhesion, *Composites Science and Technology*, Vol. 67, **2007**, p. 2838–2846
- [26] BHATTACHARYYA D., BOWIS M., JAYARAMAN K.; Thermoforming woodfibre-polypropylene composite sheets, *Composites Science and Technology*, Vol. 63, **2003**, p. 353–365
- [27] MILLER R. B.; Characteristics and Availability of Commercially Important Woods in Wood Handbook - Wood as an Engineering Material by Forest Products Laboratory, **2001**, ISBN: 978-1-59124-170-6
- [28] Market Growth wood plastic composites, May 2013 [online] <http://www.woodplasticcompositefloor.com/company-news/market-growth-wood-plastic-composite/>
- [29] Eder A.; Conference Charts the progress of WPCs, *Compounding World*, May **2013**, p. 27–36
- [30] WPC News and Events, January-February 2013 [online] <http://woodplasticcomposites.org/wpcnews.html>

- [31] KUČEROVÁ I.; Atmosferická degradace dřeva, Korozie a ochrana materiálu, Vol. 49, **2005**, p. 9–12
- [32] Willis A., Furey J., Franco E., Hurd J.; Pyrolysis Chemistry [online]. From: http://blogs.princeton.edu/chm333/f2006/biomass/bio_oil/02_chemistryprocessing_the_basics/01_chemistry/
- [33] PELTOLA P.; Alternative fibre sources: paper and wood fibres as reinforcement in Green Composites - Polymer Composites and the Environment, Edited by: Baillie, Caroline, **2004**, ISBN: 978-1-85573-739-6
- [34] IOANNIS S. ARVANITOYANNIS, A. KASSAVETI; Starch–Cellulose Blends, in Biodegradable Polymer Blends and Composites from Renewable Resources, Edited by: Yu, Long, **2009**, ISBN: 978-1-61583-602-4
- [35] WYPYCH, G.; Handbook of Fillers - A Definitive User's Guide and Databook (2nd Edition), **2000**, ISBN: 978-1-884207-69-3
- [36] KIGUCHI M., et al.; Surface deterioration of wood/flour polypropylene composites by weathering trials, Journal of Wood Science, Vol. 53, **2007**, p. 234–238
- [37] MADSEN HANSEN; Biofuels and the prospect of converting plant fibres into gasoline using enzymes [online]. From: <http://www.scq.ubc.ca/biofuels-and-the-prospect-of-converting-plant-fibres-into-gasoline-using-enzymes/>
- [38] KOPAČ J., ŠALI S.; Wood: an important material in manufacturing technology, Journal of Materials Processing Technology, Vol. 133 (1-2), **2003**, p. 134–142
- [39] WIEDENHOEFT A. C., MILLER R. B.; Structure and function of wood, in Handbook of wood chemistry and wood composites, Edited by Roger M. Rowell, **2005**, ISBN: 978-0-203-49243-7
- [40] VICK CH. B.; Adhesive Bonding of Wood Materials in Wood Handbook - Wood as an Engineering Material by Forest Products Laboratory, **2001**, ISBN: 978-1-59124-170-6
- [41] SIMPSON W. T.; Drying and Control of Moisture Content and Dimensional Changes in Wood Handbook - Wood as an Engineering Material by Forest Products Laboratory, **2001**, ISBN: 978-1-59124-170-6
- [42] ROWELL R. M.; Moisture Properties in Handbook of wood chemistry and wood composites, Edited by Roger M. Rowell, **2005**, ISBN: 978-0-203-49243-7
- [43] NOURBAKHSI A., ASHORI A.; Wood plastic composites from agro-waste materials: Analysis of mechanical properties, Bioresource technology, Vol. 101, **2010**, p. 2525–2528
- [44] GODARA A., RAABE A., BERGMANN I., PUTZ R., MÜLLER U.; Influence of additives on the global mechanical behavior and the microscopic strain localization investigated using digital image correlation, Composites Science and Technology, Vol. 69, **2009**, p. 138–146
- [45] KUO P. Y., TSAI M. J., et al.; Effect of material compositions on the mechanical properties of wood-plastic composites manufactured by injection holding, Materials and Design, Vol. 30, **2009**, p. 3489–3496

- [46] BORYSIAK S.; Supermolecular structure of wood/polypropylene composites: I. The influence of processing parameters and chemical treatment of the filler, *Polymer Bulletin*, Vol. 64, **2010**, p. 275–290
- [47] BORYSIAK S., DOCZEKALSKA B.; Influence of chemical modification of wood on the crystallization of PP, *European Journal of Wood and Wood Products*, Vol. 64, **2006**, p. 451–454
- [48] ROWELL R. M.; Chemical modification of wood in *Handbook of wood chemistry and wood composites*, Edited by Roger M. Rowell, **2005**, ISBN: 978-0-203-49243-7
- [49] CAO J. Z., WANG Y., XU W. Y., WANG L.; Preliminary study of viscoelastic properties of MAPP-modified wood-flour/polypropylene composites, *Forestry Studies in China*, Vol. 12, **2010**, p. 85–89
- [50] GUNDUZ G., AYDEMIR D., KARAKAS G.; The effects of thermal treatment on the mechanical properties of wild Pear (*Pyrus elaeagnifolia* Pall.) wood and changes in physical properties, *Materials and Design*, Vol. 30, **2009**, 4391–4395
- [51] BENGTSSON M., LE BAILIF M., OKSMAN K.; Extrusion and mechanical properties of highly filled cellulose fibre- polypropylene composites, *Composites: Part A*, Vol. 38, **2007**, p. 1922–1931
- [52] YOUNGQUIST J. A.; *Wood-based Composites and Panel Products in Wood Handbook - Wood as an Engineering Material* by Forest Products Laboratory, **2001**, ISBN: 978-1-59124-170-6
- [53] MAIER C.; CALAFUT T.; *Polypropylene - The Definitive User's Guide and Datebook*, William Andrew Publishing/Plastics Design Library, **1998**, ISBN: 978-0-8155-1871-6
- [54] BRYDSON J.; *Plastics Materials (7th Edition)*, Oxford: Elsevier, **1999**, ISBN: 978-0-7506-41326
- [55] MONASSE B., HAUDIN J. M.; Crystalline structures of polypropylene homo- and copolymers in *Polypropylene: Structure Blends and Composites*, J KARGER-KOCSIS Chapman & Hall, **1995**, ISBN: 978-0-412-61440-8
- [56] VARGA J.; Crystallization, melting and supermolecular structure of isotactic polypropylene in *Polypropylene: Structure Blends and Composites*, J KARGER-KOCSIS Chapman & Hall, **1995**, ISBN: 978-0-412-61440-8
- [57] BRUCKNER S., MEILLE, S. V.; Polymorphism in crystalline polypropylene in *Polypropylene - An A-Z Reference*, J. KARGER-KOCSIS Dordrecht: Kluwer Publishers, **1999**, ISBN: 978-0-412-80200-3
- [58] WHITE J. L., CHOI D.; *Polyolefins - Processing, Structure Development, and Properties*, Hanser Publishers, **2005**, ISBN: 978-1-60119-160-1
- [59] GEN D. E., PROKHOROV K. A., NIKOLAEVAA G. Y., et al.; Raman Spectra of Various Polymorphs of Isotactic Polypropylene, *Laser Physics*, Vol. 21, **2011**, p. 125–129
- [60] CHENG D. Z. S., JANIMAK J. J., RODRIGUEZ J.; Crystalline structures of polypropylene homo- and copolymers in *Polypropylene: Structure Blends and*

- Composites, J KARGER-KOCSIS Chapman & Hall, **1995**, ISBN: 978-0-412-61440-8
- [61] LOTZ B.; α - and β -phases of isotactic polypropylene: a case of growth kinetics phase reentrancy in polymer crystallization, *Polymer*, Vol. 39, **1998**, p. 4561–4567
- [62] LOTZ B.; Molecular aspects of structure and morphology of isotactic polypropylene, *Journal of Macromolecular Science, Part B: Physics*, Vol. 41, **2002**, p. 685–709
- [63] OBADAL M. et al.; Structure evolution of α - and β -polypropylenes upon UV irradiation: a multiscale comparison, *Polymer Degradation and Stability*, Vol. 88, **2005**, p. 532–539
- [64] OBADAL M. et al.; Tensile and Flexural Properties of β -Nucleated Polypropylenes, *Intern. Polymer Processing*, Vol. 19, **2004**, p. 308–312
- [65] HAN CH. D.; Relationships between polymer rheology and polymer processing, *Rheology and Processing of Polymeric Materials (Volume 1 Polymer Rheology)*, Oxford University Press, **2007**, ISBN: 978-0-19-518782-3
- [66] MOTTAHEDI M., DADALAU A., HAFLA A., VERL A.; Numerical Analysis of Relaxation Test Based on Prony Series Material Model in Integrated Systems, *Design and Technology*, Springer Science, **2010**, p. 79–82 , eISBN: 978-3-642-17384-4
- [67] SHENOY A. V.; Basic rheological concepts. *Rheology of Filled Polymer Systems*, Kluwer Academic Publishers, **1999**, ISBN: 0-412-83100-7
- [68] UTRACKI L. A.; Viscoelastic behavior of polymer blends, *Polymer Engineering & Science*, Vol. 28, **1988**, p. 1401–1404
- [69] LABAIG J. J., MONGE P. H., BEDNARIK J.; Steady flow and dynamic viscoelastic properties of branched polyethylene, *Polymer*, Vol. 14, **1973**, p. 384
- [70] GARCIA-FRANCO C. A., MEAD D. W.; Rheological and molecular characterization of linear backbone flexible polymers with the Cole-Cole model relaxation spectrum, *Rheologica Acta*, Vol. 38, **1999**, p. 34–47
- [71] LANFRAY Y.; Thesis, Docteur de 3^e cycle, **1988**
- [72] LEROY E. A.; *X-Ray Diffraction Methods in Polymer Science*, John Wiley & Sons. Inc. New York: **1969**, ISBN 471-02183-0
- [73] TURNER-JONES A., AIZLEWOOD J.M., BECKETT D.R.; Crystalline forms of isotactic polypropylene, *Die Makromolekulare Chemie*. 75, **1964**, p. 134–158
- [74] TURNER-JONES A., COBBOLD A.J.; The β crystalline form of isotactic polypropylene, *Journal of Polymer Science Part B: Polymer Letters*. 6, **1968**, p. 539–546
- [75] KONISHI T., NISHIDA K., KANAYA T.; Crystallization of Isotactic Polypropylene from Prequenched Mesomorphic Phase, *Macromolecules*. 39, **2006**, p. 8035–8040
- [76] KOCH T., SEIDLER S., HALWAX E., BERNSTORFF S.; Microhardness of quenched and annealed isotactic polypropylene, *Journal of Materials Science*. 42, **2007**, p. 5318–5326.

- [77] CHEREMISSINOFF. N. P.; Polymer Characterization – Laboratory Techniques and Analysis, **1996**, p. 251
- [78] WUNDERLICH B.; Crystal Melting. Macromolecular physics, Vol. 3, Academic Press, New York, **1980**, ISBN: 0-12-765603-0
- [79] VARGA J., MUDRA I., HRENSTEIN G.W.; Highly active thermally stable β -nucleating agents for isotactic polypropylene, Journal of Applied Polymer Science, **74**, **1999**, p. 2357–2368
- [80] GALESKI A.; Crystallization. Polypropylene An A-Z Reference, J. Karger-Kocsis (Ed.), Kluwer Academic Publishers, Dordrecht, **1999**, p. 992
- [81] BRANDRUP J., IMMERGUT E.H., GRULKE E.A.; Polymer Handbook, John Wiley & Sons, Inc., New York, **1999**
- [82] AZIZI H., GHASEMI I.; Investigation on the Dynamic Melt Rheological Properties of Polypropylene/Wood Flour composites. Polymer Composite, Vol. 30, **2009**, p. 429–435
- [83] WOJDYR M.; Fityk: a general-purpose peak fitting program. Journal of Applied Crystallography, Vol. 43, **2010**, p. 1126–1128.
- [84] GRAY D. G.; Transcrystallization of polypropylene at cellulose nanocrystal surface. Cellulose, Vol. 15, **2008**, p. 297–301
- [85] BOUAFIF H., KOUBAA A., PERRÉ P., CLOUTIER A., RIEDL B.; Wood Particle/High-Density Polyethylene Composites. Thermal Sensitivity and Nucleating Ability of Wood Particles. Journal of Applied Polymer Science, Vol. 113, **2009**, p. 593–600
- [86] WUNDERLICH B.; Crystal Nucleation, Growth. Annealing Macromolecular Physics, Vol. 2, Academic Press, New York, **1976**, ISBN: 0-12-765602-2

LIST OF THE FIGURES

<i>Figure 1 Effect of wood particle size with various filler content on tensile modulus (a) and maximum tensile strength (b) [8]</i>	- 14 -
<i>Figure 2 Wood-plastic composites used worldwide in 2002 [23]</i>	- 16 -
<i>Figure 3 Structure of cellulose monomer [32]</i>	- 18 -
<i>Figure 4 Structure of hemicellulose [32]</i>	- 18 -
<i>Figure 5 Structure of lignin [37]</i>	- 19 -
<i>Figure 6 Mechanism of coupling agent activity between hydrophilic fiber and hydrophobic polymer matrix [23]</i>	- 21 -
<i>Figure 7 Basic wood elements (largest → smallest) [52]</i>	- 22 -
<i>Figure 8 The orientation of the pendant methyl groups in PP: a) tail-to-tail, b) head-to-head, c) head-to-tail [55]</i>	- 24 -
<i>Figure 9 Stereochemical configurations of PP: a) isotactic, b) syndiotactic, c) atactic (random) [53]</i>	- 24 -
<i>Figure 10 iPP chain in the crystal lattice – the four possible insertions [57]</i>	- 26 -
<i>Figure 11 The crystalline structure of α form [57]</i>	- 27 -
<i>Figure 12 Structural model of β-iPP as determined by electron crystallography [58, 62]</i>	- 28 -
<i>Figure 13 The crystal unit cell of the γ form on the ab plane [60]</i>	- 29 -
<i>Figure 14 Cole-Cole plot</i>	- 35 -
<i>Figure 15 Schematic illustration of Bragg's law</i>	- 36 -
<i>Figure 16 Illustration of the polymer DSC thermograms [77]</i>	- 39 -
<i>Figure 17 The variation of the Newtonian viscosity vs. the average molecular weight</i> ..	- 41 -
<i>Figure 18 Illustration of Cole-Cole plots for PP(1, 12, 20, 27)</i>	- 42 -
<i>Figure 19 Dependence of viscous dissipation (η') on frequency in composites with PP(1)</i>	- 43 -
<i>Figure 20 Dependence of viscous dissipation (η') on frequency in composites with PP(12)</i>	- 44 -
<i>Figure 21 Dependence of viscous dissipation (η') on frequency in composites with PP(20)</i>	- 44 -

<i>Figure 22 Dependence of viscous dissipation (η') on frequency in composites with PP(27).....</i>	- 45 -
<i>Figure 23 Dependence of η'' on frequency in composites with PP(1).....</i>	- 46 -
<i>Figure 24 Ratio of η'' of PP(1) and composites in function of the amount of WF at $w=0.2$ rad/s</i>	- 46 -
<i>Figure 25 Dependence of η' on frequency in composites with PP(12)</i>	- 47 -
<i>Figure 26 Dependence of η' on frequency in composites with PP(20)</i>	- 47 -
<i>Figure 27 Dependence of η' on frequency in composites with PP(27)</i>	- 48 -
<i>Figure 28 Ratio of η'' of PP(27) and composites in function of the amount of WF at $w=0.2$ rad/s</i>	- 48 -
<i>Figure 29 Cole-Cole plot of composites with PP(1).....</i>	- 49 -
<i>Figure 30 Cole-Cole plot of composites with PP(12).....</i>	- 50 -
<i>Figure 31 Cole-Cole plot of composites with PP(20).....</i>	- 50 -
<i>Figure 32 Cole-Cole plot of composites with PP(27).....</i>	- 51 -
<i>Figure 33 Dependence of viscous dissipation (η') on frequency in composites with pine and PP(27).....</i>	- 52 -
<i>Figure 34 Dependence of viscous dissipation (η') on frequency in composites with oak and PP(27).....</i>	- 52 -
<i>Figure 35 Viscosity of PP(27) and nu-PP(27).....</i>	- 53 -
<i>Figure 36 Comparison of Cole-Cole plots of PP(27) and nu-PP(27).....</i>	- 54 -
<i>Figure 37 Dependence of viscous dissipation (η') on frequency in composites with pine and oak and PP(27).....</i>	- 55 -
<i>Figure 38 Dependence of viscous dissipation (η') on frequency in composites with pine and oak and nu-PP(27).....</i>	- 55 -
<i>Figure 39 Dependence of η' on frequency in composites with pine and oak and PP(27).....</i>	- 56 -
<i>Figure 40 Dependence of η'' on frequency in composites with pine and oak and nu-PP(27).....</i>	- 56 -
<i>Figure 41 Cole-Cole plots with pine and oak and PP(27)</i>	- 57 -
<i>Figure 42 Cole-Cole plots with pine and oak and nu-PP(27).....</i>	- 58 -
<i>Figure 43 Dependence of viscous dissipation (η') on frequency in composites after various solvent extraction of pine with PP(27).....</i>	- 59 -

<i>Figure 44 Dependence of viscous dissipation (η') on frequency in composites after various solvent extraction of oak with PP(27).....</i>	<i>- 60 -</i>
<i>Figure 45 Dependence of η'' on frequency in composites after various solvent extraction of pine with PP(27)</i>	<i>- 60 -</i>
<i>Figure 46 Dependence of η'' on frequency in composites after various solvent extraction of oak with PP(27)</i>	<i>- 61 -</i>
<i>Figure 47 Dependence of viscous dissipation (η') on frequency in composites after various solvent extraction of pine with nu-PP(27).....</i>	<i>- 62 -</i>
<i>Figure 48 Dependence of viscous dissipation (η') on frequency in composites after various solvent extraction of oak with nu-PP(27).....</i>	<i>- 62 -</i>
<i>Figure 49 Dependence of η'' on frequency in composites after various solvent extraction of pine with nu-PP(27).....</i>	<i>- 63 -</i>
<i>Figure 50 Dependence of η'' on frequency in composites after various solvent extraction of oak with nu-PP(27)</i>	<i>- 63 -</i>
<i>Figure 51 Cole-Cole plot for PP(27)/pine composites.....</i>	<i>- 64 -</i>
<i>Figure 52 Cole-Cole plot for PP(27)/oak composites</i>	<i>- 65 -</i>
<i>Figure 53 Cole-Cole plot for nu-PP(27)/pine composites.....</i>	<i>- 65 -</i>
<i>Figure 54 Cole-Cole plot for nu-PP(27)/oak composites.....</i>	<i>- 66 -</i>
<i>Figure 55 Decomposition of experimental data with two Pearson VII peaks</i>	<i>- 67 -</i>
<i>Figure 56 Decomposition of experimental data with two Pearson VII peaks</i>	<i>- 68 -</i>
<i>Figure 57 Example of WF/PP spectrum decomposition (nu-PP(27)-50CzOak-eth).....</i>	<i>- 69 -</i>
<i>Figure 58 X-ray diffraction patterns of composites with PP(27)</i>	<i>- 70 -</i>
<i>Figure 59 X-ray diffraction patterns of composites with nu-PP(27).....</i>	<i>- 70 -</i>
<i>Figure 60 Crystalline phase amount and composition in studied composites</i>	<i>- 72 -</i>
<i>Figure 61 X-ray diffraction patterns of extracted wood flour composites with PP(27). -</i>	<i>73 -</i>
<i>Figure 62 X-ray diffraction patterns of extracted wood flour composites with nu-PP(27)</i>	<i>- 73 -</i>
<i>Figure 63 Decomposition of experimental data with two Pearson VII peaks</i>	<i>- 75 -</i>
<i>Figure 64 Decomposition of experimental data with two Pearson VII peaks</i>	<i>- 75 -</i>
<i>Figure 65 Crystallization thermograms of composites with PP(27)</i>	<i>- 77 -</i>
<i>Figure 66 Melting thermograms of composites with PP(27)</i>	<i>- 77 -</i>
<i>Figure 67 Crystallization thermograms of composites with nu-PP(27).....</i>	<i>- 78 -</i>

<i>Figure 68 Melting thermograms of composites with nu-PP(27)</i>	- 78 -
<i>Figure 69 Comparison of crystallization temperatures</i>	- 80 -
<i>Figure 70 Comparison of crystalline phase amount in each material</i>	- 81 -
<i>Figure 71 Crystallization thermograms of composites with PP(27)</i> <i>and extracted pine WF</i>	- 82 -
<i>Figure 72 Melting thermograms of composites with PP(27) and extracted pine WF</i>	- 82 -
<i>Figure 73 Crystallization thermograms of composites with PP(27)</i> <i>and extracted oak WF</i>	- 83 -
<i>Figure 74 Melting thermograms of composites with PP(27) and extracted oak WF</i>	- 83 -
<i>Figure 75 Crystallization temperature comparison of both matrices</i> <i>with extracted WF</i>	- 84 -
<i>Figure 76 Crystallinity comparison of both matrices with extracted WF</i>	- 85 -
<i>Figure 77 Crystallization thermograms of composites with nu-PP(27)</i>	- 85 -
<i>Figure 78 Melting thermograms of composites with nu-PP(27)</i>	- 86 -
<i>Figure 79 Crystallization thermograms of composites with nu-PP(27)</i>	- 86 -
<i>Figure 80 Melting thermograms of composites with nu-PP(27)</i>	- 87 -

LIST OF THE TABLES

Table 1 Typical chemical compositions of wood [31, 32]	- 17 -
Table 2 Characteristics of PP samples [15]	- 31 -
Table 3 Constants used for calculation of lamellar thickness.....	- 40 -
Table 4 Rheological parameters for used polymer matrix.....	- 42 -
Table 5 Calculated peak parameters and their mutual difference.....	- 68 -
Table 6 Calculated characteristic of PP and composites with unextracted woods	- 71 -
Table 7 Calculated characteristic of PP and composites with extracted woods	- 74 -
Table 8 Calculated characteristic of nu-PP(27)composites with extracted woods	- 76 -
Table 9 Calculated characteristic of composites PP and wood flour without extraction -	79 -
Table 10 Calculated characteristic of PP(27) composites with extracted woods	- 84 -
Table 11 Calculated characteristic of nu-PP(27)composites with extracted woods	- 87 -

AUTHOR'S PUBLICATIONS

BENÍČEK, L., CHVÁTALOVÁ, L., BERKOVÁ, K., ČERMÁK, R., OBADAL, M., VERNEY, V., COMMEREUC, S; Effect of annealing temperature on phase composition and tensile properties in isotactic poly(1-butene), *Journal of Applied Polymer Science*, Vol. 124, 2012, p. 3407–34012

BERKOVÁ, K., BENÍČEK, L., ČERMÁK, R., CHVÁTALOVÁ, L.; Vývoj fyzikálních a mechanických vlastností během fázové transformace v poly(1-butenu), **Plasty a kaučuk**, Vol. 7–8, 2011

Accepted: ASKANIAN H., COMMEREUC S., VERNEY V, MASSARDIER-NAGEOTTE V., BENICEK L., **MONTAGOVA-BERKOVA K.**, CERMAK R.; Chapter 9: Natural fibres polyolefin composites: Processing, melt rheology and properties in *Bio-Based Composites for High-Performance Materials: From Strategy to Industrial Application*, CRC Press – Taylor&Francis Group

Conference contributions

MONTÁGOVÁ K., ČERMÁK R., VERNEY V.; Processing and properties of unmodified wood flour/polypropylene composites, **Conference Plastko 2010, Tomas Bata University in Zlín, Czech Republic, 2010.** ISBN 978-80-7318-909-9

BENÍČEK L., CHVÁTALOVÁ L., **MONTÁGOVÁ K., ČERMÁK R., OBADAL M.;** Phase transformation in injection-molded and extruded polybutene-1, **Conference Plastko, Tomas Bata University in Zlín, Czech Republic, 2010.** ISBN 978-80-7318-909-9

MONTÁGOVÁ K., BENÍČEK L., ČERMÁK R., CHVÁTALOVÁ L.; Evolution of physical and mechanical properties during phase transformation in poly(1-butene), **Conference WSEAS 2010, Greece–Corfu Island.** ISSN: 1792-4294. ISBN: 978-960-474-203-5

BERKOVÁ K., ČERMÁK R., VERNEY V.; Fundamental study of polypropylene/wood flour composites, **1st Central and Eastern European Conference on Thermal Analysis and Calorimetry 2011, Craiova, Romania,** ISBN 978-606-11-1893-9

BERKOVÁ K., ČERMÁK R., VERNEY V.; On wood-filled polypropylene: A calorimetric study, rheology and X-ray scattering, **1st Central and Eastern European Conference on Thermal Analysis and Calorimetry 2011, Craiova, Romania,** ISBN 978-606-11-1893-9

CURRICULUM VITAE

Personal data:

Name: Kristýna Berková

Birth's name: Montágová

Date of Birth: 1985, August 24

Address: Zálavčí 364, Leština 789 71

E-mail: montagova@ft.utb.cz

Nationality: Czech

Education:

2009–present *Blaise Pascal University, Laboratoire de Photochimie Moleculaire et Macromoleculaire, Clermont Ferrand, France, **Ph.D. Degree***

Programme: Physical Chemistry

*Thomas Bata University in Zlín, Faculty of Technology, Department of Polymer Engineering; **Ph.D. Degree***

Programme: Technology of Macromolecular Compounds

Specialization: Processing, structure and properties of composites based on natural fillers and stereoregular polyolefins: Environmentally benign concept

2007–2009 *Thomas Bata University in Zlín, Faculty of Technology,*

Master's degree

Programme: Chemistry and materials technology

Specialization: Polymer engineering,

(Master thesis: Evolution of physical and mechanical properties during phase transformation in poly(1-butene))

2004–2007 *Thomas Bata University in Zlín, Faculty of Technology,*

Bachelors's degree

Programme: Chemistry and materials technology

1996–2004 *Grammar School – Gymnazium Zábřeh*

School leaving exams: Czech language, Mathematics, German language, English language

Employment:

April–October 2011 *Tomas Bata University in Zlín, Centre of Polymer Systems*

2012–Present *Hella Autotechnik s.r.o., Development and testing laboratory*